

Durham E-Theses

I surface waves from the Atlantic II The crust and upper mantle beneath Iceland

M. G. Mitchell

How to cite:

Mitchell, M. G. (1969) I surface waves from the Atlantic II The crust and upper mantle beneath Iceland. Doctoral thesis, Durham University.

Use policy

The full-text may be used and/or reproduced, and given to third parties in any format or medium, without prior permission or charge, for personal research or study, educational, or not-for-profit purposes provided that:

- a full bibliographic reference is made to the original source
- a <https://etheses.durham.ac.uk/id/eprint/9237/> is made to the metadata record in Durham E-Theses
- the full-text is not changed in any way

The full-text must not be sold in any format or medium without the formal permission of the copyright holders.

Please consult the [full Durham E-Theses policy](#) for further details.

- I SURFACE WAVES FROM THE ATLANTIC
- II THE CRUST AND UPPER MANTLE BENEATH ICELAND

A thesis submitted for the degree of
Doctor of Philosophy
in the
University of Durham
by
Malcolm George Mitchell

Hatfield College

August 1969



ABSTRACT

1. Surface waves from the Atlantic

It is shown that Rayleigh wave arrivals can be used to locate small earthquakes which are not detectable using normal body wave techniques. Using Rayleigh wave arrivals at four stations, six small earthquakes have been located on the Reykjanes Ridge. They appear to be foreshocks preceding two larger events, with mb magnitudes of 4.5 and 4.6, which were reported in the U.S.C.G.S. bulletins. It is suggested that the apparently large Rayleigh waves from the eight events are mainly due to their shallow foci. Assuming zero focal depths, the mb magnitudes of the foreshocks appear to range from 4.2 to 4.4. It is suggested that these events were not reported in the bulletins because of the low detection probability, using body waves, for low-magnitude earthquakes occurring in the mid-Atlantic. If this interpretation is correct, then the appearance of surface wave trains from unlocated sources, on the records of seismic stations around the Atlantic, can be explained in a similar manner.

2. The crust and upper mantle beneath Iceland

A description is given of the data obtained from two temporary array stations which were installed in Iceland during the summer of 1967. P-wave delay times are measured

using data from stations in Iceland, Scotland, Sweden and Greenland. A delay time of 1.5 seconds, relative to Eskdalemuir in Scotland, appears to be constant over Iceland. Relative to Kiruna in Sweden, the Icelandic delay is approximately 2.3 seconds. The delay times are interpreted in terms of the crust and upper mantle beneath the recording stations and they can be explained if the 7.4 km/sec layer beneath Iceland extends to a depth of 200 km.

CONTENTS

Acknowledgements

I Surface waves from the Atlantic

II The crust and upper mantle beneath Iceland

ACKNOWLEDGEMENTS

I wish to thank Professors K. C. Dunham, G. M. Brown and M. H. P. Bott for the privilege of working in the department. I am very grateful to Dr. R. E. Long for his supervision and advice during the course of the work.

I should like to thank Dr. H. I. S. Thirlaway and his colleagues at Blacknest for their assistance and advice and for permitting me to use the processing equipment at Blacknest. In particular, I should like to thank Mr. P. D. Marshall for his advice on surface wave problems. I should like to thank Professor P. L. Willmore and his colleagues at the I.S.C. Edinburgh for supplying data from various seismic stations. Further, I should like to thank Mr. G. Palmason of the National Energy Authority, Iceland, and Mr. R. Stefansson of the Icelandic Meteorological Service, for their assistance and advice during the planning and execution of the Iceland experiment.

Finally, I should like to thank the Natural Environment Research Council for financial support for three years.

I SURFACE WAVES FROM THE ATLANTIC

CONTENTS

	Page
Introduction	1
CHAPTER 1:	
(1.1) The properties of Rayleigh waves	2
(1.2) The generation of Rayleigh waves	4
(1.3) Measurement of the group velocity	5
(1.4) Possible methods of epicentral location using Rayleigh waves	7
(1.5) The data used in this study	9
(1.6) The appearance of the data	10
(1.7) The group velocity curves from the test data	16
(1.8) Assessment of the location methods	23
(1.9) Theory of the third location method	24
(1.10) Results of the location program	27
(1.11) General discussion	35
CHAPTER 2:	
(2.1) The problem of amplitudes	37
(2.2) The measurement of magnitude	38
(2.3) The mb magnitude scale	39
(2.4) The Ms magnitude scale	39
(2.5) The relation between mb and Ms	43
(2.6) The results of the magnitude measurements	44
(2.7) Errors in the magnitude measurements	50

	Page
(2.8) mb values for the previously unlocated events	57
Conclusions	60
References	61
Appendix, the location program	65

FIGURES

	Page
1. Map showing the location of epicentres and stations used.	13
2. Examples of arrivals on vertical seismometers	15
3. Dispersion at Eskdalemuir	19
4. Dispersion at Godhavn	20
5. Dispersion at Blacksburg	21
6. Dispersion at Malaga	22
7. Group velocities from the location program, for Eskdalemuir	29
8. Group velocities from the location program, for Malaga	29
9. Group velocities from the location program, for Blacksburg	30
10. Group velocities from the location program, for Godhavn	30
11. Epicentres from surface wave location	34
12. Log B for focal depth = 33 km.	42
13. mb versus mb/s using I.S.C. focal depths for all data	49
14. mb versus mb/s assuming zero focal depths for group A events and others as in Fig. 13	49

TABLES

	Page
1. Station positions	11
2. Details of the test data	12
3. Epicentral positions and origin times from the location program	28
4. Locations of events using all combinations of three stations	32
5. Depth corrections to Ms	40
6. Magnitudes for the test data	46
7. Magnitudes for the previously unlocated events	59

Introduction

Surface wave trains from unlocated sources comprise 20 per cent of the arrivals which are recorded by the long-period instruments at the United Kingdom Atomic Energy Authority's seismic station at Eskdalemuir in Scotland (P. Marshall, personal communication). A similar proportion is observed by other recording stations around the Atlantic. At Eskdalemuir, the unlocated events give rise to Rayleigh waves which have similar dispersion characteristics to those received from earthquakes in the North Atlantic.

The amplitudes of the arrivals are often large enough to lead one to expect associated body waves to be recorded. However, most of the arrivals appear to be unassociated with any body waves, and in all cases body waves are recorded by too few stations for the normal methods of epicentral location to be used.

The work reported here is a preliminary investigation of one group of these events. A method was developed for locating earthquakes using Rayleigh waves. This method was applied to six events which were found to have epicentres on the Reykjanes Ridge. The magnitudes of a selection of well documented events were investigated using surface and body wave arrivals in an attempt to provide an explanation for the lack of recorded body waves from the previously unlocated events.

CHAPTER 1

(1.1) The properties of Rayleigh waves

Surface waves from earthquakes most commonly consist of both Love and Rayleigh waves. While both types appear on the horizontal component records, only Rayleigh waves appear on the vertical component. As Rayleigh waves are therefore the more clearly seen of the two, they alone are considered here for the purpose of locating earthquakes.

The properties of Rayleigh waves can be predicted mathematically from the elastic wave theory by specifying the necessary boundary conditions and by making certain assumptions about the nature of the material through which they travel. The mathematics of these processes are given in many text books and only the results will be described here. (Ewing et al 1957 give a full treatment and give a comprehensive list of references.)

The mathematics predict several types of Rayleigh waves which are referred to as different modes. However, the fundamental mode is the most conspicuous; higher modes are not commonly seen over mixed paths and are therefore not considered here. (Crampin 1966, Ossing 1964.)

The actual wave disturbance is made up of Fourier components of different wavelengths which interfere to form the

visible disturbance which contains the wave energy. Each component decays in amplitude with increasing depth, z , according to its wavelength, λ , so that the longer wavelengths penetrate farthest. The speed with which these components travel, called the phase velocity, c , depends on the medium through which they pass. In the earth, the velocity of elastic waves generally increases with depth which, combined with the increased penetration of long-wavelength components, results in an increase of phase velocity with period.

The velocity of the actual disturbance is called the group velocity, U . The relation between the phase and the group velocities is given by the equation

$$U = d(kc)/d(k) \quad (1)$$

where the wave number, $k = 2\pi/\lambda$. Thus for Rayleigh waves in the earth, U and c are not equal. The result of this relationship is that the group velocity is a function of the period and it generally increases with the wavelength. However, because of the form of equation 1, there may be maxima and minima in the group velocity curve. Although the positions of the maxima and minima depend on the structure of the medium through which the waves pass, the presence of a minimum does not necessarily imply the existence of a low-velocity layer. For a continental structure, the minimum

occurs at about nine seconds period and the maximum at about sixty seconds with a further minimum at about 230 seconds.

Waves with periods as short as that at which the first minimum occurs are heavily attenuated over oceanic paths and they are only seen if the path is predominantly continental. In the latter case they cause a build-up in amplitude towards the end of the wave train where waves of different periods arrive at the same time - this is referred to as the Airy Phase.

The Rayleigh wave particle motion is of the form of a retrograde ellipse, where the ellipse lies in the vertical plane containing the direction of wave propagation. Thus the motion may be recorded on all three components and the ratio of the amplitudes on the horizontal components depends on the direction of approach of the wave.

(1.2) The generation of Rayleigh waves

The problem of the generation of Rayleigh waves from a source at a finite depth was studied by Lamb (1904). It is necessary that they should be generated in order to provide zero stress over the free surface; this condition cannot be fulfilled in any other way when the incident wavefront is curved. Rayleigh waves may be considered to be generated by the interaction of P or S waves with the free surface at some

distance, X , from the epicentre. The distance, X , is governed by the depth of the source, H , according to the equation

$$X = Cr H / \sqrt{\delta^2 - Cr^2} \quad (2)$$

(Ewing et al 1957)

where Cr is the Rayleigh wave velocity and δ is either the P-wave or the S-wave velocity. However, the travel times of the Rayleigh waves are the same whether they are considered to be generated at the epicentre or at X .

The amplitudes of the generated waves depend on the depth of the source and on the wavelengths of the wave components. The expression for the amplitudes contains a factor of the form $\exp(-sH/\lambda)$, where λ is the wavelength and s is a constant which depends on the nature of the source i.e. whether it is shear or compressional (Jeffreys 1962). This is analagous to the way in which the components of the Rayleigh wave penetrate according to their wavelengths. Thus the generated waves contain proportionally less high-frequency energy as the focal depth increases.

(1.3) Measurement of the group velocity

Measurements of the group and phase velocities can be made by following the progress of a wave train from its source. The group velocity is given simply by the travel time of the envelope divided by distance; the phase velocity

can be determined by following the progress of some recognisable feature of the wave train, such as a peak or a trough, over a short distance. The group velocity is the more easily determined of the two and it can be measured using one station if the source parameters are known; this is difficult to do for the phase velocity because there is an ambiguity about the phase of the Fourier components at the source (Brune et al 1960).

The method used here for the measurement of group velocities is described by Brune et al (1960). The method consists of assigning numbers to consecutive peaks, troughs and cross-over points so that peaks are assigned integer numbers, cross-overs quarter-integers and troughs half-integers. If a plot is then made of the peak numbers versus arrival times, then the slope of the curve will give the period as a function of arrival time. Thus, knowing the origin time and the distance from the source, the group velocity of each period can be calculated.

In order to obtain the true group velocity, the effect of the instruments on the recorded wave train must be taken into account. It is well known that all instruments, whether they are mechanical or electrical, cause a change of phase between the input and the output. In the case of seismic recording equipment, this is expressed in terms of a phase

response curve which gives the phase change in radians as a function of period. This phase change, Θ , effects the Fourier components of the recorded wave; the effect on the actual wave train, which is delayed, is expressed in terms of the group delay. The relationship between the group delay and the phase change is analogous to that between the group and the phase velocities and it may be expressed as

$$\text{Group delay} = d \Theta / d \omega \text{ secs.} \quad (3)$$

Where ω is the angular frequency = $2 \pi / T$

T being the period of the wave. (Brune et al 1960)

Therefore, in the calculation of the group velocities, the group delay corresponding to the particular period is subtracted from the measured travel time.

(1.4) Possible methods of epicentral location using Rayleigh waves

Considering the properties of Rayleigh waves, it may be seen that there are three possible methods of location. Firstly, because the wave trains are dispersed, the separation of the periods is proportional to the distance which the waves have travelled. If this separation is measured at at least two stations, so that the epicentral distance to each station can be found, then the position of the epicentre can be calculated.

Secondly, because of the orbital motion of particles during the passage of a Rayleigh wave, the direction from which a wave has approached a station can be found by comparing the amplitudes of the motion recorded on the two horizontal-component instruments. The 180 degree ambiguity can be resolved by considering the motion on the vertical component; when the vertical motion is approaching its maximum, then the horizontal motion is away from the source. If they are used together, the first two methods may enable one to make an estimate of the epicentral position from the records of one station.

A third method is possible using the absolute arrival times of any period, or group of periods, at at least three stations. This method is analagous to the usual method of earthquake location using p-waves.

The first and the third methods depend on a prior knowledge of the dispersion characteristics of arrivals from the epicentral region; this would have to be obtained from observations on well-documented events in the area of interest. Each of the methods requires that the stations should be well distributed about the epicentral area and for maximum accuracy, they should be equally-spaced in azimuth from the epicentre.

In order to test these location methods, and to obtain the necessary information on group velocities, a selection of

well documented events, located in the North Atlantic Ocean were chosen for study at four stations.

(1.5) The data used in this study

A group of six arrivals were recorded by the long period system of the U.K.A.E.A. station at Eskdalemuir on August 22nd 1964. None of the arrivals corresponded to any events reported by the United States Coast and Geodetic Survey (U.S.C.G.S.) although from their dispersion characteristics, it seemed likely that some of them had originated in the North Atlantic Ocean. In order to test the feasibility of the location methods, with the object of eventually locating these six events in particular, a group of twenty events which had already been located by the U.S.C.G.S., were selected for test purposes. As the International Seismology Centre (I.S.C.) at Edinburgh had kindly made available film of records from the U.S.C.G.S. stations for 1964, the events were selected from those which occurred during that year.

The records from four stations were chosen according to the following criteria: firstly, each station should have recorded as many of the events of August 22nd as possible, and, secondly, the stations should be well distributed about the Atlantic in accordance with the requirements of the proposed location methods. The stations selected were Eskdalemuir in Scotland, Godhavn in Greenland, Blacksburg in

Virginia U.S.A. and Malaga in Spain. In order that the instruments should be the same at each station, the U.S.C.G.S. station at Eskdalemuir was used rather than the U.K.A.E.A. station in the same region.

It would have been convenient to use stations at Akureyri in Iceland, Ponta Delgada in the Azores and at Bermuda because for North Atlantic events, these stations would receive waves which had travelled over almost totally oceanic paths and thus partly avoiding the disturbing effects of the continental boundary. However, these were not selected as no records were available for Akureyri and Bermuda for August 22nd and the Ponta Delgada records were too noisy.

The events which were chosen were located on the North Atlantic Ridge between 30 and 60 degrees North. Details of the stations and the test data are given in Tables 1 and 2. The positions of the stations and of the events are marked on the map in Fig. 1.

(1.6) The appearance of the data

All the wave trains appeared to consist almost entirely of Rayleigh waves. Very little Love wave motion was seen, at the most, a half or one cycle was seen on the horizontal-component records merging into the beginning of the Rayleigh wave. Higher mode Rayleigh waves were not recognised on any

TABLE 1

STATION	CODE	LATITUDE			LONGITUDE		
		deg	min	sec	deg	min	sec
Eskdalemuir	ESK	55	19	00N	03	12	18W
Godhavn	GDH	69	19	00N	53	32	00W
Blacksburg	BLA	37	12	40N	80	25	14W
Malaga	MAL	36	43	39N	04	24	40W
Toledo*	TOL	39	52	53N	04	02	55W

* This station is used in the magnitude measurements discussed in Chapter 2.

TABLE 2

EVENT No.	DATE (1964)	ORIGIN TIME			EPICENTRE		DEPTH		MAG (mb)	NO. STATIONS USED FOR mb
		hr.	min.	sec.	deg N	deg W	km.	H ± h		
2	Aug 17	09	07	06.5	54.9	30.1	64.	18	4.8	13
3	Aug 17	22	47	31.4	52.0	30.1	25	22	5.0	13
4	Aug 22	17	04	29.7	51.9	30.2	19	20	5.0	14
5	Aug 26	03	18	43.7	52.1	30.1	28	22	5.2	20
9	Sept 16	22	23	38.5	22.9	45.1	50	14	5.5	25
10	Sept 17	15	02	01.5	44.6	31.3	24		5.5	31
20	Dec 2	08	20	45.6	30.5	42.0	33		5.2	14
24	May 17	19	26	21.6	35.4	36.1	33		5.6	30
27	June 5	04	44	53.4	47.6	27.3	82	14	4.7	13
33	July 1	20	09	31.0	30.8	41.5	33		5.0	17
36	July 11	22	34	42.6	41.3	29.1	62	21	4.8	8
37	July 13	16	22	27.5	53.9	35.1	39	27	4.2	6
39	Aug 23	02	56	13.3	59.4	30.3	30	41	4.5	12
40	Aug 23	04	47	46.8	59.5	30.2	33		4.6	11
41	Sept 6	18	55	49.1	38.4	26.7	44	30	4.8	6
42	Sept 13	23	01	23.1	58.7	30.9	190	24	4.1	5
43	Sept 13	23	23	34.9	59.0	31.6	25		4.1	4
44	Sept 14	06	19	49.2	58.9	31.1	47	47	4.3	5
45	Sept 14	06	34	44.0	59.2	31.1	56	19	4.4	3
49	Oct 29	13	40	36.3	41.4	29.5	33		4.5	6
U2	Aug 22	17	24	30.9	59.8	30.3	69	25	4.5	3

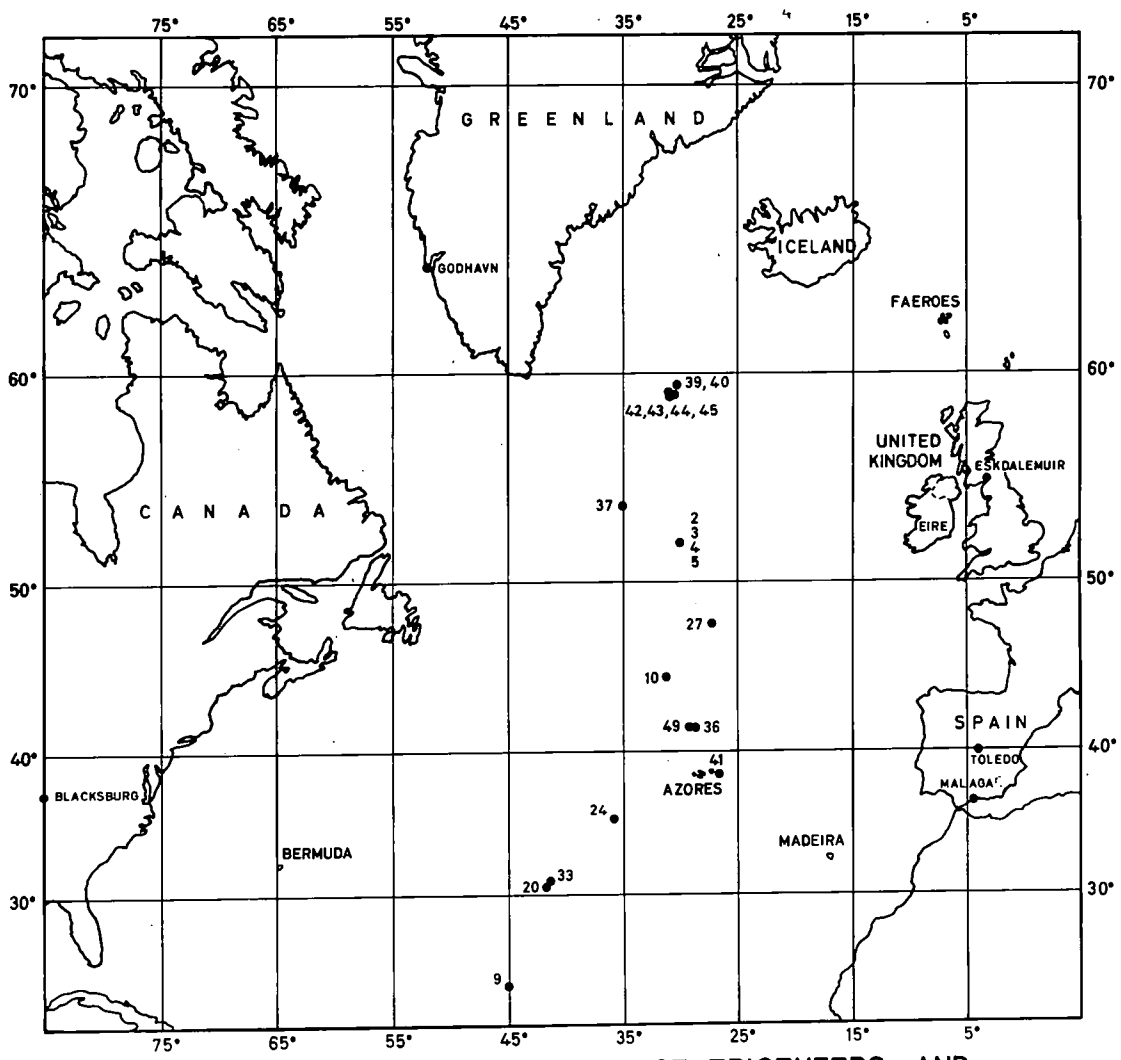


FIG. 1 MAP SHOWING THE LOCATION OF EPICENTERS AND STATIONS USED.

of the records.

As seen on the vertical component records, the Rayleigh wave arrivals sometimes appeared to be in two or more parts. Such multiple arrivals were particularly conspicuous at Eskdalemuir from the more northerly events when the arrivals appeared to be in three parts (Fig. 2 a). The first arrivals ranged in period from approximately 35 to 12 seconds, while the later arrivals which were of smaller amplitude, contained a more restricted range of periods down to about 12 seconds. Some of the Blacksburg arrivals were also complex. For example, arrivals from events 2 and 3 (Fig. 2 c) appeared to be in two parts, the first part having a long period and consisting of one cycle and the second part of shorter period and with a complex amplitude envelope.

The multiplicity of the arrivals appeared to be a characteristic of the path rather than the event and it seems unlikely that it is due to a multiple source function. The effect is attributed to lateral refraction at the continental boundary which results in the simultaneous arrival of waves which have travelled via paths of different lengths. These arrivals interfere causing beating and modulation of the amplitude envelope. (Evdenden 1954, Pilant and Knopoff 1964, Knopoff et al 1966, Savarensky et al 1968)

Where several events were clearly recorded by one station,

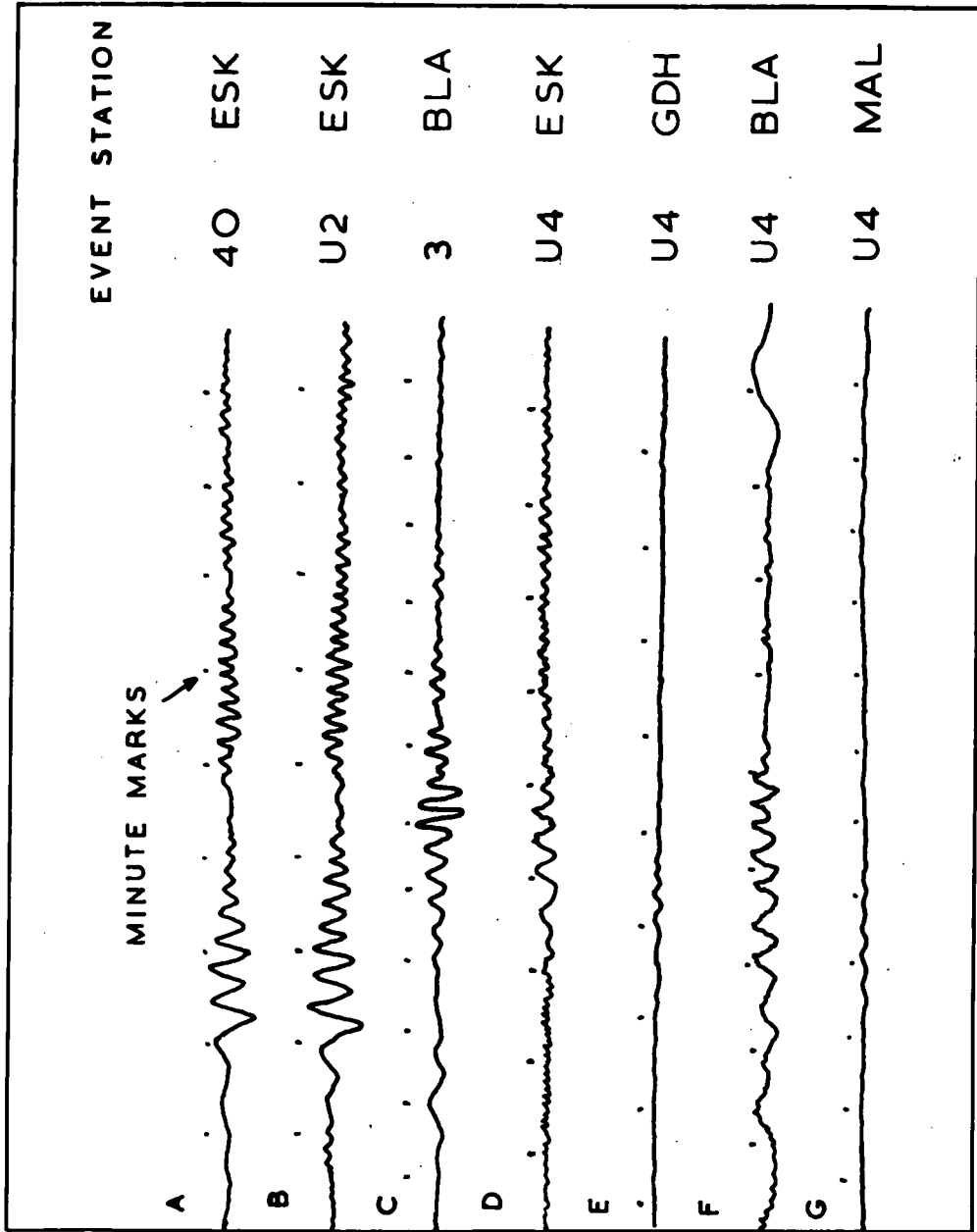


FIG.2 EXAMPLES OF ARRIVALS ON VERTICAL SEISMOMETERS. U = UNLOCATED EVENT.

it was possible to identify those which came from the same epicentral region by comparing the recorded motion on the vertical records. Most of the unlocated events were not recorded well enough for this to be a useful diagnostic in their location, except to indicate that they originated at the same order of distance from the station as the test data and that the structures of the paths over which they had travelled were similar. The unlocated event U2 provides an exception to this. It was clearly recorded at all stations, particularly at Eskdalemuir where the wave train was almost identical with that from event 40 (Fig. 2 a and 2 b). This event was located by the method described later in this thesis and, afterwards, by the I.S.C. when it was found to have an epicentre within 60 kms of event 40.

(1.7) The group velocity curves from the test data

Group velocity curves for the test data were calculated using the method described earlier. Most of the records were on two-inch film strips which were analysed at Durham on a special viewer. The image was enlarged so that one minute of recording time corresponded to approximately 1.65 cm on the viewing screen. The clarity of the image permitted measurements of distance to within a minimum of 0.25 mm which corresponded to a time resolution of approximately one second.

Other records, which were in photocopy form, permitted a similar resolution.

Inaccuracies in the measurements are introduced by the broadness of the peaks and troughs, the sharpness of the trace and perturbations due to background noise. Where the records were sufficiently clear, crossover points were measured in addition to peaks and troughs.

For certain arrivals the effects of beating were clearly shown in the curve of peak number versus arrival time. These resulted in discontinuities in the curve though, where possible, a smooth curve was drawn through the points, otherwise only the first portion of the curve was used. Differentiation of the curve to determine the periods was done graphically by drawing tangents and measuring their slopes. The distances from each station were calculated using a computer program based on the equations given by Bullen (1963, p.154).

The measured travel times were corrected for the effects of instrumental group delay. The corrections ranged from 2 seconds at 15 seconds period to approximately 14 seconds at 40 seconds period. These corrections were calculated from the instrumental phase response curves (Ben-Menahem et al 1965) according to the theory described earlier. The corrections were applied for the sake of completeness and so that the group velocity curves could be compared with those

obtained by others; it is not necessary for the application of the location methods as the unlocated events and the test data were recorded on the same instruments.

Not all of the test data were used to compute group velocity curves. Some of the larger events were unusable because the large recorded motion produced a very faint trace, while the smaller events were sometimes obscured by noise. The curves which were obtained for Eskdalemuir, Godhavn, Blacksburg and Malaga are reproduced in Figures 3, 4, 5 and 6.

It should be noted that the curves represent the observed dispersion which is needed for the location methods; no corrections were made for the effects of continental path length. The curves for Eskdalemuir and Malaga are very similar and show oceanic dispersion. However, the Blacksburg and Godhavn curves vary considerably from event to event. This is due to the effect of the varying proportion of continental path (which for some of the northerly events received at Blacksburg is up to 65%) and to the effects of lateral refraction due to the small angle of incidence of the wavefront to the continental boundary. It may be seen that the dispersion measured at these stations for the more southerly events (e.g. 33, 20) is very similar to that obtained at Malaga and Eskdalemuir.

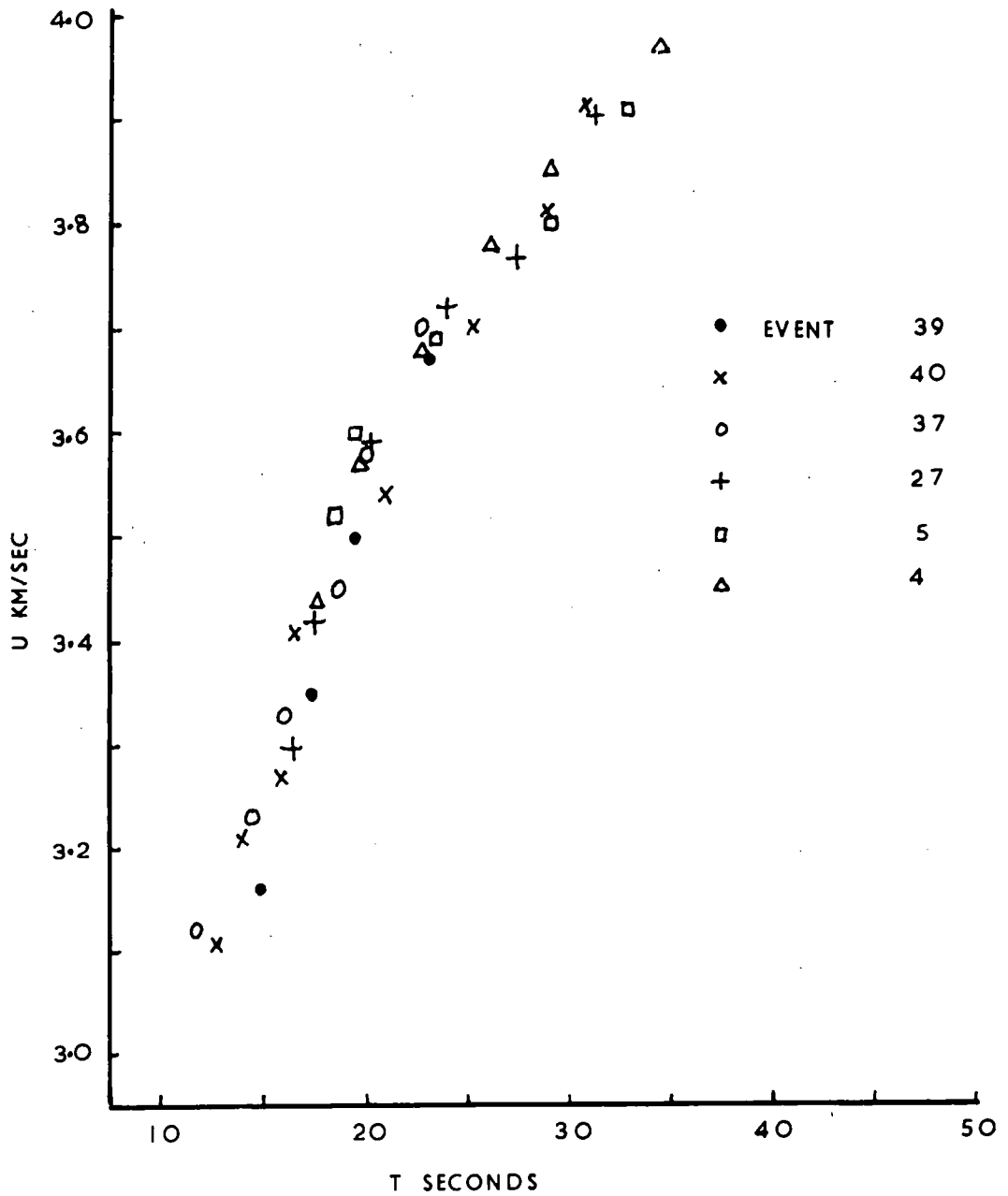


FIG 3. DISPERSION AT ESKDALEMUIR

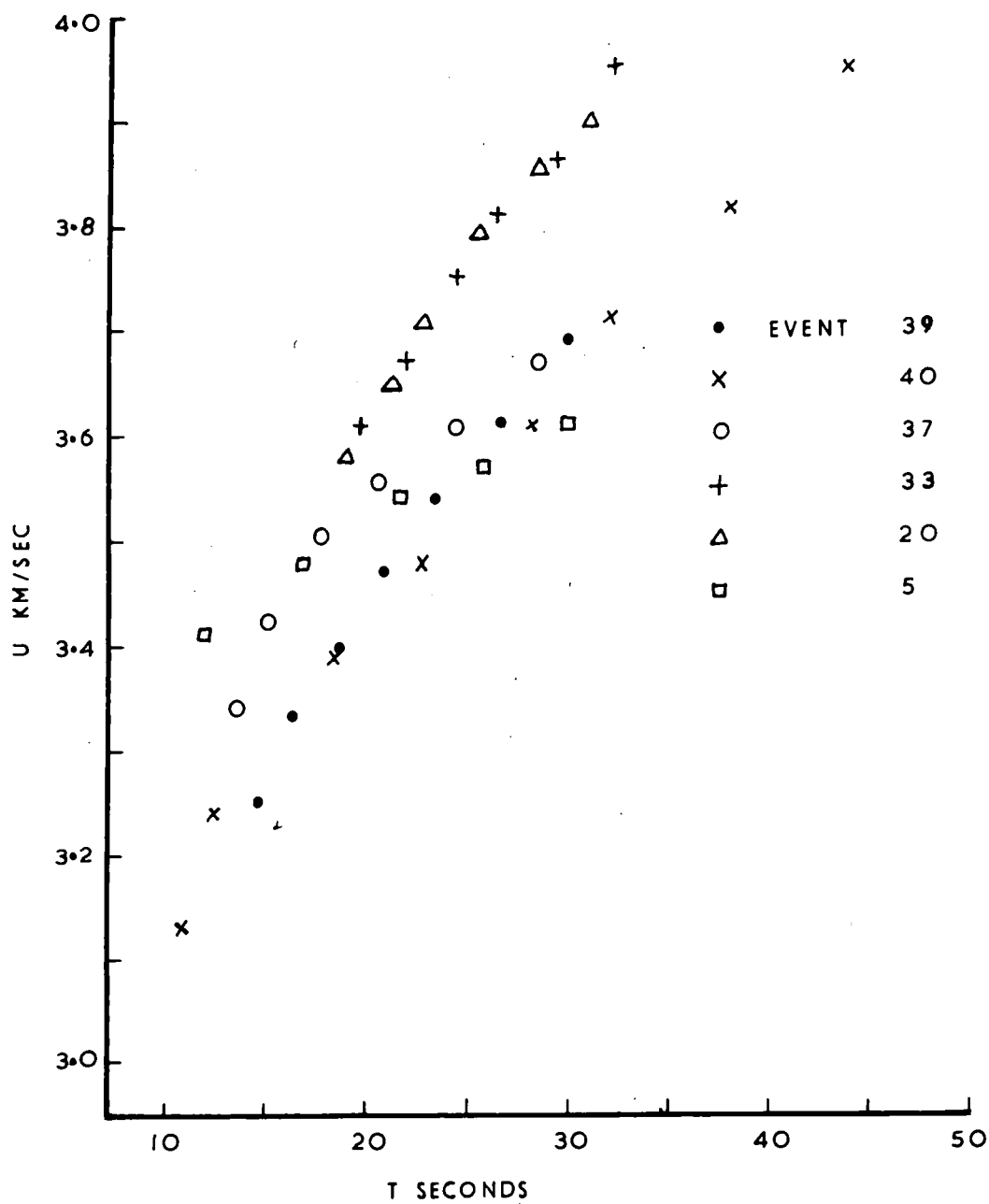


FIG 4. DISPERSION AT GODHAVN

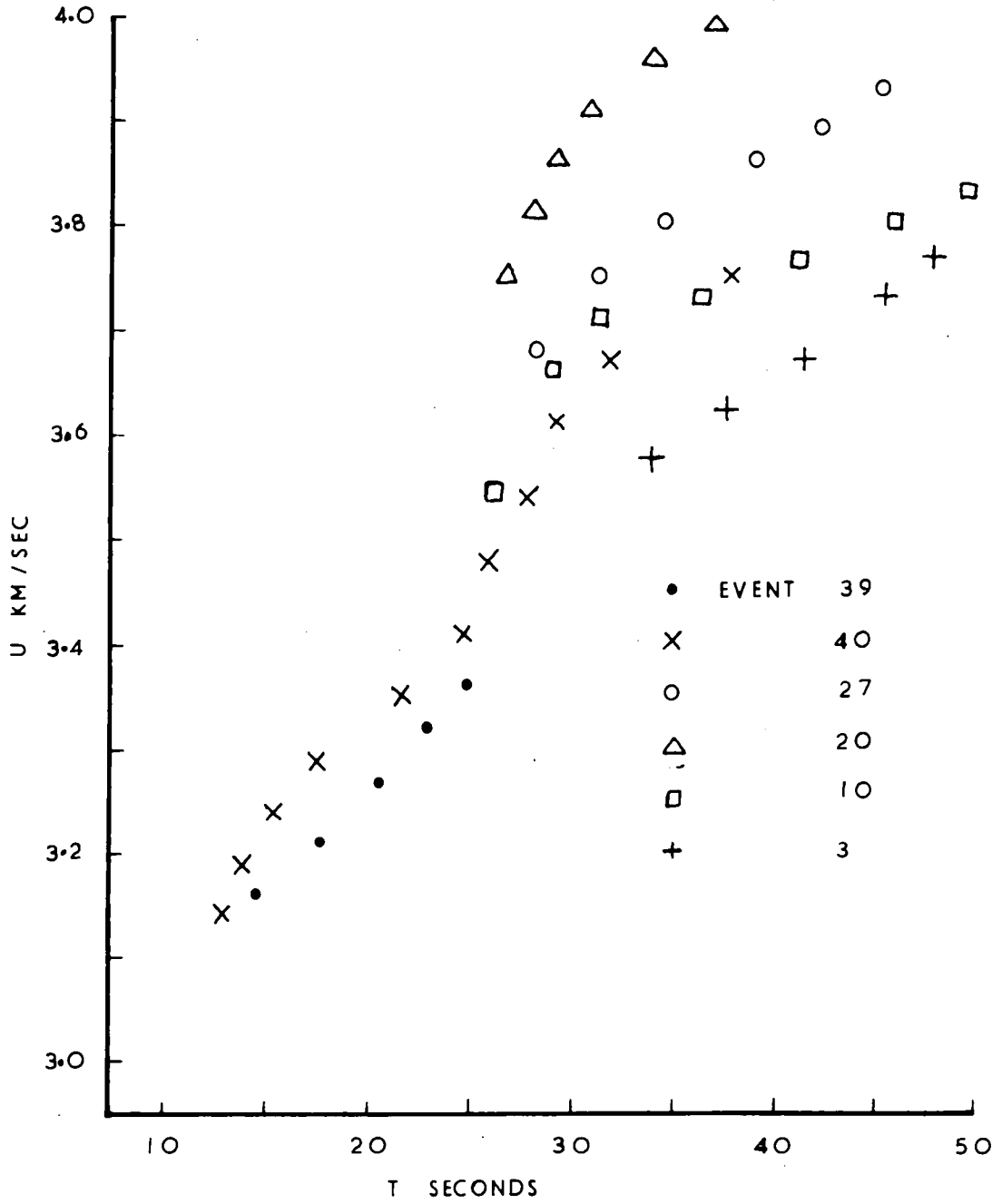


FIG 5. DISPERSION AT BLACKSBURG

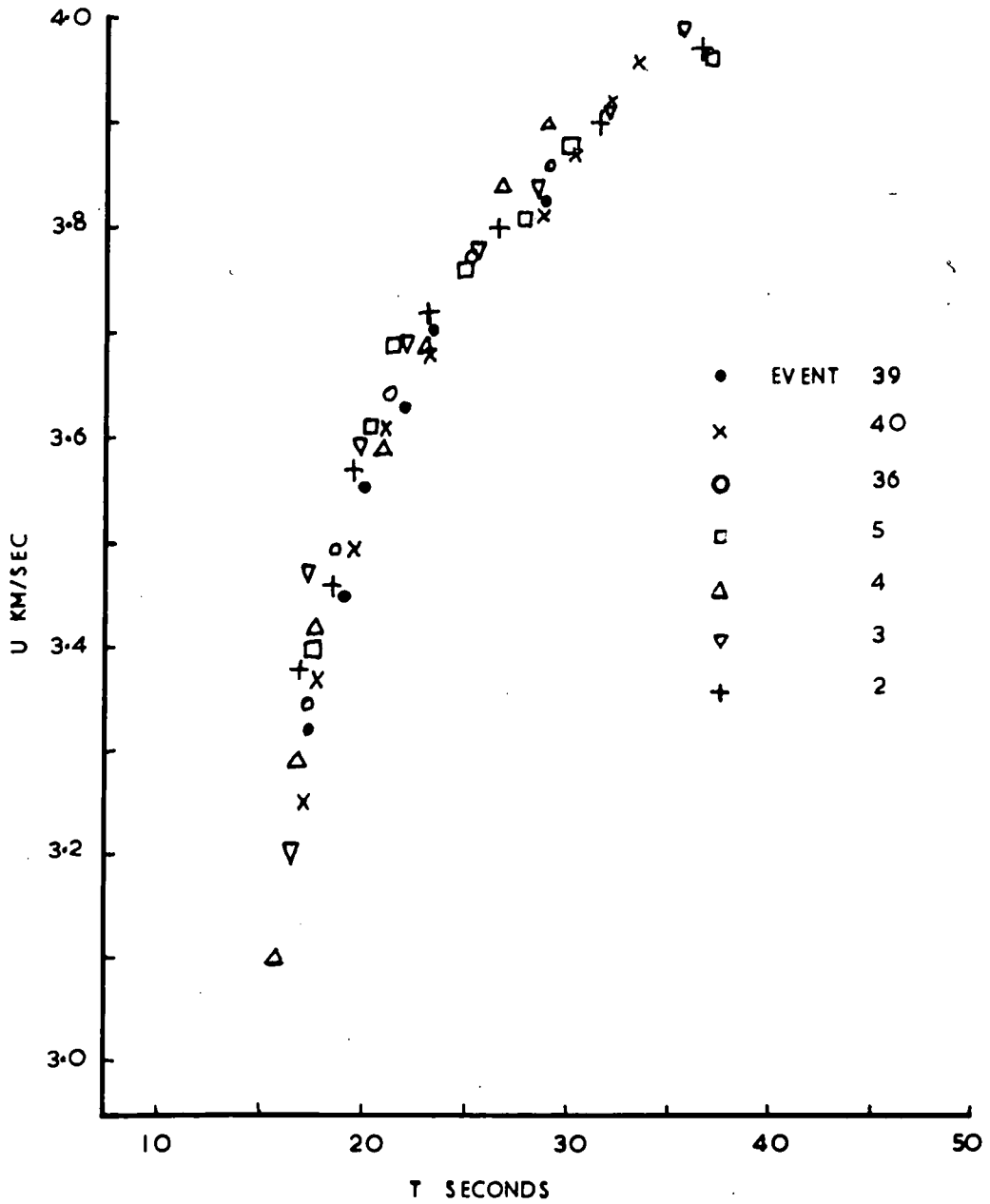


FIG 6. DISPERSION AT MALAGA

(1.8) Assessment of the location methods

The three methods of location were assessed using the test data. The first method, that of calculating the distance from the epicentre to each station from the separation of the periods, can give the distance to within 400 kms from any station at which the arrivals are clearly received and are not complex. The method is very limited by the quality of the records and by the range of periods received by each station. For the location of small events, which are often greatly disturbed by noise, the method is not usable.

The second method, that of finding the azimuth of the source from each station by using the horizontal component records, works only with very clear records, with large horizontal motions which are relatively undisturbed by noise. Even under these conditions, the azimuth is only accurate to within ± 10 degrees. It was found that the horizontal component records were generally more noisy than the vertical records. They are particularly susceptible to wind noise which often renders them useless. With noise-free records the method is still frustrated by the effect of Love wave motion, which results in a different amplitude ratio between the horizontal component records for the first arrivals - which are otherwise the most clearly recorded. The method is limited further by the effects of lateral refraction so

that the plane of polarisation of the wave does not necessarily correspond to the direction from the source to the station (Evenden 1954, Savarensky et al 1968).

Thus although the first two methods may be used to obtain a rough epicentral position when clear records are obtained, their accuracy is very poor, and for locating small events, which are rarely recorded clearly, both methods are impractical. However the third method, which makes use of the absolute arrival times of the periods at each station, was tested with more success. It is capable of locating events to within a 100 km square and is therefore considered to give useful information on events whose epicentral positions would otherwise be unknown. It has the advantage that the arrival times of several periods are used from each station, therefore inaccuracies in the determination of individual periods may average out over each wave train.

(1.9) Theory of the third location method

Let the arrival time at a station i of a period j be

$t(i, j)$. If the group velocity over the path from the source to the station is $V(i, j)$ and the epicentral distance is Δ_i then we can write:

$$T_0 = t(i, j) - \Delta_i/V(i, j) \quad (4)$$

where T_0 is the origin time of the event.

If surface waves are recorded at several stations at which the group velocities of similar arrivals are known, then a series of equations can be obtained each giving values of the apparent origin time $T(i, j)$ according to trial values of the epicentral position. As the correct position is approached, so the terms $T(i, j)$ will converge towards the true origin time, T_0 .

A computer program was written in Fortran IV in order to test this method of location using an IBM 360 computer. The program computes the values of the terms $T(i, j)$ for each of a series of trial epicentres which are placed in a uniform reticulate manner over a specified area in which the true epicentre is expected to lie. For each trial position, the onset times at each station are used to find the average estimate of the origin time, $TBAR(i)$, for each station i , where

$$TBAR(i) = \sum_{j=1}^j \Delta_i/L(i) [t(i, j) - \Delta_i/V(i, j)] \quad (5)$$

and where $L(i)$ = the number of observations at each station. Next, the average value of the terms $TBAR(i)$ is calculated to give an estimate of the origin time (ETO). A measure of the goodness of fit of each trial position is then obtained by calculating a term referred to as TSSQ which is a function of the variance of the terms $TBAR(i)$, i.e.

$$TSSQ = \sum_{i=1}^{i=n} [ETO - TBAR(i)]^2 \quad (6)$$

Where $ETO = \sum_{i=1}^{i=n} [1/n TBAR(i)]$, n being the number of stations.

Thus each trial epicentral position has associated with it a value of TSSQ. As the different positions are tried, the one with the currently lowest value of TSSQ is stored as the best position. When all the positions have been tried, the process is repeated with more closely-spaced positions about the previously-chosen best position. The new search area is chosen to overlap with the eight positions surrounding it in the previous search. The program iterates in this manner until the distance between trial positions is less than 0.1 degrees, which is well within the accuracy of the data.

When the process is completed, the final estimate of the epicentral position and the origin time are printed out with the corresponding value of TSSQ. In addition, the calculated group velocities are given so they may be compared with those

which were assumed for the location in order to give a measure of the accuracy of the solution.

A printout of the program and examples of the output, together with a description of the necessary input details, are given in Appendix I.

(1.10) Results of location program

The program was used to compute the epicentres and the origin times of the unlocated events which are designated U1-U6. A preliminary location using the average group velocity curves at each station showed that they all occurred in the Reykjanes Ridge in the vicinity of the test events 39 and 40. The locations were then repeated using the mean values of the group velocity curves from events 39 and 40 for each station. Details of the epicentral positions and origin times are given in Table 3.

The accuracies of these locations may be estimated by comparing the calculated group velocities obtained from the program with those which were assumed in the location. These are compared in Figures 7, 8, 9 and 10 for events received at Eskdalemuir, Malaga, Blacksburg and Godhavn, where the solid curves show the group velocities which were used in the location. It may be seen that the average difference between the calculated and the assumed group velocities at each station is approximately 0.05 km/sec. If the error in the

TABLE 3

EVENT	TSSQ	ORIGIN TIME			LATITUDE		LONGITUDE	
No.		hr	min	sec	deg	min	deg	min
(Aug. 22nd)								
U1	0	17	19	39	59	14.3N	30	16.9W
U2	9	17	24	24	59	20.8N	30	23.1W
U3	0	18	30	27	59	22.5N	30	30.5W
U4	16	19	12	16	59	01.8N	30	45.2W
U5	113	21	18	23	59	12.8N	30	11.6W
U6	24	21	25	22	59	25.8N	30	38.8W

N.B. The origin times given by the I.S.C. for events U2, 39 and 40 are:

U2	Aug 22	17hr	24min	30.9 sec
39	Aug 23	02hr	56min	13.3 sec
40	Aug 23	04hr	47min	46.8 sec

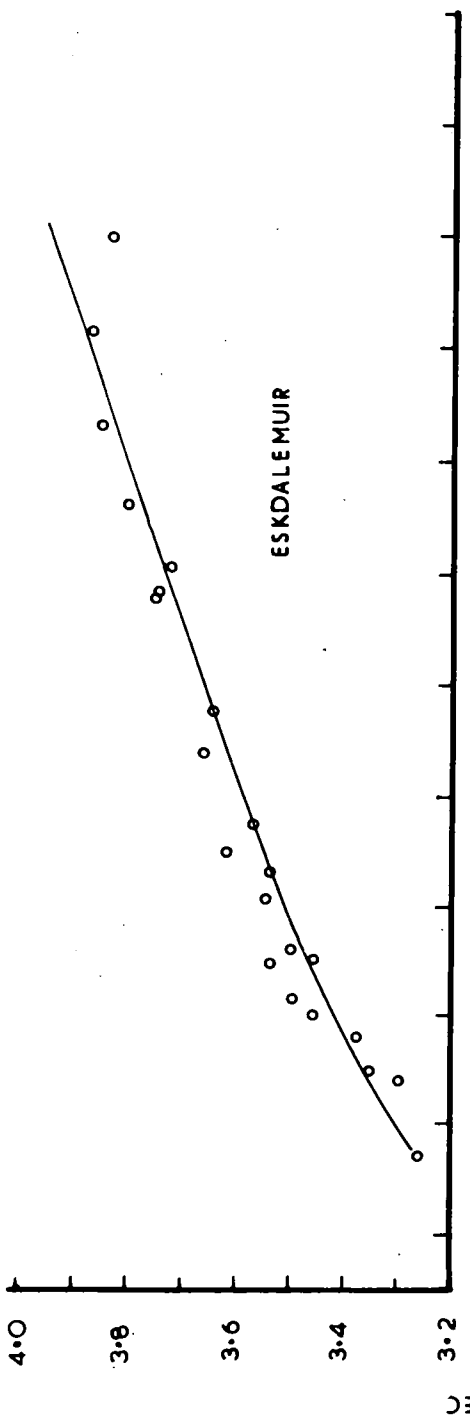


FIG 7.

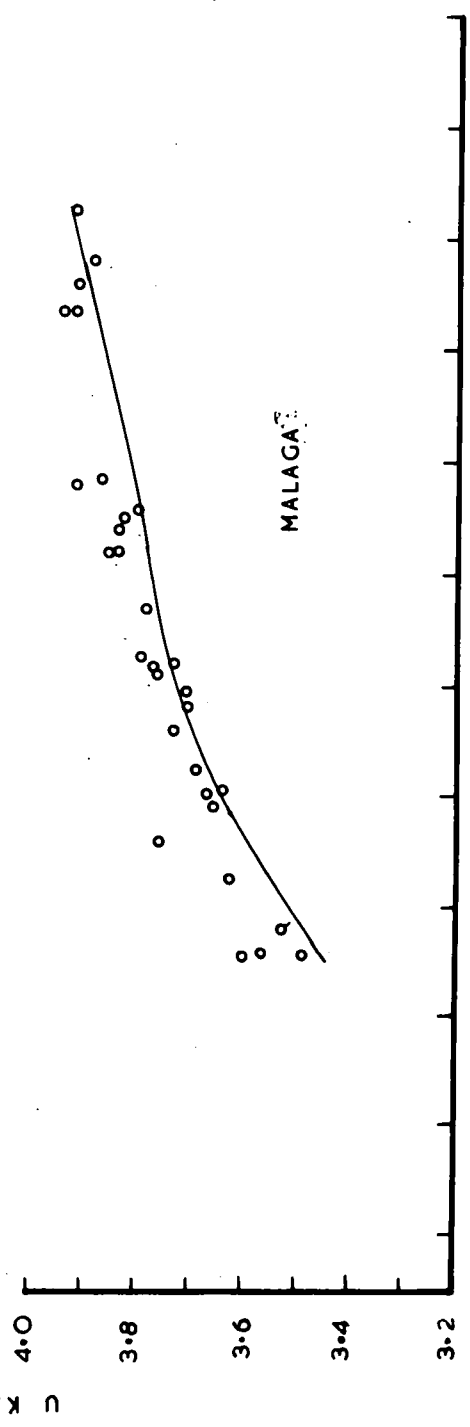


FIG 8.

14

18

22

26

30

34

T SECONDS

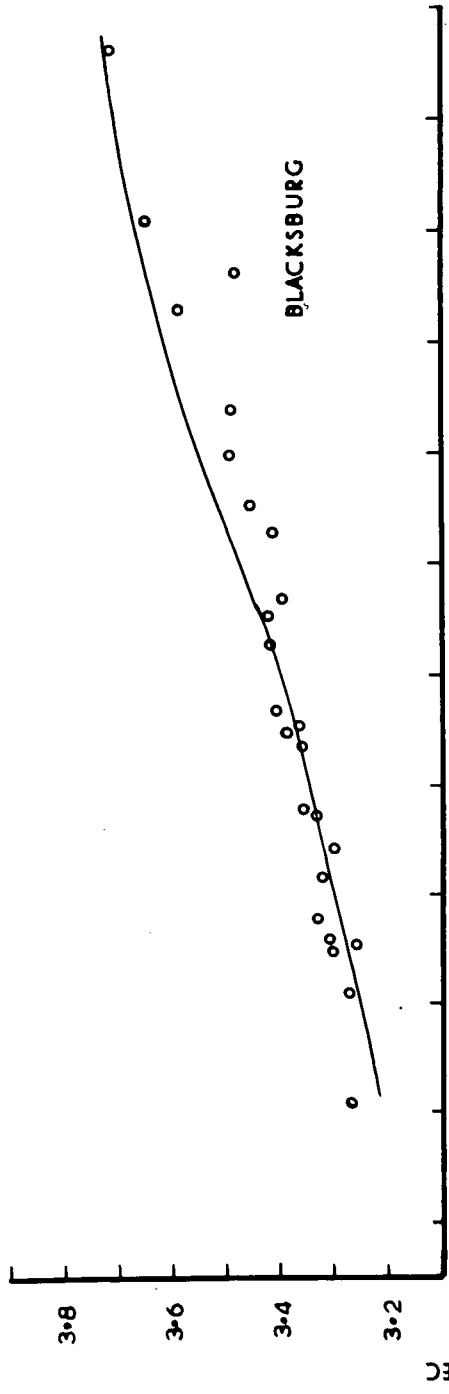


FIG 9.

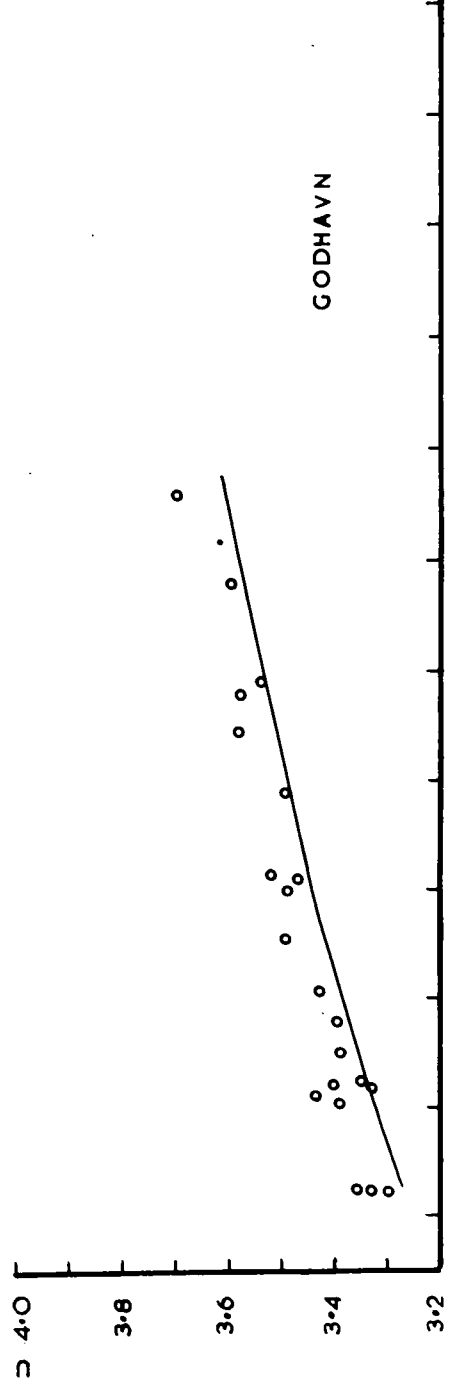


FIG 10.

group velocity is dV sec. and the travel time is T sec., then the calculated distance to a station may be in error by an amount $d\Delta$ given by

$$d\Delta = T dV \quad (7)$$

Assuming that $dV = 0.05$ km sec at each station and remembering that this is negative at Blacksburg, then we have $d\Delta = 25, 23, -65$ and 45 km for Eskdalemuir, Godhavn Blacksburg and Malagar respectively.

However, these represent the maximum errors in distance which the incorrect velocities at each station are likely to cause. Some of these errors will be absorbed in the calculated origin time which, in this instance, will be depressed, and the errors in the epicentral positions may be less than indicated.

In order to check the errors which may arise in this way, the locations were repeated, for those events which were received at four stations, using all selections of three stations for each event. The results of these locations are shown in Table 4 where the values E show the change in latitude and longitude (in minutes) and T shows the change in origin time (in seconds) relative to the locations using four stations. It may be seen that with the exception of event U5, the variation in latitude and

TABLE 4

EVENT No.	STATION OMITTED	E min N	E min W	T sec
U2	ESK	2	-8	-1
	GDH	-12	-1	2
	BLA	-8	16	-2
	MAL	4	2	1
U3	ESK	0	0	0
	GDH	0	0	0
	BLA	0	0	0
	MAL	0	0	0
U4	ESK	-3	10	2
	GDH	16	1	-3
	BLA	11	-11	3
	MAL	-6	-3	-1
U5	ESK	8	-26	5
	GDH	-43	-3	2
	BLA	-28	53	8
	MAL	14	7	-4
U6	ESK	-3	11	-2
	GDH	21	1	4
	BLA	11	-26	3
	MAL	-6	-4	2

longitude is generally less than 26 minutes which is equivalent to approximately 48 km. The variation in origin time is within ± 4 seconds.

However, these locations are made using the means of the group velocity curves for events 39 and 40 at each station and these curves are slightly different from both the event 39 and the event 40 curves. In order to check the effect of this difference, the events 39 and 40 were relocated using the average curves. The resulting epicentres were each within a radius of 15 km from the I.S.C. epicentres and the origin times were correct to within 4 seconds. Therefore the other events (U1 - U6) are probably located relative to events 39 and 40 to within 65 km of their true (relative) epicentres.

The positions of the events U1 - U6, the calculated epicentres of the reference events 39 and 40 and the I.S.C. epicentres of events 39, 40 and U2 are shown in Figure 11. It is noticeable that the calculated position of event U2 is closer to events 39 and 40 than is the epicentre given by the I.S.C. This change in epicentral position is unlikely to be due to the use in the location program of the dispersion curves from events 39 and 40, as the dispersion characteristics are unlikely to be different whether the wave path to any of the stations used here is from the I.S.C. epicentre

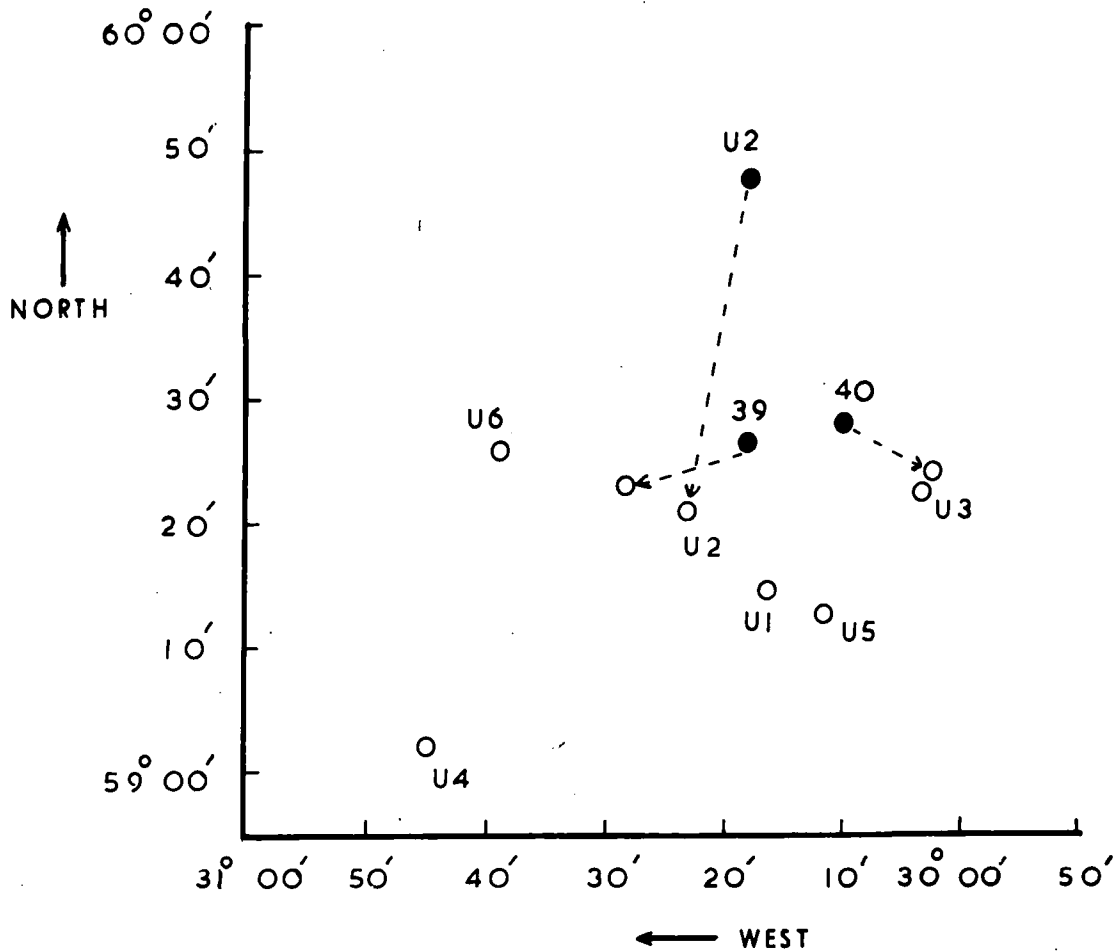


FIG II. EPICENTRES FROM SURFACE WAVE LOCATION

○ FROM SURFACE WAVES

● " I. S. C. BULLETINS

of event U2 or from the epicentres of events 39 and 40. The eight events appear to lie within an area approximately 80 km (E-W) by 55 km (N-S) on the Reykjanes Ridge. Considering their similar positions and their temporal sequence (Table 3), it seems likely that they are all part of the same foreshock sequence ending with event 40.

(1.11) General discussion

The efficacy of this location method depends on the availability of appropriate group velocity curves. For stations such as Eskdalemuir and Malaga, this requirement is easily satisfied for events occurring in the North Atlantic. However, for stations such as Godhavn and Blacksburg, the varying continental path proportions and the effects of lateral refraction, for events in the northern half of the North Atlantic, result in apparent group velocity curves which vary greatly according to the position of the event for which they are determined. It is fortuitous that the events 39 and 40 provide suitable curves for the location of the events considered here.

These difficulties can be overcome by using such stations as Akureyri and Bermuda for which one may expect the apparent group velocity curves to be almost independent of epicentral position over a large area of the North Atlantic. In the

routine location of a large number of events from different areas, the program could be altered to work with a set of stored curves for each station - each curve being appropriate for use with events occurring within a particular region. If sufficient stations are available, then those which were furthest from the event or for which the curves were not reliable, could either be omitted from the program or they could be weighted against in the calculation of the term TSSQ.

The program could be further refined to accept in digital form the peak and trough positions of the arrivals to be located. These could be converted into period and arrival time data by the use of a polynomial fitting routine followed by differentiation.

If sufficient stations are available, then the events may be located using data on the arrival times of single periods at each station. In this case the arrival times of a specified period at each station could be reported on a routine basis and may be used to support a study of small and otherwise unlocated events from areas such as the Mid-Atlantic Ridge.

CHAPTER 2

(2.1) The problem of amplitudes

While the test data were being analysed prior to the location of the Reykjanes Ridge events, it was noticed that the amplitudes of the recorded surface waves were not always proportional to the magnitudes of the events (which are determined from P-waves) reported in the bulletins; some of the events of magnitude 4.4 produced surface waves with amplitudes approaching those of events with magnitudes of 5.0. Further, having located the group of events on the Reykjanes Ridge using surface wave observations, a question arises regarding the lack of P-wave observations for these events. With the exception of one of these events (U2), which was missed by the U.S.C.G.S. and reported later by the I.S.C., no corresponding body waves were reported in the bulletins and none was seen at any of the stations used here.

In order to investigate the surface wave amplitude variations in the test data, to predict the expected P-wave amplitudes from the events which were located in the Reykjanes Ridge, and to see whether the lack of P-wave observations was anomalous, the relationship between P and Rayleigh wave amplitudes was investigated. This was done using the test data by comparing the event magnitudes as determined from the

surface wave amplitudes at the stations used in the location routine with magnitudes determined from P-waves and reported in the I.S.C. bulletins. For most of the test data, a linear relationship between the two magnitude determinations is apparent. However, for events in the Reykjanes Ridge, such a relationship does not appear if the focal parameters determined by the I.S.C. are used in the calculations. Nevertheless, a linear relationship is found if the Reykjanes Ridge events are assumed to occur at the surface. This relationship is used to predict the P-wave amplitudes of the previously unlocated events.

(2.2) The measurement of magnitude

The magnitude of an event refers to the energy released at the focus. This is determined by measuring the amplitudes of the seismic waves generated by the event and allowing for the way in which they decay with increasing distance from the source, for the effect of focal depth and for the effect of the instruments on the recorded motion. Magnitudes can be determined either from body waves (mb) or from surface waves (Ms). Magnitudes of the test data were taken from the bulletins of the I.S.C. which report mb.

(2.3) The mb magnitude scale

The mb scale uses the ratio of the ground amplitude of the recorded motion to the period in seconds (A/T). This is usually measured on the short-period vertical instrument. The relationship between A/T and the magnitude is

$$mb = \log A/T + Q \quad (8)$$

Where Q is a depth-distance factor and A is the $\frac{1}{2}$ peak to peak amplitude in microns. (Gutenberg and Richter 1956).

(2.4) The Ms magnitude scale

The surface wave magnitude determinations in this work use Bath's (1952) method. The amplitude in microns of the 20 second period vertical Rayleigh wave motion is combined with factors to correct for the effects of distance and focal depth to give the Ms Magnitude according to the formula

$$Ms = \log A + \log B + E \quad (9)$$

Where A is the $\frac{1}{2}$ peak to peak amplitude in microns, log B is Gutenberg's distance correction factor (Richter 1958) and E is a correction for the focal depth.

The values of E used in this study are given in Table 5. These are taken from a formula of the form $\exp(-z/\lambda)$ where z is the depth and λ is the wavelength, which applies to a homogeneous earth with Poisson's ratio 0.25 (Marshall 1965).

Table 5

Depth corrections to Ms.

Depth km.	Correction, E (For T = 20 sec.)
25	0.22
33	0.28
40	0.35
50	0.47
60	0.52
75	0.65
90	0.78
100	0.84

Gutenberg's log B curve only covers distances from 20 to 180 degrees whereas most of the earthquakes used here are less than 20 degrees from the observing stations. It was therefore necessary to extend the log B curve to 10 degrees.

Log B expresses the reduction in amplitude according to absorption of the wave and the effects of geometrical spreading; it can be written as (Carpenter and Thirlaway 1966)

$$\log B = \log (1/X (e^{-X/QU^T})) - \log 0.5 \quad (10)$$

Where X is the distance in kilometers, Q is the absorption coefficient, U is the group velocity in Kms/sec and T is the

period in seconds. The factor of $\log (.5)$ is added to $\log B$ because the $\frac{1}{2}$ peak to peak amplitude is measured.

It has been shown that Gutenberg's curve can be reproduced using the above equation if a Q of 400 is assumed (Carpenter and Thirlaway 1966). For this work the curve was extended using a Q of 400 and a value of 3.6 for the group velocity. ($\log B$ is insensitive to changes in the group velocity. Using 3.3 for U , which is the observed velocity at Blacksburg for the most northerly events used here (39 and 40), only changes $\log B$ by 0.01). The extended curve together with Gutenberg's values, is shown in Figure 12. In order to make the two curves compatible, a factor of 0.28, corresponding to a depth of 33 km, has been added to the extended curve.

In addition to the effects of absorption, geometrical spreading and focal depth, the dispersion characteristics of the ray path, the source function and the instrumental response also effect the amplitudes of the recorded wave. In general, one can write the amplitude of the wave, $A(T)$, as a function of period, T , as

$$A(T) = I(T) B(T) E(T) S(T) T(T) \quad (11)$$

Where B and E are the distance and depth terms accounted for in the calculation of M_s , $I(T)$ is an instrument term, $S(T)$ is

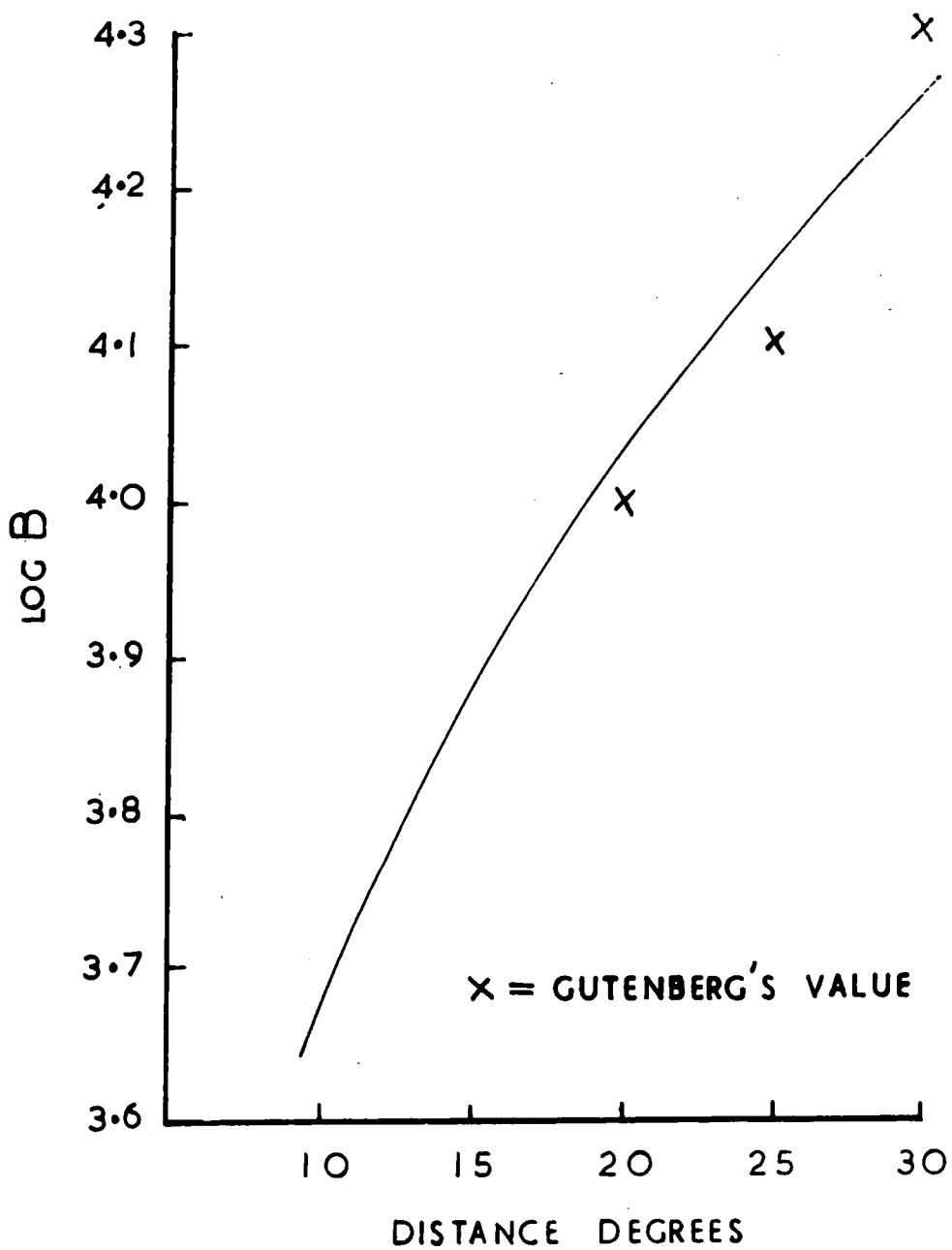


FIG 12. $\log B$ FOR FOCAL DEPTH = 33 KM.

a term due to the source function and $T(T)$ is a term due to the effects of dispersion.

The term $T(T)$ may be expressed as (Carpenter and Thirlaway 1966)

$$T(T) = U T^{-5/2} (dU/dT)^{-1/2} \quad (12)$$

This term describes the reduction in the wave amplitude as the wave is spatially spread out by dispersion. Thus $T(T)$, which is a function of the slope of the group velocity curve, will depend on the path over which the wave has travelled, and it will, for example, be different for continental and oceanic paths.

(2.5) The relationship between m_b and M_s

The variations in surface wave and body wave amplitudes due to varying crust and mantle structures which are not taken into account in the calculation of m_b and M_s , make it impossible to find a relationship between the two which has world-wide applicability. However, for the purpose of comparing earthquakes occurring in the same region, using measurements made at the same stations, any linear relationship between m_b and M_s may be assumed with equal validity. For this work, the following equation was used (Davies, 1969)

[Faint, illegible text]

$$m_b = 2.55 + 0.52 M_s \quad (13)$$

It is unlikely that any such linear relationship will hold for a wide range of magnitudes. Aki (1967) has shown that the frequency spectrum of the source is dependent on the size of the event, so that the longer periods are increased in amplitude relative to the short periods as the magnitude of the event increases. Thus, if an m_b - M_s relationship, which holds for large magnitudes, is used with small events to predict m_b from M_s measurements, then m_b may be underestimated.

(2.6) The results of the magnitude measurements

The data used in the magnitude determinations consisted of most of the events listed in Table 2 and also the event U2 for which m_b values were published in the I.S.C. bulletin. The events numbered 27, 37 and 49 were not used as only photocopies of the arrivals were available and these did not include the part of the record which gives the instrument magnification.

Measurements of the surface wave magnitude (M_s) for arrivals with a period of 20 seconds, were made according to the theory described in the previous section. The amplitudes were measured from the films of the records. The instrument magnification quoted in the records was used directly without

making corrections according to the period. (The response curves show that the magnification quoted on the records is almost the same as that at 20 seconds).

The measured values of M_s were then converted into body-wave magnitudes using the formula 13 ($m_b = 2.55 + 0.52 M_s$) these are referred to as m_b/s . The magnitudes were corrected for the effects of dispersion described by the term $T(T)$ in equation 11. The corrections were applied so that magnitudes M_s are normalised to correspond to arrivals which have travelled along a path with the same dispersion characteristics as those measured at Malagar. Where the group velocity curve for a particular station was not available for some event, then the correction was estimated from the curve for a similar event.

Where the Malagar records were not available, those from the U.S.C.G.S. station at Toledo were used instead. It was assumed that the dispersion would be the same as at Malagar. It was found that no corrections were necessary for measurements at Eskdalemuir, or for measurements at Blacksburg and Godhavn for the more southerly events.

The m_b/s values are shown in Table 6 where they compared with the m_b magnitudes determined by the I.S.C. Focal depths and epicentral positions were also taken from I.S.C. Bulletins (Table 2). Where m_b/s values are missing for certain stations

TABLE 6

EVENT No.	DEPTH Km	DEPTH Term E	STATION	DISTANCE deg.	LOG B	LOG ₁₀ amp.	T(T)	Ms	mb/s	MEAN mb/s	I.S.C. mb
2	64	0.26	ESK	16.2	3.92	-.05	0.0	4.12	4.69	4.69	4.8
			GDH	20.6	4.06	-.53	-.35	3.79	4.34	4.34	
			BLA	38.0	4.41	-.04	-.2	4.63	4.95	4.95	
3	25	-.06	MAL	23.7	4.13	-.08	0.0	4.31	4.78	4.78	5.0
			ESK	16.2	3.92	0.01	0.0	3.87	4.56	4.56	
			BLA	38.0	4.41	-.09	-.2	4.26	4.66	4.66	
4	19	-.12	MAL	23.8	4.13	0.08	0.0	4.15	4.70	4.70	5.0
			ESK	16.2	3.92	-.06	0.0	3.74	4.50	4.50	
5	28	-.04	MAL	23.6	4.13	-.05	0.0	3.96	4.61	4.61	5.2
			ESK	16.2	3.92	0.25	0.0	4.13	4.70	4.70	
9	50	0.19	MAL	23.8	4.13	0.32	0.0	4.41	4.84	4.84	5.5
			ESK	44.8	4.51	0.12	0.0	4.82	5.06	5.06	
			GDH	46.6	4.54	-.28	0.0	4.45	4.87	4.87	
10	24	-.07	BLA	33.5	4.32	0.51	0.0	5.02	5.16	5.16	5.5
			ESK	20.9	4.07	0.89	0.0	4.89	5.09	5.09	
			GDH	27.3	4.21	0.81	0.0	4.95	5.13	5.13	
			BLA	37.4	4.40	0.60	0.0	4.93	5.12	5.12	
20	33	0.00	TOL	20.7	4.06	0.64	0.0	4.63	4.96	4.96	5.2
			ESK	39.9	3.39	0.37	0.0	4.76	5.03	5.03	
			GDH	39.3	4.42	-.23	0.0	4.19	4.73	4.73	
24	33	0.00	BLA	32.4	4.30	-.71	0.0	5.01	5.15	5.15	5.6
			GDH	35.5	4.36	1.82	0.0	6.18	5.76	5.76	
			MAL	25.5	4.17	1.44	0.0	5.61	5.47	5.47	

TABLE 6 (continued)

EVENT No.	DEPTH Km	DEPTH Term E	STATION	DISTANCE deg.	LOG B	LOG ₁₀ T(T)	Ms	mb/s	MEAN mb/s	I.S.C. mb
33	33	0.00	ESK	36.4	4.37	0.0	4.32	4.80	4.76	5.0
			GDH	39.0	4.42	0.0	4.19	4.73		
36	62	0.26	MAL	31.2	4.28	0.0	4.23	4.75		
39	30	-.02	MAL	20.3	4.01	0.0	3.96	4.61		4.8
			ESK	15.1	3.88	0.0	3.86	4.55	4.57	4.5
			GDH	14.0	3.82	0.0	4.12	4.60		
			BLA	38.8	4.42	-.18	3.97	4.51		
			MAL	28.2	4.23	0.0	3.98	4.61		
40	33	0.00	ESK	15.1	3.88	0.0	4.23	4.75	4.7	4.6
			GDH	14.0	3.82	0.0	4.33	4.70		
			BLA	38.9	4.42	-.18	4.10	4.58		
			MAL	28.2	4.23	0.0	4.25	4.76		
41	44	0.13	ESK	23.2	4.12	0.0	3.59	4.42	4.59	4.8
			BLA	42.0	4.47	0.0	3.86	4.56		
			TOL	17.6	3.97	0.0	4.31	4.79		
42	70	0.32	ESK	15.4	3.90	0.0	3.99	4.62		4.1
43	25	-.06	ESK	16.2	3.92	0.0	3.50	4.37		4.1
44	47	0.16	ESK	16.1	3.91	0.0	4.02	4.64		4.3
45	56	0.22	ESK	15.6	3.90	0.0	3.99	4.62		4.4
U2	69	.31	ESK	15.1	3.88	0.0	4.54	4.91	4.87	4.5
			GDH	14.0	3.82	0.0	4.51	4.80		
			BLA	38.8	4.42	-.18	4.66	4.87		
			MAL	28.2	4.23	0.0	4.49	4.89		

and events, this is either because there was no 20 second period on the record or because the station record was not available. It may be seen that the events fall into two groups according to whether mb/s is greater or less than mb ; these groups are referred to as group A and group B respectively. This is shown more clearly in Figure 13 where the diagonal line corresponds to $mb = mb/s$.

It may be seen that a linear relationship between mb and mb/s is apparent for the group B events, i.e. in general mb increases with mb/s . However, for the group A events, which with the exception of event 24 all occur in the Reykjanes Ridge in the vicinity of 59 deg N, 30 deg W, there is no obvious relationship between the two magnitudes and they appear to form a separate group. Let us consider the errors in these measurements so that we may decide whether this apparent distinction between the two groups of events is real.

In order to minimise the effects of path differences, let us consider the magnitude errors in the group A events in the Reykjanes Ridge and the nearest group B events (group B') which occur South of the Reykjanes Ridge at approximately 52 deg N 30 deg W (i.e. events 2, 3, 4 and 5 (Fig. 1)).

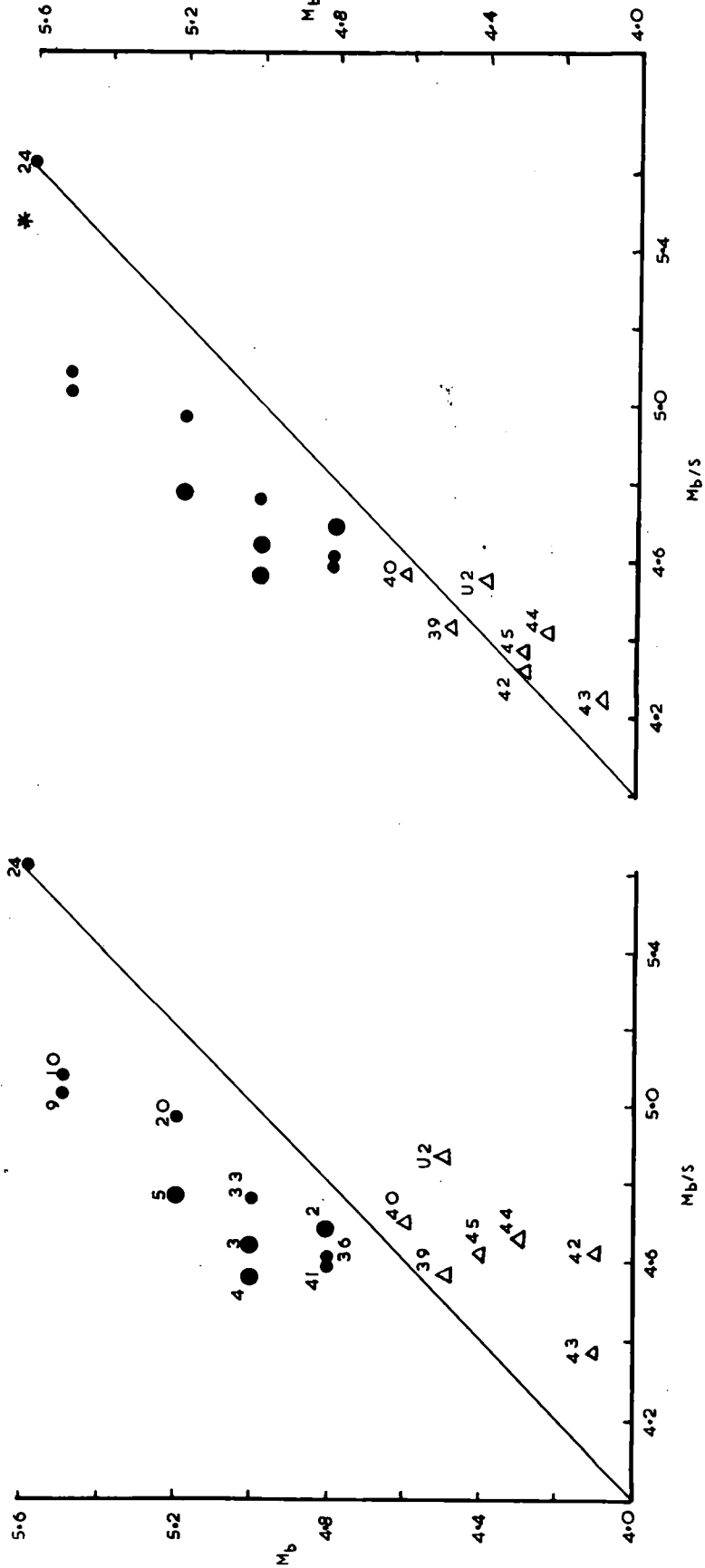


FIG 13. M_b VERSUS M_b/S USING I.S.C. FOCAL DEPTHS FOR

ALL EVENTS. ● = GROUP A', △ = GROUP A.

FIG 14. M_b VERSUS M_b/S ASSUMING ZERO FOCAL DEPTHS FOR

GROUP A EVENTS & OTHERS AS IN FIG 13.

(2.7) Errors in the magnitude measurements

The errors in these measurements, both of m_b and M_s , may be divided into two types: internal consistency errors which result from a scatter in the data used in the calculations, and errors which result from the use of false premises.

The internal consistency errors for the m_b values may be estimated from the variation in the individual station m_b values for each event. For most of the events this is of the order of 0.1 units (standard deviation) though this may be higher for events 42 to 45 and U2 where only 3 to 5 individual station magnitudes have been used to determine the event size. For the m_b/s values the consistency errors are more difficult to estimate as a maximum of four stations are used for any event. However, with the exception of events 42 to 45, for which records were only available at Eskdalemuir, an indication of the errors may be gained from the range of m_b/s values for each event. Apart from event 2, this is less than 0.15 units for the group B' events and less than 0.05 units for the group A events. For event 2 the range is 0.3 units. It is clear that these errors alone are unlikely to have caused the apparent difference between the two groups of events.

Let us consider the errors of the second type. Both in the calculation of m_b and of m_b/s we have corrected for dis-

tance according to functions (i.e. Q and $\log B$) which may not apply to the regions of interest here. However, in both calculations, the mean distance from the source to the stations is nearly the same for events in each group. Therefore the use of incorrect distance correction terms is unlikely to introduce any apparent distinction between the mb:mb/s relationship for the two groups.

Focal depth is perhaps one of the most difficult parameters to assign to an earthquake and focal depth estimates may be very inaccurate. Some of the events used here (e.g. 24, 33, 40 and 20) are assigned depths of 33 kms which is an assumed rather than a calculated depth. If the mb and the mb/s calculations are repeated for the group A events assuming that they are at the surface while the depths of the group B' events are taken as given in the bulletins, then the distinction between the two groups disappears; the scatter in the group A data is reduced and an almost linear relationship appears for all the data. This is shown in Figure 14.

Errors in the mb and mb/s determinations may also be introduced by an azimuthal dependency of the radiation pattern. Such a dependency has been demonstrated for both P-waves and Rayleigh waves for different types of source mechanism (Ben-Menahem 1961, Haskell 1963, Wu and Ben-Menahem 1965, Gupta 1966 and 1967, Wu 1968).

Both groups of events are situated on rift zones; group A events are on the Reykjanes Ridge on which there are no signs of fracture zones in the region of interest (Heirtzler et al 1966, Godby et al 1968) and the group B' events are clear of the 53 degree fracture zone defined by Johnson (1967). From the work of Sykes (1967) it is clear that rift zone earthquakes are all likely to have similar fault plane solutions - i.e. normal faulting. Thus the P-wave radiation patterns should be similar from events in both groups, with maximum energy radiated perpendicular to the Ridge axis. However, the Reykjanes Ridge is rotated clockwise relative to the Ridge further South so it is possible that the radiation patterns from the two groups interact differently with the stations used in the magnitude determinations reported in the bulletins. Most of these stations are in America and Canada so the direction of maximum P-wave amplitude for the group A events could pass to the North of these stations resulting in an underestimate of mb. An examination of the variations with azimuth and distance of the individual station mb determinations showed no difference between the two groups, though the data are sparse and do not preclude the possibility of such an effect. (The stations at Malaga and Godhavn were of little use here as they received emergent arrivals from events in both groups).

Haskell (1963) has shown that, for normal faulting, Rayleigh waves are radiated in a two-lobed pattern. This should be orientated azimuthally in the same way as the P-wave lobes, though the simple pattern may be made more complex by the effect of the moving source and by variations in focal depth (Ben-Menaham 1961, 1964). Thus it is possible that the surface wave amplitudes may also vary according to the position of the recording stations. Additional variations may also be produced by lateral refraction at the continental boundary (Savarensky et al 1968). However the mb/s determinations at each station show no indication that these effects are the cause of the distinction between the two groups.

In addition to the effects of the radiation pattern, the source function may differ for events in the two groups. It was mentioned previously (section 2.5) that Aki (1967) has investigated the effect of earthquake size on the generated amplitude spectrum. The effect described by Aki should lead to a larger mb:mb/s ratio for the group A events than for the group B' events - as the former have larger mb magnitudes - thus rather than cause the difference between the two groups this would tend to reduce it. However the assumptions made in Aki's investigation (i.e. a constant stress drop and rupture velocity for all earthquakes) may not be valid, so the

source function may depend on the geological environment, the focal depth and the orientation of the fault plane.

Further differences in the $m_b:m_b/s$ ratio for the two groups may be caused by varying attenuation beneath the Ridge. This would most likely result from a varying proportion or extent of partially melted material in the mantle beneath the Ridge. Although an increase in attenuation will reduce both m_b and M_s , the effect on the $m_b:m_b/s$ ratio is not clear; while P-waves may travel through a larger section of high-attenuation material, Rayleigh waves may be more affected because they involve shear motion. However, the group velocities of 20 second period Rayleigh waves appear to be independent of the percentage of Ridge path travelled by the wave (Ossing 1964). It therefore seems unlikely that the surface wave amplitudes will be changed by varying attenuation beneath the Ridge. It is also difficult to reconcile the idea of excessive P-wave absorption beneath the Reykjanes Ridge with the zero station correction for m_b magnitude obtained for Akureyi by Carpenter and Marshall (1967). It is therefore unlikely that attenuation alone is responsible for the differences between the two groups.

Thus apart from incorrect focal depths, there are several mechanisms which may combine to produce a bias in the $m_b:m_b/s$ determinations for events in either group. However it is

reasonable to assume that the main source of error is in the focal depth though a bias in the curve may still exist if the depth corrections, E and Q, are incorrect. The scatter in the data points may be due to any of the causes outlined above including errors in the depths of the group B events.

It may be possible to detect differences in focal depth by Fourier analysing the surface wave arrivals. This was attempted using arrivals from the two groups (A and B') recorded at Eskdalemuir. While the Reykjanes Ridge events did contain proportionally more high-frequency energy at approximately 12 seconds period, which is consistent with a shallow focus, the amplitude spectra were far from smooth and they were difficult to interpret. Particularly for the high-frequency arrivals, the effects of lateral refraction may mask the differences in amplitude spectra of arrivals from each group due to varying focal depth. To be successful, such an analysis must be carried out at some station to which the arrivals from each group travel over substantially identical paths, for example at Akureyri in Iceland.

It is noticeable that event 24 does not fit in with the general trend of the data shown in Figure 14. The focal mechanism of this particular event was investigated by Sykes (1967) who found that it corresponded to strike-slip faulting and was therefore consistent with the transform fault hypo-

thesis. Thus this event, unlike any of the others, definitely lies on a fracture zone. This implies that the radiation patterns of both the P-waves and the surface waves for this event may be different from those of the other events examined here.

Surface wave magnitudes for this event were calculated only at Godhavn and Malaga; as the traces at the other stations were too faint to be read. There is a large discrepancy between the mb/s determinations at these two stations; mb/s is larger at Godhavn by 0.29 units (Table 6) though the arrival at Malaga is very complex and the amplitude envelope is far from smooth. Comparison with the Rayleigh wave radiation patterns derived by Haskell (1963) for a strike-slip fault with a dip of 85 degrees (as determined by Sykes) shows that both the Malaga and the Godhavn stations lie between the lobes of maximum energy radiation. The radiation pattern will be modified by the effects of a moving source as described by Ben-Menahem (1961). If the fault is propagated in an East-to-West direction then this may cause the reduction in amplitude at Malaga relative to that at Godhavn which is observed. However this does not explain the apparently high value of mb/s magnitude for this event which would be more fitting if the two stations were on the maxima of the radiation lobes.

The reported depth of this event is 33 kms. If it is taken at the surface (as was done by Sykes) and the mb and mb/s values are recalculated, then its position on Figure 14 is changed to that indicated by the asterisk. This reduces, but does not remove, the apparent discrepancy between the magnitudes of this event and the extrapolated trend of the figure. The high mb/s value may be due to the effect described by Aki (1967) where the efficiency of the generation of long-period waves is disproportionately increased with an increase in magnitude. However, there are no other events on the mb:mb/s curve with which this event may be compared. It is not known whether this event is anomalous, perhaps because it occurs on a fracture zone, or whether it defines a trend in the curve which other events of high magnitude may confirm.

(2.8) mb values for the previously unlocated events

Assuming that the interpretation of shallow depth for the Reykjanes Ridge events is correct, we may use the relationship implied in Figure 14 to calculate the approximate mb magnitudes for the other events in the Reykjanes Ridge (events U1 and U3-U6) from which P-waves were not recorded.

The measurements of Ms and mb/s for these events are

listed in Table 7. It is assumed that they all occur at the surface. By comparing their mb/s values with the data shown in Figure 14, it may be seen that their mb values vary between 4.2 and 4.4 approximately. We may also put an approximate upper limit on the mb magnitude by assuming that the minimum P-wave amplitude visible at the stations used here is equal to the noise level. This leads to $mb(\max) = 4.3$ if the events occur at the surface.

The probability that an event will be detected by P-wave observations depends on the area in which it occurs and on the relative positions of the recording stations. For events in the Mid-Atlantic Ridge, the detection probability is less than 1 for events with mb magnitudes less than 4.5 and it falls off rapidly as the magnitude lowers. This is clearly seen in the cumulative frequency versus magnitude plots obtained for the Ridge by Francis (1968) where the points roll off a straight line for magnitudes less than 4.6. It appears that the detection probability changes from 0.6 for events with $mb = 4.4$ to 0.4 for events with $mb = 4.2$. Thus the fact that these events were not reported in the bulletins is not significant, though it does seem that the detection threshold is lowered for shallow events in the area if surface wave observations are used.

TABLE 7

EVENT No.	STATION	DISTANCE	LOG B	LOG	T(T)	Ms	MEAN	MEAN
		Deg.	amp			Ms	Ms	mb/s
U1	ESK	16.2	3.88	-.30	0.0	3.30	3.18	4.20
	GDH	14.0	3.82	-.23	-.18	3.13		
	MAL	23.6	4.23	-.83	0.0	3.12		
U3	ESK	16.2	3.88	-.45	0.0	3.15	3.10	4.16
	GDH	14.0	3.82	-.45	-.18	2.91		
	BLA	39.0	4.42	-.74	-.20	3.20		
U4	MAL	23.6	4.23	-.83	0.0	3.12		
	ESK	16.2	3.88	-.06	0.0	3.54	3.49	4.37
	GDH	14.0	3.82	-.15	-.18	3.24		
U5	BLA	39.0	4.42	-.36	-.20	3.58		
	MAL	23.6	4.23	-.35	0.0	3.60		
	ESK	16.2	3.88	-.83	0.0	2.77	2.94	4.08
U6	GDH	14.0	3.82	-.33	-.18	3.03		
	BLA	39.0	4.42	-1.13	-.20	2.81		
	MAL	23.6	4.23	-.83	0.0	3.12		
	ESK	16.2	3.88	-.53	0.0	3.07	3.17	4.20
	GDH	14.0	3.82	-.15	-.18	3.21		
	BLA	39.0	4.42	-.83	-.20	3.11		
	MAL	23.6	4.23	-.83	0.0	3.12		

N.B. Details of event U2 (Mean mb/s = 4.87) are given in Table 6.

Conclusions

It has been shown that Rayleigh wave arrivals can be used to locate small events which are not detectable using normal P-wave location routines. Using Rayleigh wave observations, six small events have been located on the Reykjanes Ridge. They are associated with two larger events which were reported in the U.S.C.G.S. bulletins. The locations, which were made relative to the two larger events using observations at a maximum of four stations, are accurate to within 65 km. This accuracy could be improved by using more stations.

The large Rayleigh wave amplitudes from the Reykjanes Ridge events appear to be mainly due to their shallow foci. On the assumption that they occur at the surface, the mb magnitudes of the previously unlocated events have been calculated and they appear to range from 4.2 to 4.4. It is suggested that they were not reported in the bulletins because of the low detection probability, using P-wave techniques, for small earthquakes occurring in the mid-Atlantic. The fact that the detection probability is increased for shallow events if surface wave observations are used, provides an explanation for the appearance of surface wave trains from unlocated sources on the records of seismic stations around the Atlantic.

REFERENCES

- Aki, K. 1967 Scaling law of seismic spectrum, J. Geophys. Res., 72, 1217-1231.
- Ben-Menahem, A. 1961 Radiation of seismic surface waves from finite moving sources, Bull. seism. Soc. Am., 51, 401-435.
- _____ and Harkrider, D. G. 1964 Radiation patterns of seismic surface waves from buried dipolar point sources in a flat, stratified earth, J. Geophys. Res., 69, 2605-2620.
- Ben-Menahem, A. et. al. 1965 A procedure for source studies from spectrums of long period body waves, Bull. seism. Soc. Am., 55, 211-225.
- Brune, J. N. et. al. 1960 A simplified method for the analysis and synthesis of dispersed wave trains, J. Geophys. Res., 65, 287-304.
- Bullen, K. E. 1963 Introduction to the theory of seismology, Cambridge University Press.
- Carpenter, E. W. and Thirlaway, H. I. S. 1966 Seismic signal anomalies, travel times, amplitudes and pulse shapes, Vesiac Study Conference, Willow Run Laboratories, report no., 4410-99-X.
- Carpenter, E. W. et. al. 1967 The amplitude-distance curve for short period teleseismic P-waves, Geophys. J. R. astr. Soc., 13, 61-70.

- Crampin, S. 1967 Coupled Rayleigh-Love second modes, Geophys. J. R. astr. Soc., 12, 229-235.
- Davies, D. 1969 Seismic methods for monitoring underground explosions, Stockholm International Peace Research Institute.
- Evernden, J. F. 1954 The direction of approach of Rayleigh waves and related problems (part II) Bull. seism. Soc. Am., 44, 159-184.
- Ewing, W. M. et. al. 1957 Elastic waves in layered media, McGraw-Hill Book Company, New York.
- Francis, T. J. G. 1968 The detailed seismicity of mid-ocean ridges, Earth & Planet. Sci. Lett. (Neth.) 4, 39-46.
- Godby, et. al. 1968 Aeromagnetic profiles across the Reykjanes Ridge south-west of Iceland, J. Geophys. Res., 73, 7637-7649.
- Gupta, I. N. 1966 Use of reciprocity theorem for obtaining Rayleigh wave radiation patterns, Bull. seism. Soc. Am., 56, 925-936.
- _____ 1967 Body wave radiation patterns from elementary sources within a half space, Bull. seism. Soc. Am., 57, 657-674.
- Gutenberg, B. and Richter, C. F. 1956 Magnitude and energy of earthquakes, Annali Geofis., 9, 1-15.

- Haskell, N. A. 1963 Radiation pattern of Rayleigh waves from a fault of arbitrary dip and direction of motion in a homogeneous medium, Bull. seism. Soc. Am., 53, 619-642.
- Heirtzler, J. R. et. al. 1966 Magnetic anomalies over the Reykjanes Ridge, Deep Sea Research, 13, 427-445.
- Jeffreys, H. 1962 The Earth, Cambridge University Press.
- Johnson, G. L. 1967 North Atlantic fracture zones near 53° , Earth & Planet. Sci. Lett. (Neth.) 2, 445-448.
- Knopoff, L. et. al. 1966 Structure of the crust and upper mantle in the Alps from the phase velocities of Rayleigh waves, Bull. Seism. Soc. Am., 56, 1009-1044.
- Lamb, H. 1904 On the propagation of tremors over the surface of an elastic solid, Phil. Trans. R. Soc., A, 203, 1-42.
- Marshall, P. D. 1965 A note on magnitude scales currently in use, A.W.R.E. Blacknest, note CPA/PA4/AG.50.
- Ossing, H. A. 1964 Dispersion of Rayleigh waves originating in the Mid-Atlantic Ridge, Bull. seism. Soc. Am., 54, 1137-1196.
- Pilant, W. L. and Knopoff, L. 1964 Observations of multiple seismic events, Bull. seism. Soc. Am., 54, 19-39.

- Richter, C. F. 1958 Elementary seismology, Freeman, San Francisco.
- Savarensky, E. F. et. al. 1968 On the lateral refraction of Rayleigh waves and microseisms in the North Atlantic, Geophys. J. R. astr. Soc., 15, 529-544.
- Sykes, L. R. 1967 Mechanisms of earthquakes and nature of faulting on the Mid-Ocean Ridges, J. Geophys. Res., 72, 2131-2153.
- Wu, F. T. and Ben-Menahem, A. 1965 Surface wave radiation pattern and source mechanism of the Sept. 1st. 1962 Iran earthquake, J. Geophys. Res., 70, 3943-3949.
- Wu, F. T. 1968 Parkfield earthquake of June 28, 1966: Magnitude and source mechanism, Bull. seism. Soc. Am., 58, 689-709.

APPENDIX 1Program for epicentre location using Rayleigh waves

The data cards for this program are read in to the computer as follows:

Block 1 1 card, FORMAT (I10), variable is NGOES.

This refers to the number of events to be located.

Block 2 1 card, FORMAT (72H).

This is for hollerith information which is printed out above the location results for the relevant event.

Block 3 1 card, FORMAT (6F10.2), variables are ILATS, ILONGS, RLATS, RLONGS, ISTEP, FNIT.

ILATS and ILONGS are the latitude and longitude (in degrees) of the southeast corner of the search area.

RLATS and RLONGS are the latitude and longitude (in degrees) of the northwest corner of the search area.

(The sign convention used in this program is that north and west are positive, and south and east are negative).

ISTEP (in degrees) is the spacing between trial epicentres in the first iteration. On the nth iteration, the spacing is $ISTEP/4n$ degrees. FNIT is the number of iterations.

Block 4 1 card, FORMAT (I10), variable N.

N is the number of stations used in the location.

Block 5 N cards, FORMAT (4F10.2), variables THETAD(S),
THETAM(S), PHID(S), PHIM(S).

These are the co-ordinates of latitude and longitude,
in degrees and minutes, of the locating station S, where
S = 1 to N.

Block 6a 1 card, FORMAT (I10), variable MP(S).

MP(S) is the number of observations at the Sth station.

Block 6b MP(S) cards, FORMAT (3F10.3), variables T(S,P),
V(S,P), Q(S,P).

T(S,P) is the arrival time in seconds relative to some
reference time (which is common for all observations on
the same event) of the Pth observation at the Sth station.
V(S,P) and Q(S,P) are the assumed group velocity, in
km/sec, and the measured period in seconds, of the Pth
observation at the Sth station, where P = 1 to MP(S)
and S = 1 to N.

Q(S,P) is not used in the location but it is printed out
together with the calculated group velocity as a conveni-
ence; it may be omitted without alteration to the program.

Blocks 6a and 6b are repeated for each of the stations used
in the location. Up to NGOES events may be located by repeat-
ing blocks 2 to 6 inclusive.

A listing of the program and examples of the output are
given on the pages following.


```

C
C
C
C
    RLAT = BLAT+STEP(NIT-1)
    RLONG= BLONG+STEP(NIT-1)
    STEP(NIT)=STEP(NIT-1)/4
200  LAT=ILAT-STEP(NIT)
    LONG=ILONG-STEP(NIT)
204  LONG=LONG +STEP(NIT)
    IF (LONG.GT.RLONG) GO TO 300
203  LAT=LAT+STEP(NIT)
    IF(LAT.LE.RLAT) GO TO 202
    LAT=ILAT-STEP(NIT)
    GO TO 204
202  CONTINUE
C  CALCULATES THE TERM TSSQ FOR THE TRIAL EPICENTRE.
    DO 4 S=1,N
    THETA=THETAD(S)*60+THETAM(S)
    PHI=PHID(S)*60+PHIM(S)
    CALL DELT(DIST,THETA,PHI,LAT,LONG)
    L=MP(S)
    OT=0
    DO 5 P=1,L
    OT=OT+T(S,P)-DIST/V(S,P)
    TBAR(S)=OT/L
5  CONTINUE
4  CONTINUE
    TOT=0
    DO 6 S=1,N
    TOT=TOT+TBAR(S)
6  TSSQ=0
    DO 7 S=1,N
    ETO=TOT/N
    TSSQ=TSSQ+(ETO-TBAR(S))**2
7  CONTINUE
    IF(TSSQ.LT.TSSQB) GO TO 10
    GO TO 203
C  STORES THE COORDINATES OF THE TRIAL EPICENTRE IF IT GIVES A LOWER
C  VALUE OF TSSQ THAN THE PREVIOUS POSITIONS.
10  TSSQB=TSSQ
    BLAT=LAT
    BLONG=LONG
    LATD=BLAT/60
    LATM=BLAT-LATD*60
    LONGD=BLONG/60
    LONGM=BLONG-LONGD*60
    GO TO 203
C  PRINTS OUT THE FINAL EPICENTRAL DETERMINATION,THE ESTIMATED
C  ORIGIN TIME AND THE ASSOCIATED VALUE OF TSSQ.
550 CONTINUE
552 WRITE(6,552)LATD,LATM, LONGD, LONGM, TSSQB, ETO
    FORMAT(6X, I6, 1X, F5.1, I6, 2X, F5.1, 1X, F6.1, 1X, F6.1)
    WRITE(6,444)
C
C
C
C

```

```
C
C
C
C
444  FORMAT(/46H          STAT.NO. A.TIME  V.USED  V.CALC  T.SEC)
C      CALCULATES THE GROUP VELOCITIES OF THE ARRIVALS AT EACH
C      STATION USING THE FINAL EPICENTRAL POSITION AND ORIGIN TIME.
      DO 222 S=1,N
      THETA=THETAD(S)*60+PHIM(S)
      PHI=PHID(S)*60+PHIM(S)
      CALL DELT(DIST,THETA,PHI,LAT,LONG)
      L=MP(S)
C      PRINTS OUT FOR EACH STATION,THE ARRIVAL TIME OF EACH PART OF THE
C      WAVETRAIN,THE GROUP VELOCITIES WHICH WERE ASSUMED IN THE LOCATION
C      THE CALCULATED GROUP VELOCITIES AND THE PERIOD OF EACH ARRIVAL.
      DO 333 P=1,L
      VC(S,P)=DIST/(T(S,P)-ETO)
      WRITE(6,445)S,T(S,P),V(S,P),VC(S,P),Q(S,P)
445  FORMAT(10X,I2,4X,F6.1,5X,F4.2,3X,F4.2,3X,F4.1)
333  CONTINUE
222  CONTINUE
      IF(GOES.LT.NGOES) GO TO 700
      END
```

SUBROUTINE DELT(DIST,SMINA,SMINB,EMINA,EMINB)

THIS SUBROUTINE CALCULATES THE DISTANCE IN KM BETWEEN TWO POINTS WITH COORDINATES SDEGA(DEGREES),SMINA(MINUTES) AND SSECA(SECONDS)

REFERRING TO LATITUDE NORTH,AND SDEGB(DEGREES),SMINB(MINUTES) SSECB(SECONDS) REFERRING TO LONGITUDE WEST.THE SECOND POINT IS DESCRIBED IN A SIMILAR MANNER WITH EDEGA,EMINA ETC. THE COORDINATES NORTH AND WEST ARE POSITIVE.

FOR THE LOCATION PROGRAM,THE COORDINATES OF THE TWO POINTS ARE GIVEN IN MINUTES SO THE OTHER VARIABLES ARE PUT =0 IN THE FIRST EIGHT CARDS OF THE PROGRAM.THESE MAY BE REMOVED FOR GENERAL USE.

SDEGA=0

SDEGB=0

EDEGA=0

EDEGB=0

SSECA=0

SSECB=0

ESECA=0

ESECB=0

PI=4.*ATAN(1.)

RTOD=180./PI

RADIUS=6371.024

SLAT=(ABS(SDEGA)+ABS(SMINA)/60.+ABS(SSECA)/3600.)/RTOD

IF(SDEGA)4,5,5

5 IF(SMINA)4,6,6

6 IF(SSECA)4,51,51

4 SLAT=-SLAT

51 SLATA=ATAN(0.9932/7*TAN(SLAT))

CONVERTS TO GEOCENTRIC LATITUDE

SLONG=(ABS(SDEGB)+ABS(SMINB)/60.+ABS(SSECB)/3600.)/RTOD

IF(SDEGB)7,8,8

8 IF(SMINB)7,9,9

9 IF(SSECB)7,10,10

7 SLONGA=2.*PI-ABS(SLONG)

GO TO 41

10 SLONGA=SLONG

41 SC=SIN(SLATA)

SK=COS(SLATA)

SD=SIN(SLONGA)

SE=COS(SLONGA)

SA=SK*SE

SB=SK*SD

SG=SC*SE

SH=SC*SD

SE=-SE

SK=-SK

SLAT=SLAT*RTOD

SLONG=SLONG*RTOD

```

C
C
C
ELAT=(ABS(EDEGA)+ABS(EMINA)/60.+ABS(ESECA)/3600.)/RTOD
IF(EDEGA)12,15,15
15 IF(EMINA)12,17,17
17 IF(ESECA)12,43,43
12 ELAT=-ELAT
43 ELATA=ATAN(0.993277*TAN(ELAT))

```

```

C
C
C
CONVERTS TO GEOCENTRIC LATITUDE

```

```

ELONG=(ABS(EDEGB)+ABS(EMINB)/60.+ABS(ESECB)/3600.)/RTOD
IF(EDEGB)18,19,19
19 IF(EMINB)18,20,20
20 IF(ESECB)18,24,24
18 ELONGA=2.*PI-ABS(ELONG)
GO TO 42
24 ELONGA=ELONG
42 EC=SIN(ELATA)
EK=COS(ELATA)
ED=SIN(ELONGA)
EE=COS(ELONGA)
EA=EK*EE
EB=EK*ED
EG=EC*EE
EH=EC*ED
EE=-EE
EK=-EK
COSD=SA *EA+SB *EB+SC *EC
SIND=SQRT(1.-COSD*COSD)
IF(SIND) 60,30,60
30 AZ=180.
IF (COSD) 50,99,40
40 DIST=0.
GO TO 26
50 DIST=180.
GO TO 26
60 COSECD=1./SIND
DIST=ATAN2(SIND,COSD)
GO TO 26
99 DIST=1./RADIUS
26 DIST=DIST*RADIUS
RETURN
END

```

EVENT U2. REFERENCE TIME 1731 HRS.

LATD	LATM	LONGD	LONGM	TSSQB	ETO
59	20.8	30	23.1	9.2	-396.2

STAT.NO.	A.TIME	V.USED	V.CALC	T.SEC
1	46.0	3.94	3.83	32.0
1	59.0	3.74	3.72	26.1
1	72.0	3.55	3.62	21.0
1	83.0	3.47	3.53	19.0
1	124.0	3.27	3.25	15.4
2	43.5	3.57	3.59	25.6
2	56.5	3.41	3.49	19.1
2	68.0	3.34	3.40	16.4
2	78.0	3.27	3.33	14.5
3	758.5	3.73	3.71	35.3
3	780.0	3.68	3.65	32.2
3	801.0	3.64	3.58	30.6
3	832.0	3.55	3.49	28.0
3	864.5	3.37	3.40	23.4
3	896.0	3.31	3.32	20.4
4	414.8	3.89	3.90	31.2
4	431.8	3.80	3.82	27.0
4	446.8	3.74	3.75	24.2
4	462.2	3.67	3.69	22.5
4	477.2	3.55	3.62	20.5
4	492.1	3.45	3.56	19.1

EVENT U3. REFERENCE TIME 1837 HRS.

LATD	LATM	LONGD	LONGM	TSSQB	ETO
59	22.5	30	3.5	0.0	-392.6

STAT.NO.	A.TIME	V.USED	V.CALC	T.SEC
1	40.5	3.88	3.87	30.0
1	65.0	3.62	3.66	22.8
1	86.5	3.47	3.50	19.2
2	36.4	3.61	3.69	27.2
2	50.4	3.51	3.58	22.9
2	62.5	3.44	3.48	20.0
2	74.6	3.37	3.39	17.6
2	80.6	3.34	3.35	16.5
3	842.6	3.58	3.49	28.8
3	854.8	3.52	3.45	27.1
3	867.0	3.43	3.42	25.1
3	879.2	3.36	3.39	23.0
3	891.3	3.33	3.36	21.6
3	909.0	3.29	3.31	19.2
4	407.7	3.88	3.94	30.7
4	423.4	3.81	3.86	27.7
4	439.7	3.75	3.79	24.5
4	454.5	3.70	3.72	23.2
4	469.2	3.64	3.66	22.0

II THE CRUST AND UPPER MANTLE BENEATH ICELAND

CONTENTS

	Page
Introduction	1
CHAPTER 1:	
(1.1) Iceland	3
(1.2) The crustal structure of Iceland	3
(1.3) Gravity in Iceland	8
(1.4) The trace of the Mid-Atlantic Ridge through Iceland	9
(1.5) Crustal drift in Iceland	10
(1.6) Acid rocks in Iceland	11
CHAPTER 2:	
(2.1) The Iceland experiment	13
(2.2) Seismometer arrays	14
(2.3) The equipment used in the Iceland experiment	17
(2.4) The layout of the arrays	19
(2.5) Routine running of the arrays and problems encountered	21
(2.6) Data obtained from the Iceland experiment	23
CHAPTER 3:	
(3.1) P-wave delays : Introduction	34
(3.2) The reduction of P-wave travel times to obtain relative station delays	35
(3.3) The data used in this study	44
(3.4) Results of the delay measurements	49

	Page
(3.5) Comparison with other delay time measurements	58
(3.6) Interpretation of the delay times	60
(3.7) Gravity and seismological data on the mantle beneath Iceland	67
(3.8) Discussion	71
Conclusions	74
References	76
Appendix 1. Array layouts at Hveravellir and Myvatn	85
Appendix 2. The data used in the delay time measurements at Akureyri, Eskdalemuir, Kiruna and Kaptobin	88
Appendix 3. Tryggvason's method	92

FIGURES

	Page
1. Map of Iceland	4
2. Bath's structure of Iceland. (Reproduced from Palmason, 1967a)	6
3. Epicentres of local earthquakes recorded in Iceland	25
4. Single-channel, vertical component records of local earthquakes recorded at Hveravellir	28
5. Examples of multi-channel playouts of earthquakes recorded at Hveravellir	(in wallet)
6. Azimuthal great circle projection centred on Akureyri	36
7. Differences from J-B times for a surface focus	42
8. Hveravellir teleseism records from single channels and from sum of N channels	48
9. Delay relative to Akureyri showing 95% confidence limits	52
10. Delay relative to Akureyri without Herrin's corrections	54
11. Shear wave velocity versus depth (Reproduced from Toksoz et al 1967)	65

TABLES

	Page
1. Approximate origin times of the events corresponding to the epicentres marked on the map in Figure 1	27
2. Details of the teleseisms used in the delay measurements at the Hveravellir Array relative to the Eskdalemuir Array	46
3. Delay at Akureyri relative to Eskdalemuir	50
4. Delay at Akureyri relative to Kiruna	50
5. Delay at Akureyri relative to Kaptobin	51
6. Delays at Reykjavik and Sida relative to Akureyri	51
7. Delay at the Hveravellir Array relative to those at the Eskdalemuir Array	51
8. Comparison of the delay time measurements with those made by other authors	59
9. Crustal structures for Iceland, Eskdalemuir and Kiruna	62
10. The depth of the 7.4 km/sec layer beneath Iceland calculated from the delays at Akureyri relative to those at Eskdalemuir and Kiruna	62

Introduction

This part of the thesis is mainly concerned with the investigation of the crust and upper mantle of Iceland using earthquake seismology. Two temporary array stations were installed in Iceland during the summer of 1967 by the Geology Department of Durham University. The aims of the experiment were twofold; firstly, to record teleseismic arrivals which could be used to measure accurate P-wave delay times, and secondly, to obtain data on local earthquakes which would be used in an investigation of the local earthquakes themselves and in an investigation of the deeper crustal structure of Iceland.

A brief description of the geology and geophysics of Iceland is given in Chapter 1. Chapter 2 deals with the Iceland experiment. A description is given of the apparatus which was used and of the way in which it was exploited in the experiment. A description is also given of the data which were recorded on local events though they have not been analysed in detail.

Chapter 3 deals with the measurement and interpretation of P-wave delay times. Delay times at Reykjavik were measured by Tryggvason in 1964 but the recent revision of the Jeffreys-Bullen travel time tables by other authors points to the need

for a re-evaluation of the Iceland delay times. Further, it has been suggested by Stefansson that the delay times measured by Tryggvason might be due to the onsets at Reykjavik being obscured by the high level of microseismic noise.

The delay times reported here were made using the three permanent Icelandic stations at Reykjavik, Akureyri and Sida and at one of the temporary array stations in Central Iceland. The delays are measured relative to those at stations in Scotland, Sweden and Greenland and they are interpreted in terms of the crust and upper mantle structures beneath the recording stations.

CHAPTER 1

(1.1) Iceland

Iceland is a large volcanic island situated at the junction of the Mid-Atlantic Ridge and the Faeroes-Greenland Ridge. It provides a convenient place for the study of the geophysical processes and conditions of the Mid-Atlantic Ridge though how typical it is of a ridge area is open to conjecture. While both the Mid-Atlantic Ridge and Iceland are seismically active, the Faeroes-Greenland Ridge is aseismic. Its origin is not clearly understood but it may be the trail of volcanic material which was erupted from a 'hot spot' on the Ridge during the separation of Greenland and the continent of Europe (Wilson 1965); that 'hot spot' is now represented by Iceland.

(1.2) The crustal structure of Iceland

Iceland is completely covered by Tertiary basalts which have been dated at 12.5 my (Moorbath et al 1968). In the central part of Iceland which is referred to as the neovolcanic zone, the Tertiary basalts are covered by a thin layer of Quaternary and recent volcanic products (Fig 1).

Few refraction experiments have so far been carried out to determine the deep crustal structure of Iceland. Figure 2 shows a model for the crustal structure obtained by Bath (1960)

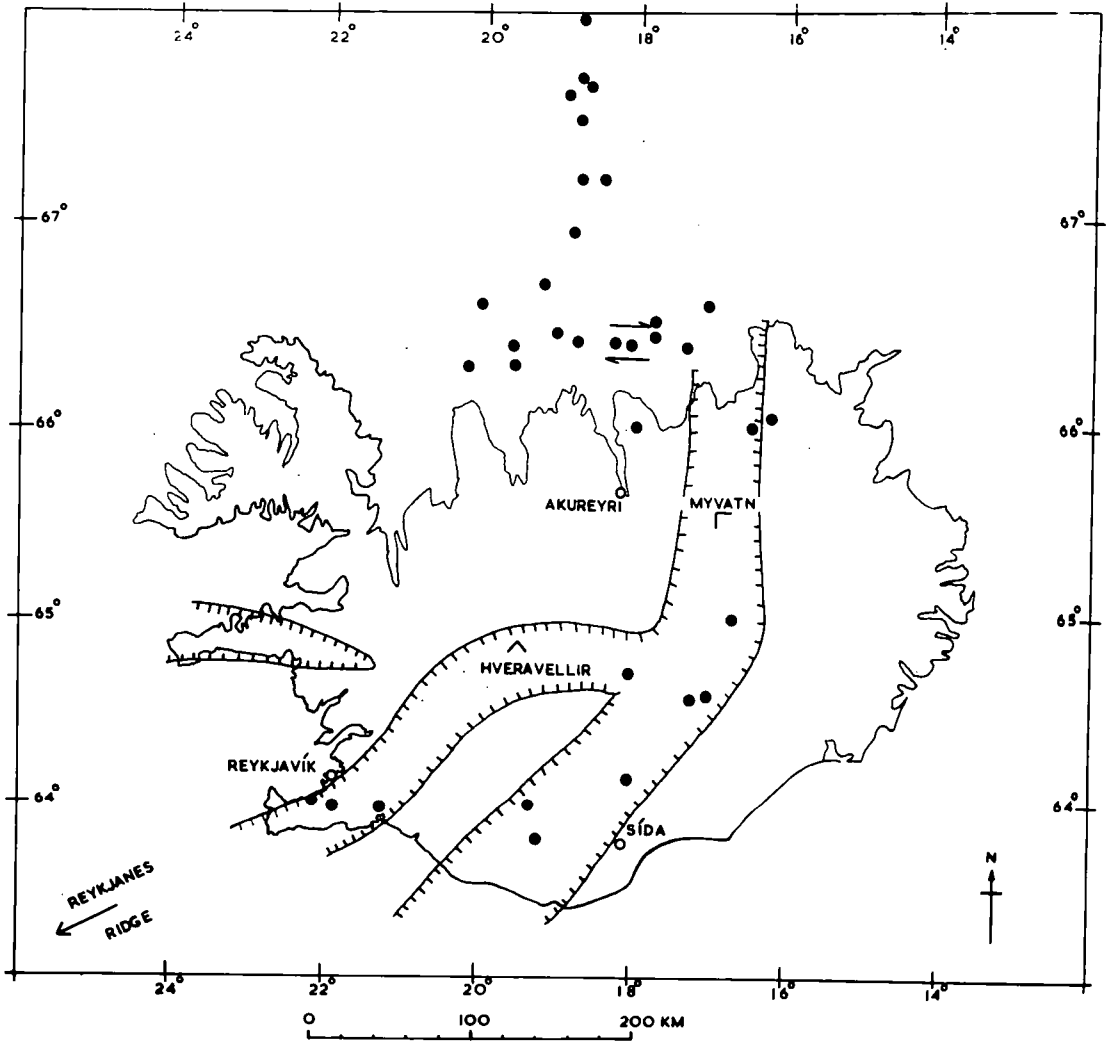


FIG 1

MAP OF ICELAND
 EPICENTERS, ●, FROM SYKES 1965

ARRAY STATION = Γ
 PERMANENT " = \parallel = G
 NEOVOLCANIC ZONE = ---|---|---|---

from a 250 km long refraction profile in western Iceland. The two deeper layers with velocities of 6.71 and 7.38 km/sec are interpreted as basalts. The position of the Moho at 27.8 km depth was deduced on the basis of reflected waves and must be regarded as rather uncertain.

Numerous short refraction profiles have resulted in a fairly detailed mapping of the upper part of the crust which appears to have a more complex structure than Bath's model indicates (Tryggvason and Bath 1961, Palmason 1963, Palmason 1967a). The upper layer, layer 0, is found at the surface in the neovolcanic zone and has a velocity which ranges from 2.1 to 3.4 km/sec; it consists of Quaternary volcanic rocks. The second layer, layer 1, with an average velocity of 4.15 km/sec is found at the surface in western, northern and eastern Iceland and it is generally found beneath layer 0 in the Neovolcanic Zone; it is interpreted as the upper part of the Tertiary Flood Basalts. The lower part of the Tertiary Flood Basalts (layer 2) has an average velocity of 5.04 km/sec and usually underlies layer 1 except in the Reykjanes Peninsular where it is absent (Palmason 1967a). These three layers correspond to the uppermost layer in Bath's model.

Between 2 and 4 km below the surface, layer 3 occurs with a velocity ranging from 5.9 to 6.8 km/sec. From the short refraction profiles there are indications that the

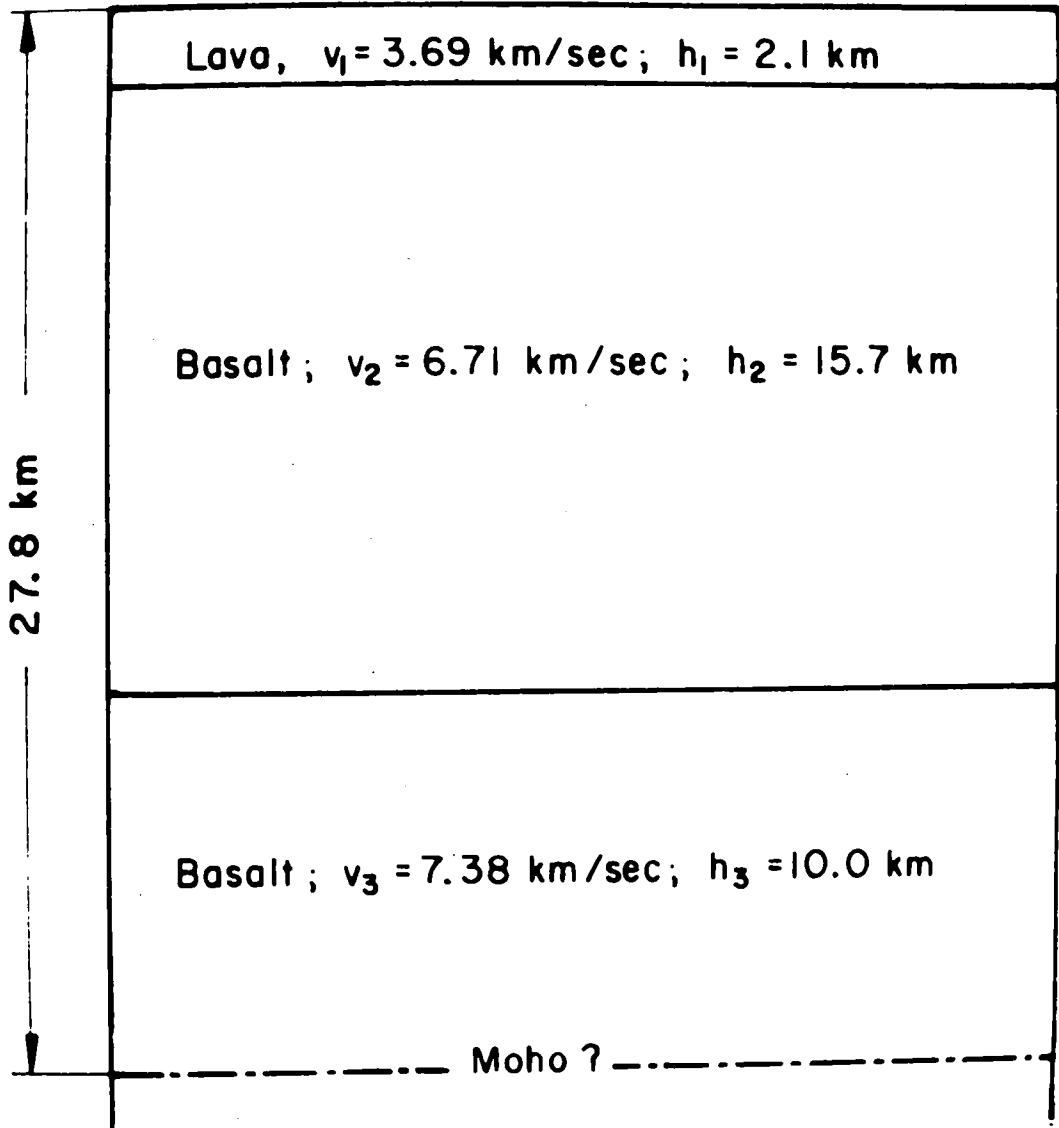


Fig 2

velocity determinations for this layer fall into two groups with average values of 6.19 and 6.48 km/sec. Layer 3 does not appear at the surface so its nature is largely unknown, though, from its velocities, it appears to be analogous to the main continental and oceanic crustal layers.

At a depth of about 15 km beneath Iceland, the P-wave velocity increases to 7.4 km/sec. This fourth layer, the 7.4 layer, has been detected beneath Iceland many times. Tryggvason (1959) found layers with such velocities from an investigation of the apparent velocities of P-waves from earthquakes in Iceland and from surface wave studies (Tryggvason 1962). It has also been detected beneath the Mid-Atlantic Ridge (Ewing and Ewing 1959), the East Pacific Rise (Raitt 1956), and the Red Sea (Girdler 1963). The vertical extent of this layer has been a matter of some speculation. Bath tentatively placed its lower limit at 28 km though other workers have estimated that it is much deeper. From a study of earthquakes occurring between Norway and Greenland, Tryggvason (1961a) concluded that the depth to the lower boundary was between 100 and 140 km. In a later study, using the delay times of P-waves recorded at Reykjavic and Kiruna from teleseismic events, Tryggvason (1964) found that a depth of 240 kms to the base of the 7.4 layer could explain the observed delay times. A similar result was obtained by

Francis (1969) from measurements of $dT/d\Delta$ using earthquakes from the North-Atlantic Ridge which were recorded at the local Icelandic stations and in eastern Greenland.

(1.3) Gravity in Iceland

Gravity measurements in Iceland reveal a saucer-shaped Bouger anomaly with a minimum of -30 mgal near the centre of the island and maxima of 40-60 mgal near the coast (Einarsson 1954). Bodvarsson and Walker (1964) suggested that the anomaly was caused by a thickening of the Tertiary Basalts towards the centre of Iceland. However, following the seismological evidence for a thin crust and for a great thickness of the 7.4 layer, Bott (1965a and 1965b) interpreted the gravity anomaly as being the result of a low-density upper mantle. If the 7.4 layer extends to 240 km as suggested by Tryggvason, then the gravity can be explained if the 7.4 velocity is the result of a partially fused upper mantle with a consequent reduction in density. This requires a magma fraction of approximately 10 per cent which is possible if there is an uprising convection cell beneath Iceland.

This interpretation is in keeping with the high heat flow measurements in Iceland. Extreme values of up to $7.4 \mu\text{cal}/\text{cm}^2$ sec have been recorded though Palmason (1967b) has suggested that $2.9 \mu\text{cal cm}^2$ sec may be the best available value on

regional heat flow in Iceland. Further evidence for high subsurface temperatures in Iceland comes from work on magnetotelluric soundings by Hermance and Garland (1968) which indicates the presence of a highly conductive layer at a depth of some 25 kms. They interpret this as the effect of a temperature enhancement of 300 to 400 deg.K.

(1.4) The trace of the Mid-Atlantic Ridge through Iceland

The magnetic anomalies mapped by Heirtzler et al (1966) clearly show that the Mid-Atlantic Ridge extends up the Reykjanes Ridge to southwestern Iceland. Magnetic data over Iceland obtained by Serson (Sigurgeirsson 1967) show that zones of high intensity can be traced along both sections of the Neovolcanic Zone to approximately 65 deg North. However, the central anomaly of the Reykjanes Ridge cannot readily be traced north of the western tip of the Reykjanes Peninsula.

Earthquake epicentres clearly show the northward extension of the Ridge from an area some 40 km North of Iceland at about 19 degrees West. (Fig 1). Within Iceland the path of the Ridge is not so well defined. The large earthquakes are confined to east-west running zones in south and north Iceland, while a zone in which mainly small earthquakes occur lies further east with a nearly north-south direction (Stefansson 1967). With the aid of one strike-slip focal

mechanism solution (which was investigated independently by Stefansson, 1966), Sykes (1967) interpreted the north zone as a transform fault. Ward et al (1969), interpreting the results of a micro earthquake study, have suggested that the southern zone is also a transform fault. Further evidence for these proposed transform faults come from magnetic anomalies in the Norwegian Sea, east and north of Iceland (Avery et al 1968), where there are disturbances in the magnetic lineations characteristic of old fracture zones north of 66 deg N and just south of 64 deg N. These zones strike at approximately N 80 deg W and appear to line up with the suggested transform faults.

(1.5) Crustal drift in Iceland

Crustal drift in Iceland is believed by some authors to result mainly from crustal extension by dyke injection (Bodvarsson and Walker 1964). Crustal spreading rates for Iceland have been estimated by Moorbath et al (1968). By comparing the K-Ar age determinations for rocks in the east of Iceland with the distance from the active zone, they computed a spreading rate of 1.2 cm/yr. Similarly, by comparing the age of the Faroe Islands, 55-60 m.y. (Tarling and Gale, in press) with their distance from the Reykjanes Ridge, the apparent spreading rate is approximately 1 cm/yr. These

estimates are in excellent agreement with the rate of 1.0 cm/yr obtained from the magnetic patterns across the Reykjanes Ridge just south of Iceland (Pitman and Heirtzler, 1966, Vine, 1966).

(1.6) Acid rocks in Iceland

Acid rocks make up an estimated 10-12% of the Tertiary plateau in eastern Iceland (Walker, 1959) and on the Snaefellsnes peninsula northwest of Reykjavik (Sigurdsson, 1967). If this figure is representative of the volume of Tertiary rocks, then such a high proportion is difficult to explain by differentiation from a basic magma as such a process is likely to yield only 2-5% of acid residuum, although a theoretical maximum is of the order of 7-12% (Carmichael, 1964).

Walker (1965) has suggested that there may be sial under Iceland which, by remelting, has contributed to the acid rocks at the surface. However, the constant Sr $^{87}/\text{Sr}^{86}$ ratio for both acid and basic igneous rocks suggests a common origin for both fractions (Sigurdsson, 1967). Sigurdsson (1967) suggests that petrological and isotopic evidence indicates fractionation from a basaltic parent rock as the most likely source of the acid rocks in Iceland. McBirney (1967) noted the relation between the Niggli quartz number of oceanic vol-

canic rocks and their distance from the crest of ocean ridges. A close relation to the heat flow data suggests that the more siliceous rocks near the crests are produced by melting at shallow depths.

CHAPTER 2

(2.1) The Iceland experiment

Two temporary array stations were installed in Iceland during the summer of 1967 by the Geology Department of Durham University. The aims of the experiment were to gather seismic data for the study of the crust and upper mantle of Iceland. The array stations were placed in the north of Iceland at Myvatn and in the central region at Hveravellir (Fig. 1). Together with the three permanent Icelandic stations at Reykjavik, Akureyri and Sida (Fig. 1), they provide a good coverage of the island for the investigation of local earthquakes. It was hoped that the local earthquake data might be used for an investigation of the epicentral positions and focal depths of the earthquakes, and, using array processing techniques, for an investigation of the deeper crustal structure of Iceland. Further, the measurement of P-wave delay times at these stations would enable a study to be made of the variations in the velocity structure of the upper mantle beneath the island.

The experiment lasted from May 1st to September 4th 1967. The author was in Iceland for the whole period assisting in the setting up of both the array stations and then running the Hveravellir station. Because of extremely harsh weather conditions, both sites were inaccessible during the early

months of the "summer". Myvatn was not reached until May 18th and Hveravellir was reached on July 5th. Because of difficulties with the equipment, the Myvatn station was only operational intermittently and the records obtained were of poor quality. The Hveravellir station operated more or less continuously from July 20th and both stations were dismantled on September 3rd.

(2.2) Seismometer arrays

A full description of the theory of seismometer arrays is given by Birtill and Whiteway (1965). Seismometer arrays are normally situated in a horizontal plane and are arranged in some uniform geometrical pattern. Most arrays, including those which were set up in Iceland, consist of short-period vertical-component seismometers whose outputs are recorded on magnetic tape.

Each signal component travels across the array with an apparent ground velocity which is dependent on the path and the mode of propagation. The apparent ground velocity of the first P-wave arrival increases from approximately 8 km/sec at 2 degrees distance to about 24 km/sec at 90 degrees distance. For local events, the apparent velocity of refracted arrivals is equal to the velocity of the refractor providing that the structures through which the rays pass are horizontally

homogeneous and providing that the dimensions of the array are small compared with the distance to the source.

Because of the finite velocity of propagation across the array, a seismic signal will, in general, arrive at different seismometers at different times. Thus for a given array layout, the relative onset times at each seismometer will be a function of the apparent velocity of the arrival and its direction of approach. The advantages of an array of seismometers are that the apparent velocity vector of the signal can be determined from the relative onset times across the array, and that the outputs of the individual seismometers can be combined to increase the signal:noise ratio and thus to enhance the onset of a signal component. Either function may be carried out by electronic means.

The determination of the azimuth and the apparent velocity of the signal (azimuth and velocity filtering) can be effected by combining the outputs of the individual seismometers after inserting delays corresponding to a particular velocity and azimuth condition. The amplitude of the resulting signal will be greatest when the inserted delays exactly cancel those incurred at the seismometers during the recording of the signal, because only then will the individual signals be in phase on summation. The seismometer outputs may also be combined in other ways after the delays are inserted;

for example, two halves of the array may be summed and then multiplied together, or they may be summed and then cross-correlated.

In a similar manner the signal:noise ratio may be increased. Consider an array which is perturbed by random noise. A coherent signal travelling across the array will incur delays between seismometers which may be cancelled on playback without affecting the noise which is unrelated between seismometers. If the outputs are then added so the signal components are in phase, then the mean signal power is proportional to n^2 , where n is the number of seismometers. However, as the mean noise power is only proportional to n , the signal:noise power ratio is increased by n . For small arrays, such as those used in Iceland, a signal:noise ratio improvement may be gained for teleseismic arrivals by summing the outputs directly without inserting delays, because the wavelengths of the signal are much greater than those of the noise.

The apparent velocity and azimuth of a signal can also be determined by onset time analysis. This technique is normally used only with first arrivals since they are the clearest. The onset times are read from playouts of the individual seismometer channels. They may be determined from the first break if it is sufficiently clear, or by tracing one of the typical waveforms and then fitting it to the other arrivals.

The apparent velocity vector of the signal may then be determined using a computer to solve a set of equations relating the onset times to the apparent velocity and azimuth of the signal. This method may be used with local or teleseismic arrivals and it may provide more accurate information on first arrivals than any other processing technique.

(2.3) The equipment used in the Iceland experiment

Apart from the tape deck and the seismometers, the equipment was designed and built in Durham. A complete description of the apparatus and details of the electronics are given in a paper by Long (1968).

The array is fully portable and independent of mains power supplies. For the Iceland experiment, Willmore mark 1 seismometers were used as detectors. These comprised ten vertical instruments and two horizontals. Recording was done on one-inch magnetic tape using a Geotech Portable Recorder. At the recording speed used, 15/160 i.p.s., each tape lasted approximately ten days. The recorder has provision for fourteen tracks plus two edge tracks, therefore with twelve seismometers, two full tracks are left for recording the radio time checks and signals from the electronic clock. The two edge tracks were used to record a reference signal for flutter correction during replay.

The equipment can be divided into two basic parts, firstly, the seismometers and field amplifiers, and secondly, the central recording equipment which includes the tape deck and associated electronics, the clock, the radio and the power supplies. These two parts are connected by twin-conductor, field-telephone cable.

The field amplifiers amplify the signal from the seismometers and send it down the land line in F.M. form to the central recording apparatus. The land lines also carry power from the central recording apparatus to the field amplifiers. The system has a facility for remote calibration of the seismometers and the amplifiers, and for remote control of the amplifier gains. This control is exercised from the central recording apparatus where a single-channel pen recorder is used to monitor the signals from each seismometer. The maximum gain in the amplifiers before modulation is about 16,000; this can be reduced in 8 stages of $\div 2$.

The time is recorded from a crystal clock which emits pulses every second. The pulses are of differing lengths so that second, ten-second and minute marks can be distinguished, and after each minute mark, they are long or short according to a binary code which enables the minute, hour and the day to be read. A visual binary-coded time display is also provided so that clock can be synchronized with the radio time

signals.

The total power consumption of the system is less than 50 watts which were obtained from four six-volt car batteries connected in series. These were charged, while they were running the equipment, from portable, petrol-driven Honda generators.

The seismometers were adjusted to be critically damped. Where necessary, damping was provided by placing high-stability resistors (approx. 1 Kohm) across the seismometer coils. The instruments were adjusted to have a period of 0.8 seconds.

(2.4) The layout of the Arrays

The arrays were intended for use with teleseismic arrivals to increase the signal:noise ratio and with local earthquakes for velocity and azimuth filtering. For signal to noise improvement, the array design is not critical. In order to achieve good velocity and azimuth discrimination, an L-shaped layout was used.

The seismometer spacing was chosen so that, for local earthquakes, the array dimensions would be comparable with the signal wavelengths; this condition is necessary for the array to have a sharp response. In order to prevent aliasing, the seismometers were spaced so that at least three samples

per wavelength were recorded. Therefore, assuming that the apparent velocity of local arrivals is 7.4 km/sec and that their frequencies range from 3 to 5 cps., each arm must be 2.5 km long and the seismometers must be 0.5 km apart. The equipment for the array was sufficient for twelve seismometers of which two were used as horizontals to help in the identification of S-waves from local earthquakes. In order to satisfy the spacing requirements, the following layout was chosen: The arrangement of vertical seismometers should be identical on each arm of the array with the first seismometer placed 0.25 km from the crossover point and the others at intervals of 0.5, 0.5, 0.5 and 1.0 km. The horizontal instruments were installed in the first pit on one arm of each array. These were arranged so that they recorded motion parallel to each arm.

The orientation of each array was chosen according to convenient local landmarks which, with the aid of sighting poles and tape measures, were used to survey the arrays after suitable seismometer locations had been found. Details of the actual array layouts at Hveravellir and Myvatn are given in Appendix 1.

Both arrays were situated on recent lava fields which, in common with most of Iceland, were devoid of trees. The lava was considerably broken up and interspersed with sandy

material some of which was covered by coarse grass and herbage. Wherever possible, the seismometers were completely buried and located on large blocks of lava to obtain good seismic coupling. Where they could not be buried, the seismometers were covered by mounds of sand to shelter them from the wind.

The central recording equipment was located at the cross-over points of the arrays. The electronics were housed in a small tent while the batteries and the generators were kept outside beneath improvised stone shelters.

(2.5) Routine running of the arrays and problems encountered

The routine running of the arrays was straightforward. The generators ran on average for eighteen hours per day which was sufficient to keep the batteries charged. Time checks were taken whenever possible from the hourly time signals broadcast by the B.B.C. Overseas Service. At the Hveravellir station, the radio was left on continuously so that all available time checks were recorded on tape. The gain settings of the amplifiers were checked twice daily and altered according to the prevailing noise levels. The amplifiers usually operated at maximum gain except during very high winds when they operated at near the minimum gain. The seismometers were calibrated daily. All these operations were noted in

the station log book against the corresponding clock time. Particular note was made of the times at which the generators were started as the initial voltage surge sometimes caused the clock to jump. The tapes were changed every ten days and then sent back to Durham for inspection.

Recording was delayed for some time at both stations while the equipment was repaired after suffering damage in transit to the sites. Having successfully installed the arrays, the biggest problem was to keep pace with the breakdowns in the equipment. These occurred for a variety of reasons but mostly because of moisture in the electronics, faults with the generators caused by sand and dust, and sheep damage to the cables.

Naturally, the problem of moisture was foreseen and the seismometers and amplifiers, which were out in the open, were sealed with grease and rubber gaskets and included bags of silica gel to absorb moisture. However, the P.V.C. tubes which encased the amplifiers still leaked and, once they were damp, drying them out in field conditions proved very difficult. The main problem with the seismometers was to prevent water from reaching the output plug: when this happens the damping characteristics of the instrument is altered and the signal is attenuated. These problems were partially solved by sealing all the joints with liberal applications of grease and

covering the apparatus with polythene sheeting.

Sheep damage to the cables could not be prevented as it was impractical to bury the cables. The F.M. form of the signal sent down the land lines proved very resilient to cable damage. However, complete breaks or shorts did occur frequently and a lot of time was spent on cable repairs.

The generators continually broke down because of sand and dust in the carburettors. They were very difficult to service and were often more vulnerable to damage after repair than before. Because of the generator failures, it was difficult to keep the batteries fully charged. The worst consequence of this was that the clocks ran erratically. This was a particularly bad problem at Myvatn where the conditions were more dusty than at Hveravellir. As a result the Myvatn records are unusable when absolute onset times are needed. Further difficulties at Myvatn were caused by failures in the driving belts in the tape deck. This resulted in the closing down of the Myvatn station for some weeks while spare belts were sent out from America.

(2.6) Data obtained from the Iceland experiment

A large number of local earthquakes and several teleseisms were recorded by the array stations at Hveravellir and Myvatn. Because of difficulties with the equipment, the data

recorded at the Myvatn station are of comparatively limited use. The data recorded at the Hveravellir station have been examined and some of the teleseisms which were recorded have been used in the P-wave delay work reported in the next chapter. Because of a lack of time, no results have been obtained from the data on local earthquakes though the data have been examined with a view to their use in an investigation of the local earthquakes and of the deeper crustal structure of Iceland.

During the operation of the Hveravellir array, 95 local earthquakes were recorded of which 69 were also recorded by at least one of the three permanent stations at Reykjavik, Akureyri and Sida. Two of the local events were reported by the U.S.C.G.S. who calculated their magnitudes as 4.1 and 5.0. Both events overloaded most of the recording channels at Hveravellir.

Approximate locations of 18 local events were calculated using the S-P times reported in the bulletins from the three local stations. The locations were made assuming that an S-P time of 1 second is equivalent to an epicentral distance of 7.4 km. This relationship was used because it appeared to give the smallest error as indicated by the overlap of the distance arcs from each locating station. The epicentres of these events are marked on the map in Figure 3 together with

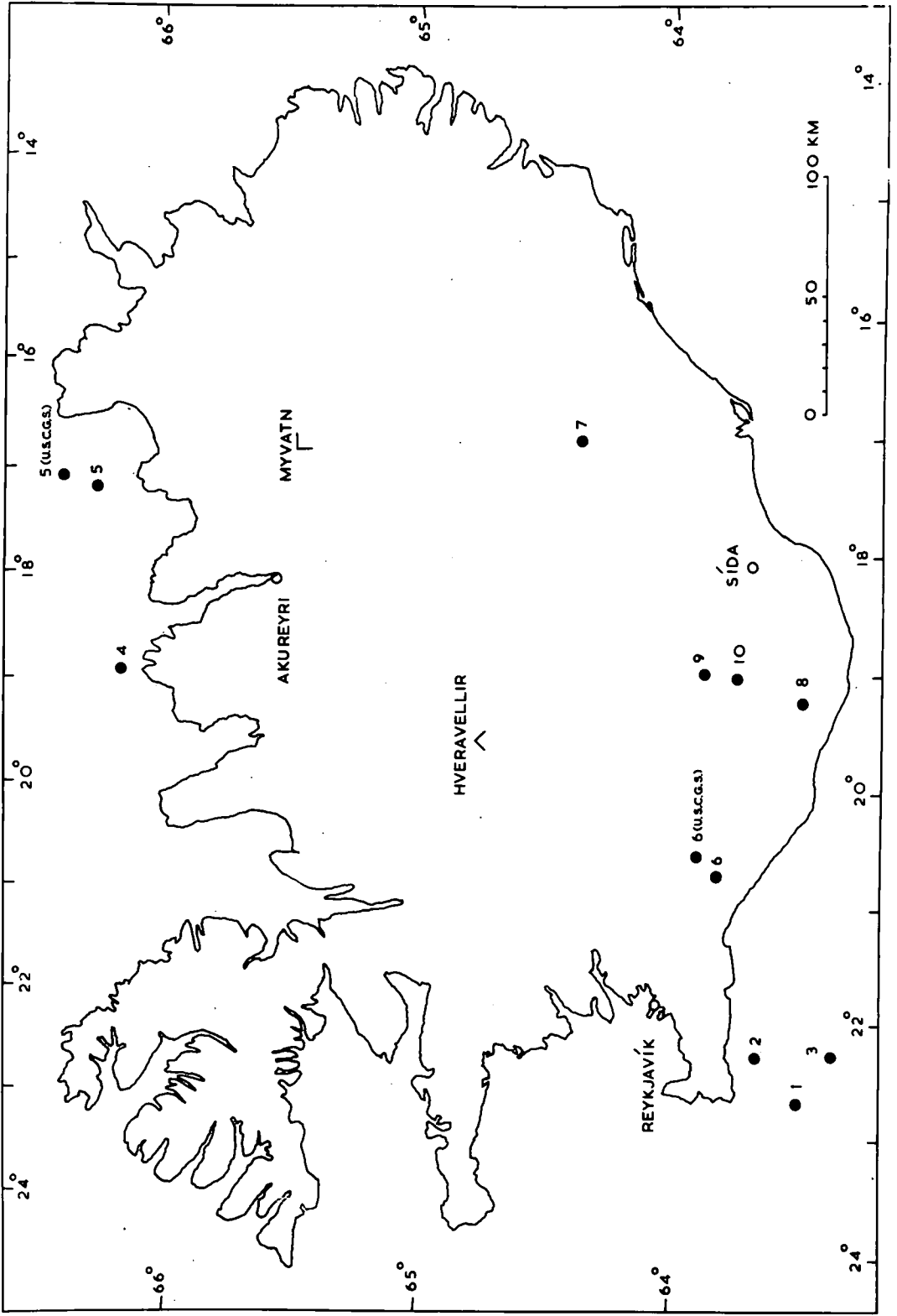


FIG. 3

the two U.S.C.G.S. epicentres, one of which (number 5) has also been located using S-P times. The origin times, to the nearest minute, for the events corresponding to the various epicentral positions in Figure 3, are given in Table 1. From the overlap of the distance arcs from each station, it appears that most of the locations are accurate to within a radius of 15 km. It is clear that these events occur in the main earthquake zones in Iceland (cf. Figure 1).

Examples of single-channel records from seven of these events are shown in Figure 4. The epicentral distances for each event are taken from Figure 3. Most of the records show several phases with a clear first P-wave arrival which is probably P_n (corresponding to the 6.7/7.4 interface on Bath's model, Figure 2). The second P-wave arrival appears to be P_g though the identification is uncertain. The first S-wave arrival, which is referred to as S_g, could be identified with certainty on comparatively few records. Where the two phases are clear, the S_g-P_g time corresponds to the epicentral distance to within approximately 15 km assuming that an S_g-P_g time of 1 second is equivalent to a distance of 7.4 km. On certain records, for example 6a in Figure 4, clearly defined pulses are present between P_g and S_g. It is notable that these pulses are either absent or considerably reduced in amplitude in the record 6c though the two records are otherwise identi-

TABLE 1

EVENT NUMBER	DATE (1967)	ORIGIN TIME	
		hr	min
1a	July 20	15	36
1b	21	16	52
2	25	11	20
3	25	11	31
1c	25	12	14
4	26	19	45
5*	26	22	00
6a**	27	00	06
6b	27	00	47
6c	27	00	50
6d	27	05	32
6e	27	06	58
7	Aug 4	10	32
8a	4	13	22
8b	17	01	52
9	28	08	13
10	28	10	31

* The U.S.C.G.S. data on this event are: Depth normal, origin time = 21 hr 59 min 50.2 sec, mag.(mb) = 4.1, epicentre = 66.5°N, 17.1°W.

** These events are foreshocks and aftershocks of a larger event for which the U.S.C.G.S. reported the following data: Depth normal, origin time = 05 hr 17 min 54.0 sec, mag.(mb) = 5.0, epicentre = 64.0°N, 20.7°W.

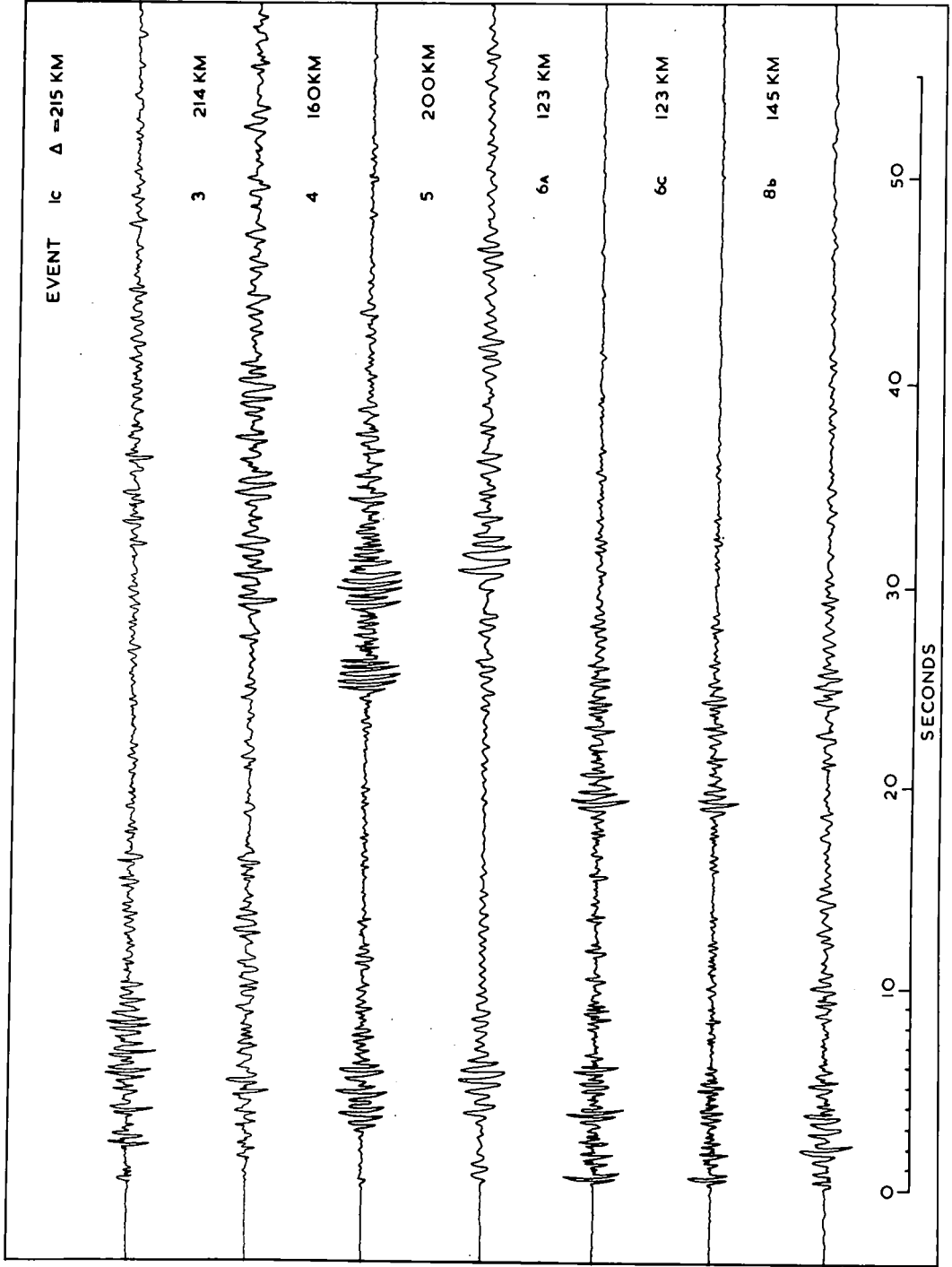


FIG. 4

cal. Both records are from events which are clearly part of a foreshock-aftershock sequence about a larger event which was reported by the U.S.C.G.S. (Table 1). The differences between the records obtained from events in the sequence may provide a valuable clue to the variation in their focal depths.

With the exception of six small events, which appear to originate within 7 km of Hveravellir, all the events which were recorded and for which Sg-Pg times are known, originate at distances between 65 km and 230 km from Hveravellir. All of these events presumably occur within the main earthquake zones. The majority of local events recorded by the array occurred during the early stages of the experiment when the array was incomplete. Consequently, comparatively few records are suitable for array processing techniques.

An unsuccessful attempt was made to velocity-filter the records from eight local events which were recorded at Hveravellir. This was done using the analogue equipment at the U.K.A.E.A. Laboratory at Blacknest. The equipment is not entirely suitable for use with the Iceland data. As the equipment is intended for use with data from larger arrays, the delay increments were too large to permit accurate phasing on the Iceland data. Although the correlator outputs did vary according to the phasing conditions, the correlator response was very poor and in some instances apparent velocities

of 14 km/sec were indicated for first arrivals.

A preliminary onset-time analysis was made using first-arrival data from the eight events which were velocity-filtered. The analysis was made using a computer program which was run at Blacknest by Mr. D. Corbishly. Corrections for the variations in pit heights were made using 2 km/sec for the velocity of the uppermost layer. All the events occurred at epicentral distances of at least 100 km from Hveravellir so a first arrival with an apparent velocity of 6.7-7.4 km/sec would be expected. The epicentres of three of the events which were analysed are shown in Figure 3; these are events 8b, 9 and 10 and they gave apparent velocities of 9.0, 9.6 and 7.8 km/sec respectively. There are discrepancies between the event azimuths as measured from the map in Figure 3 and those determined from onset-time analysis of $+2^{\circ}$, $+15^{\circ}$ and $+12^{\circ}$ for events 8b, 9 and 10 respectively. These errors may be explained if the epicentres are located too far east by up to 25 km. The apparent velocities are obviously too large and cannot be reasonably explained entirely on the basis of a dipping refractor. They are probably due to non-uniform strata in the neovolcanic zone and beneath the array. The other events which were analysed gave apparent velocities between 6.3 and 7.5 km/sec. One of these originated near epicentre 6 on Figure 3 and the others originated in the North

of Iceland near epicentres 4 and 5. There appears to be no correlation between the azimuth, and the epicentral distance of the event, and the apparent velocity of the arrivals. Although the apparent velocities determined for the second group of events are reasonable, they are probably affected by the structure beneath the array and therefore they do not necessarily represent the velocity of the refractor. A multi-channel payout of one of the northern events which was onset-time analysed is contained in the wallet at the back of this thesis. The horizontal channels show the S-wave phases with unusual clarity.

It is clear that the velocities and azimuths obtained from the processed data are unreliable for the determination of refractor velocities or event azimuths. Nevertheless, the use of a computer velocity-filtering program, operating on digitised data from the array, may enable different phases to be recognised on the records. In conjunction with accurate epicentral locations, found by using the absolute arrival times of phases recorded at the various stations in Iceland, the arrival times of different phases on the array records may be used to verify models for the crustal structure. Alternatively, a crustal structure could be assumed (e.g. Bath's structure, Fig. 2) and then the focal depths of the earthquakes could be investigated using array data on the

basis of the arrival times of Pn, Pg and Sg, using, for example, the method described by Thirlaway (1961) or Greensfelder (1965). This could be supplemented by using other phases such as the pulses on the record 6a which probably correspond to reflections within the crustal layers.

Sixteen teleseismic events were recorded by the Hveravellir array; seven of these were also recorded by the Myvatn array. The majority of these events provided clear records at both stations. A multi-channel playout of records obtained at Hveravellir from a magnitude 6.0 event at Honshu is in the wallet at the back of this thesis. Because of unknown clock errors, only four of the events recorded at Hveravellir could be used for P-wave delay measurements and none of the Myvatn records could be used. No S-waves were detected at either station from any of the teleseismic events recorded.

To summarise, we may say that many useful data were obtained from the Iceland experiment. The teleseismic data have been used to measure P-wave onset times which show clearly that delays do occur beneath Iceland and that they are not due to late reading of the onsets. The data on local events are probably unique since the records obtained show more detail, in terms of subsidiary phases, than is revealed by the records from the local stations which are produced with

a scale of 1 mm per second. Further, the appearance of various phases on the array records can be enhanced by means of array processing techniques.



CHAPTER 3

(3.1) P-wave delays: Introduction

The travel time residuals relative to the Jeffreys-Bullen travel time tables (Jeffreys and Bullen, 1940), were measured for teleseismic P-waves recorded at Reykjavik in Iceland by Tryggvason (1964). By comparing the residual at Reykjavik with the residual which he measured for Kiruna in Sweden, Tryggvason deducted that the difference in residuals was consistent with an extension of the 7.4 km/sec layer to a depth of 240 km beneath Iceland. It has been shown that the J-B travel time tables have the wrong shape, in the region of interest, which could lead to residual differences of the order of one second (Carder 1964, Carder et al 1966, Cleary and Hales 1966, Herrin et al 1968, Liljwall and Douglas 1969). Thus part of the residual difference measured by Tryggvason may be due to incorrect travel time tables. Further, it has been suggested that the large residual measured by Tryggvason for Reykjavik may be due to the onsets being obscured by the high level of microseismic background noise (Stefansson, 1967).

The work presented here is a re-evaluation of the measurements made by Tryggvason, using a more refined analysis of the data from a wider range of stations and incorporating corrections to the J-B tables. Further, the use of processed data from an array station in central Iceland, and data from the

U.S.C.G.S. station at Akureyri, which operates at more than eight times the gain of Reykjavik, may permit a more accurate detection of onsets than at Reykjavik. Relative residuals are measured at pairs of stations by comparing the onset times of events recorded at each station. The events used are in the distance range 40 to 90 degrees from Iceland.

The method employed here attempts to separate from the gross travel time residuals the relative delays between station pairs caused by the different crust and upper mantle structure beneath each station. Delays are measured at Akureyri (AKU) in Iceland, Eskdalemuir Array station (EKA) in Scotland, Kiruna (KIR) in Sweden and at Kaptobin (KTG) in Greenland. To estimate the variation in delay over Iceland, delays at Reykjavik and Sida are compared with those at Akureyri. A further comparison is made between delays obtained using processed data from the array stations at Hveravellir in central Iceland and at Eskdalemuir. (The Icelandic stations are marked on the map in Figure 1 and the others are shown in Figure 6). The relative delays presented here are interpreted in terms of the structure beneath Iceland.

(3.2) The reduction of P-wave travel time residuals to obtain relative station delays

The delay time, T_s , arising from the anomalous structure

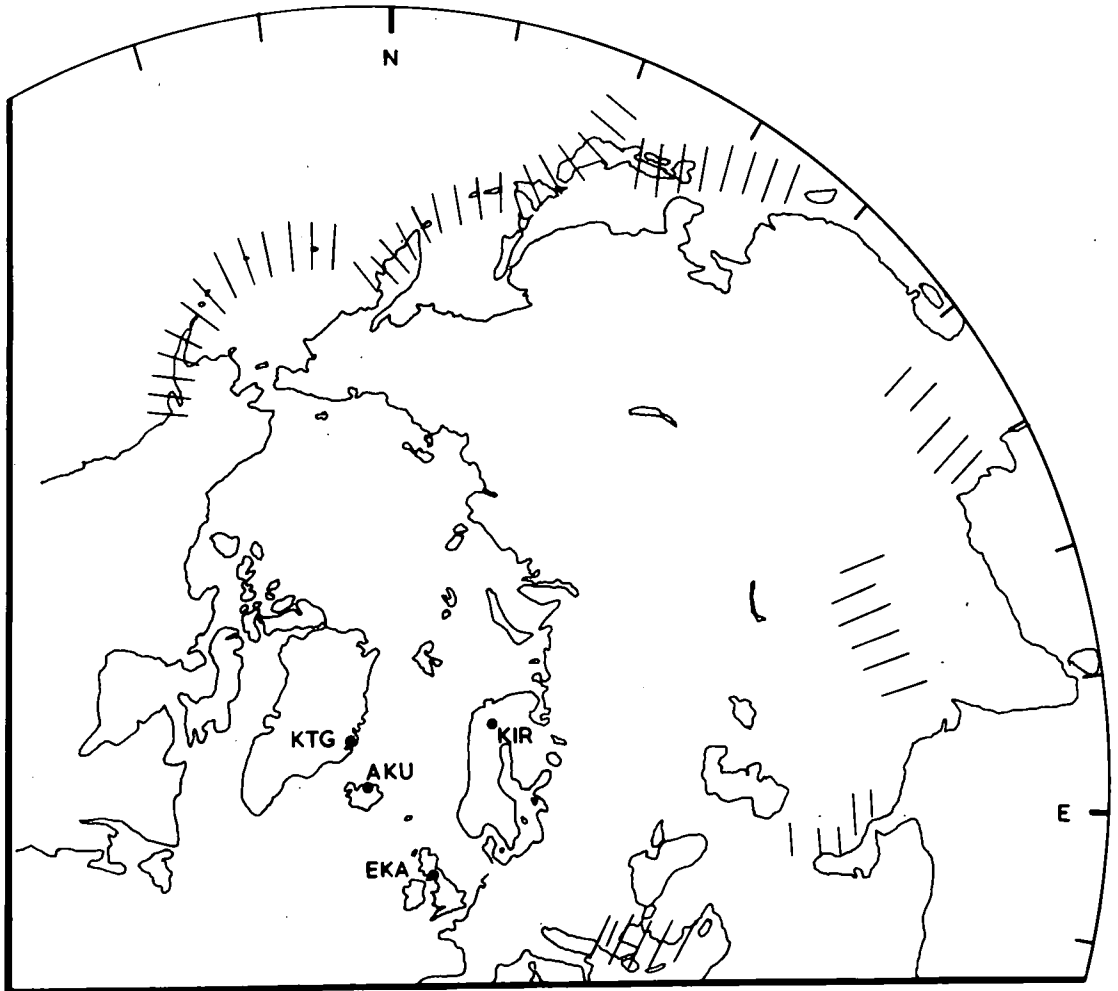


FIG. 6 AZIMUTHAL GREAT CIRCLE PROJECTION CENTRED ON AKUREYRI RADIAL DISTANCE = 90° DISTANCE AND AZIMUTH ARE CORRECT FROM AKUREYRI
 /// = MAJOR EARTHQUAKE ZONE

beneath the recording station, is incorporated in the travel time residual, R . We define the travel time residual as the difference between the observed and the expected travel times, i.e.,

$$R = \text{observed travel time} - \text{expected travel time} \quad (1)$$

We may express the residual, R , in more detail as the sum of five terms:

$$R = T_s + T_o + T_e + T_t + E \quad (2)$$

Where, T_o arises from errors in the assumed focal data.

Incorrect focal data, particularly incorrect epicentres, arise from a non-symmetrical distribution of the stations used in the event location, combined with errors in the travel time tables used in the location. Further errors may arise from station delay times. These may both lead to systematic errors in R since most earthquakes in a given distance range from any station tend to come from a single seismic region. The term T_o may differ for two earthquakes from the same epicentre if they originate at different depths or if they are of different magnitudes, since they may then be recorded by a different selection of stations.

T_e is the effect of anomalies in the crust and upper mantle

in the region of the earthquake.

Tt is the error in the calculated travel times resulting from errors in the travel time tables.

and

E represents errors which may arise from poor timing and misreading of the seismogram.

The effects of T_o and T_e can be greatly reduced by direct measurement of the relative residual as the difference between the residuals measured at two stations observing the same event. The residual difference is then the result of the subtraction of two equations of the above type (eqn.2) so that the relative station delay ($T_s - T_s'$) is contaminated with difference terms in T_o , T_e , T_t , and E .

In the case of errors due to uncertainties in the source parameters ($T_o - T_o'$), it is clear that the effect of an error in the origin time cancels from the difference equation, but this is not true of errors due to incorrect epicentres and incorrect focal depths. The delays measured here are calculated relative to those at Akureyri. The distance from Akureyri is largest for Eskdalemuir (approx. 13.5 deg) and Kiruna (approx. 17 deg), whereas the minimum epicentral distance (measured from Akureyri) is 40 degrees. We can calculate the approximate effect of errors in epicentral positions and focal depths assuming that the station at which delays

are measured relative to Akureyri is 15 degrees from Akureyri.

The error in the relative delay caused by errors in the focal depth depends on the epicentral distance to the reference station and on the focal depth; for a given depth error, the effect on the relative delay will be greatest for deep and near events (though the variations are small for the events used here). For an error of 50 km in a quoted depth of 50 km, for an event at 50 and 65 degrees from the observing stations, the error in the relative delay will be approximately 0.3 seconds. The error will be zero if the epicentral distances to the two stations are the same.

Consider the effect on the relative delay if the error in epicentral position is 25 km. If (a), the true epicentre lies on the great circle bisecting, and perpendicular to, the line joining the two stations, then the maximum error in relative delay will be caused when the epicentre is displaced perpendicular to the great circle. The error will then vary from approximately 0.8 to 0.3 seconds as the epicentral distance varies from 40 to 90 degrees. If (b), the true epicentre lies on the great circle passing through the two stations, then the maximum error in the relative delay will be caused when the epicentre is displaced along the great circle. This results from the difference in the slope of the travel time curve at Δ deg and at $\Delta + 15$ deg; this will cause an error

of approximately 0.3 seconds for observations between 25 and 95 degrees. Thus the maximum error in the relative delay, which will be caused by an error of 25 km in the epicentral position of an event recorded at two stations 15 deg apart, will range from 0.3 to 0.8 seconds.

The results of the Longshot explosion show that the U.S.C.G.S. epicentres in that region are generally located approximately 25 km North of their true positions (Marshall et al 1966). In this work, most of the earthquakes used originate in the North Pacific and U.S.C.G.S. epicentres have been assumed. If the magnitude and direction of the epicentral errors for the North Pacific data are the same as those for the Longshot region, then the displacements are close to the station bisectors and the errors will largely cancel with a residual effect on the relative delay probably not exceeding 0.4 seconds.

Since the angles between rays to the station pairs used here are small, their paths are likely to be sensibly equal at the source so that the term $(T_e - T_e')$ will tend to zero in the difference equation unless there is a strong distance or azimuth dependency.

The epicentral distances to each station in a pair are rarely equal and so errors in the travel time tables $(T_t - T_t')$ will not necessarily cancel. For this work, the calculated

travel times were taken from the Jeffreys-Bullen tables. Departures from these tables have been noted by several authors and apart from a base line shift, which cancels in the difference equation, their curves are closely similar (see references in the introduction to P-wave delays). Thus in order to minimize the error due to the term $(T_t - T_t')$, the observed residual differences were corrected according to the curve derived by Herrin et al (1968) showing departures in travel times from the Jeffreys-Bullen curve for a surface focus (Fig 7). Herrin's curve was used here because it appeared to be the best-documented curve available at the time. The surface-focus correction curve was used throughout. The corrections, which were applied to individual delay differences, were taken to the nearest 0.1 second and they ranged between plus and minus 0.8 seconds.

The reading error, E , can be large depending on the noise conditions and on the nature of the arrival. In order to remove the effects of very large values of E , which may otherwise contaminate the average residual difference between any station pair, the following procedure was adopted: Firstly, residual differences greater than ten seconds (of which there were two) were rejected, secondly, for each station pair, values of residual difference greater than two (Bessel-corrected) standard deviations from the mean were rejected.

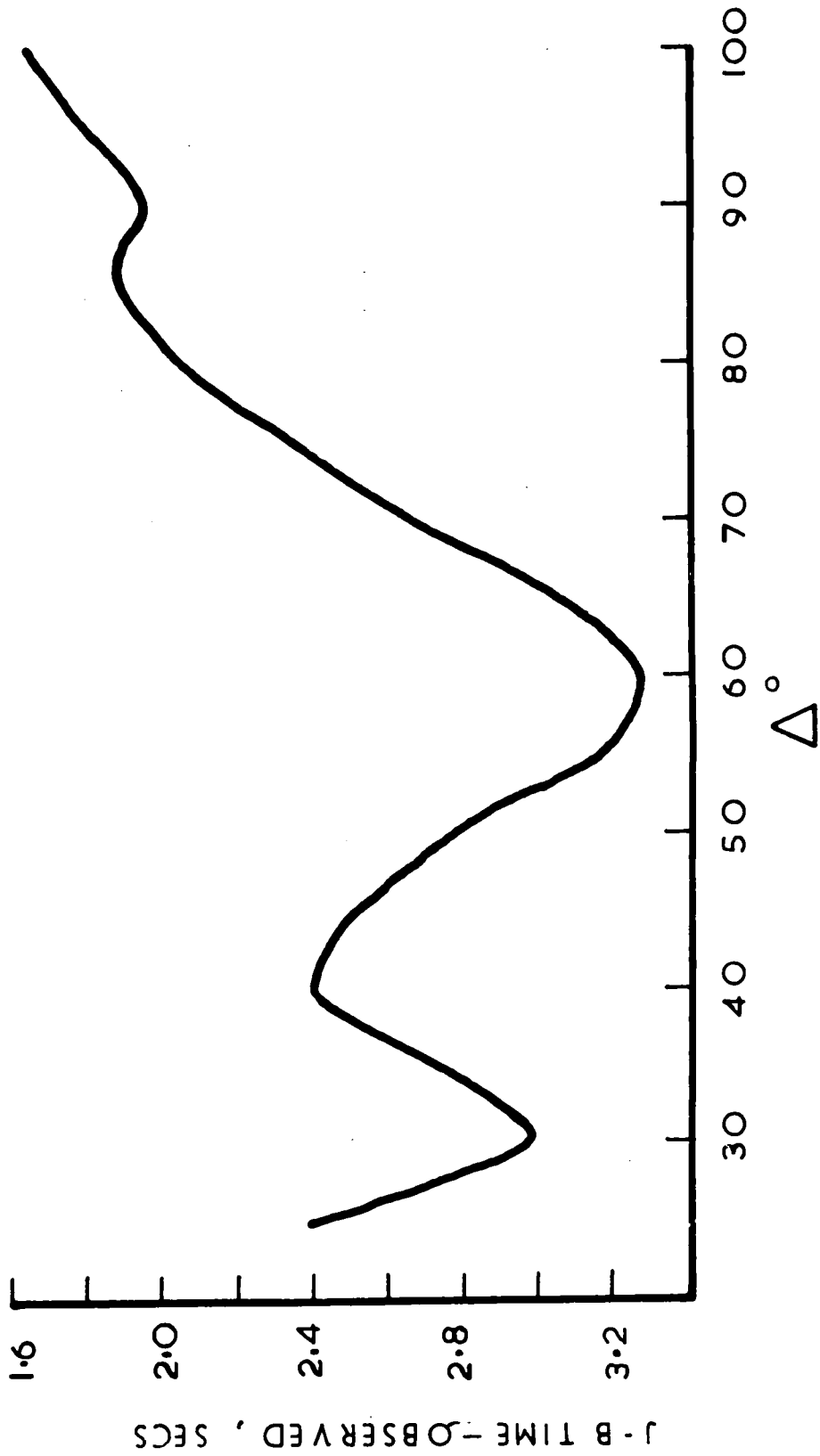


FIG 7 DIFFERENCES FROM J - B TIMES FOR SURFACE FOCUS

FROM HERRIN 1968

In this way, approximately five per cent of the data for each station pair were discarded; the remainder is referred to as culled data.

Having thus reduced the data, we may use the average of many individual measurements of residual difference to obtain an estimate of the relative delay, $(T_s - T_s')$, due to the differences in the crust and upper mantle beneath the two stations. It may however still be perturbed by the various factors in the difference equation of which T_0 (due to errors in position) and T_e (due to anomalies at the source) will probably be the greatest.

The average delay differences between station pairs were corrected, where necessary, for the effects of station elevation according to the equation:

$$dt = dh[1/V_c \cos(i_c) - \tan(i_c)/V_a] \quad (3)$$

Where: dt is the extra travel time due to the station elevation h .

i_c is the angle made by the ray at the base of the crust.

V_a is the apparent surface velocity of the ray
and V_c is the crustal velocity.

This correction was made for delays at Hveravellir (620m), Eskdalemuir (229m) and Kiruna (390m). The value used for V_c at Hveravellir was 3.0 km/sec (Tryggvason and Bath, 1961).

For Eskdalemuir, V_c is not known exactly though Agger and Carpenter (1964) assumed a velocity of 4.7 km/sec for the topmost layer. This is similar to the values found elsewhere off the coast around the British Isles (Blundell and Parks, 1967) and 4.7 km/sec was assumed for V_c in the height corrections for the delay times at Eskdalemuir. In the absence of detailed refraction data, a value of 4.7 km/sec was assumed for V_c at Kiruna. The correction is only significant for Hveravellir. As the variation in dt with epicentral distance is small, the corrections were calculated to the nearest 0.05 sec and then held constant for all distance ranges. The actual corrections used were 0.05 sec, 0.07 sec and 0.2 sec for Eskdalemuir, Kiruna and Hveravellir respectively.

(3.3) The data used in this study

Delays relative to Akureyri (AKU) were measured for stations at Kiruna (KIR) in Sweden, Kaptobin (KTG) in Greenland and for Eskdalemuir: Array Station in Scotland (Figure 6). Additional measurements were made at the Icelandic stations at Sida (SID) and Reykjavik (REY) relative to delays at Akureyri (Figure 1). The data for these measurements were taken from the monthly station picking lists for 1964, 1966, 1967 and 1968 up to and including April. Calculated onset times were taken from a Gedess printout (Young and Gibbs

1968) which was kindly prepared by Mr. J. B. Young. These were calculated using U.S.C.G.S. focal data, ellipticity corrections and Jeffreys-Bullen travel time tables. Only onsets which were reported as iP were used in this analysis; this considerably reduces the amount of usable data from the Icelandic stations and from Eskdalemuir. A complete list of the data for Akureyri, Eskdalemuir, Kiruna and Kaptobin is given in Appendix 2.

Delay measurements between the array stations at Hveravellir and Eskdalemuir were made using four teleseismic events which were recorded by both stations. Direct comparison between Hveravellir and Akureyri was impossible because of uncertainties in the clock corrections at Akureyri while the Hveravellir station was operating.

The measurements between Hveravellir and Eskdalemuir were made using the events listed in Table 2. Onset times at Eskdalemuir were taken from phased and summed channels, using the analogue equipment at U.K.A.E.A. Blacknest. The Eskdalemuir onset times determined in this way were accurate to within 0.05 sec. Onset times at Hveravellir were taken from summed channels with no inserted delays. Hveravellir onsets taken from phased and summed channels (using the analogue equipment at U.K.A.E.A. Blacknest) gave similar results with the onset apparently slightly later by approximately

TABLE 2

EVENT	DATE	ORIGIN TIME	EPICENTRE	DEPTH	MAG	Δ°	Az. ^o	Δ°	Az. ^o
		hr min sec	deg N deg E	km	mb	EKA	EKA	HVR	HVR
	1967								
A	July 20	14 26 14.1	51.4 178.3	33	5.3	73.6	359	63.3	348
B	Aug. 10	11 21 22.3	45.4 150.3	37	5.7	77.2	19	69.8	8
C	Aug. 13	20 06 50.6	35.3 135.3	357	6.0	83.0	33	78.2	21
D	Aug. 24	03 21 17.6	43.5 147.5	70	5.4	78.4	21	71.5	10

0.1 seconds.

The records of the arrivals used at Hveravellir are shown in Figure 8 where the top trace in each pair is the output from an unfiltered, single, vertical channel and the bottom trace is the output from the unphased and unfiltered sum of N channels. The gains are similar for each event, with the single-channel record of event C, for example, representing a gain of approximately 30,000. The summed channels produced onsets which were clear though not different from those which might be picked from single-channel records. However, the onsets on the summed channel records are unambiguous. The channels used for the summation were those which were closest to the crossover point of the array; poor channels, i.e. those which were very noisy or which showed ringing, were excluded from the sum. The onsets at Hveravellir, which were taken from the summed channel records, are marked with a dash in Figure 8. These could be read to within 0.1 sec.

A comparison between the waveforms recorded at each station showed that, while the arrivals from common events were similar, they were not sufficiently alike for a common part of the waveform to be used for the measurement of relative delays. This is partly due to the difference in instrument response at the two stations and partly due to the different crust and upper mantle structure beneath the two

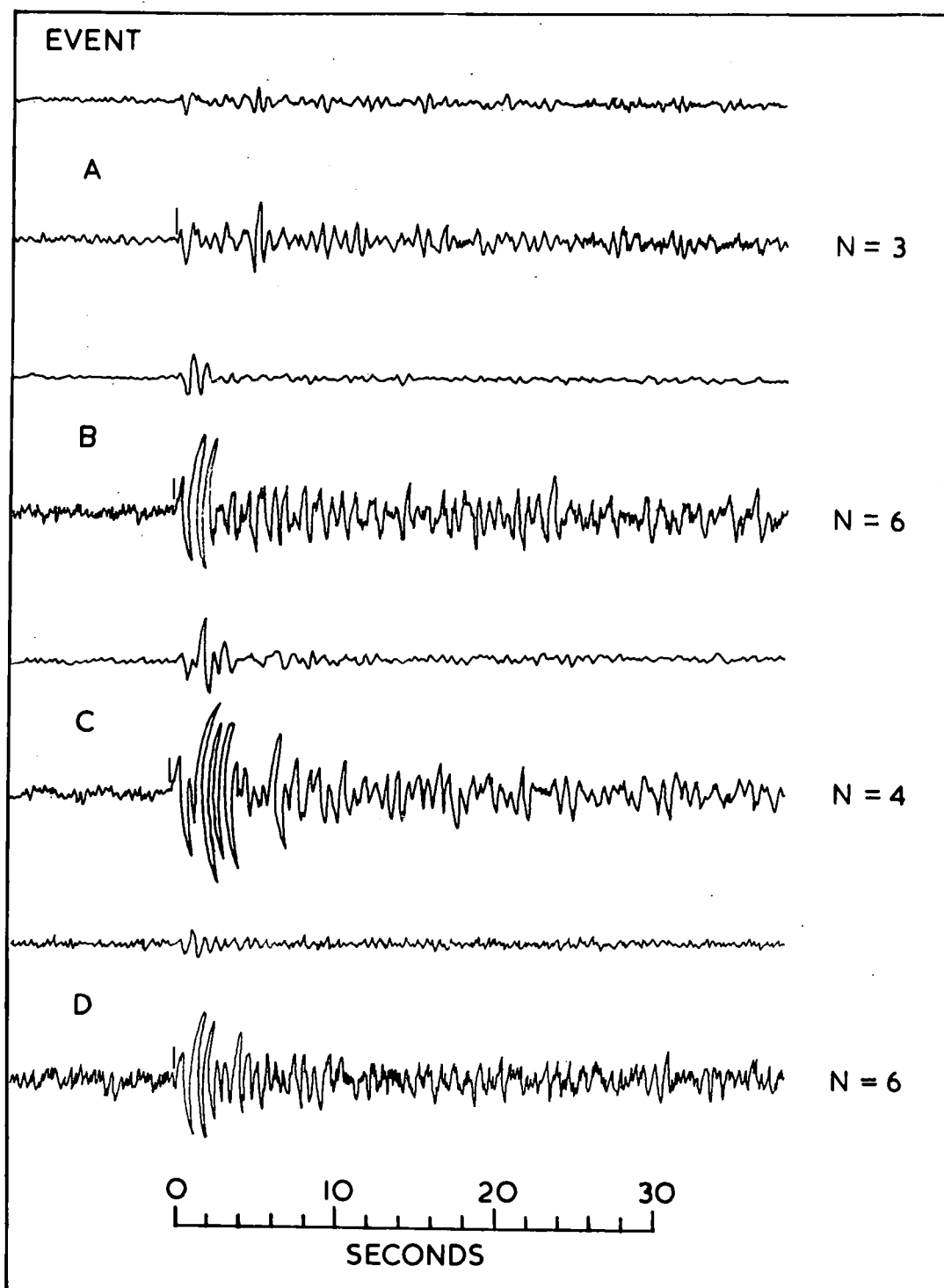


FIG. 8. HVERAVELLIR TELESEISM RECORDS FROM SINGLE CHANNELS AND FROM SUM OF N CHANNELS.

stations.

(3.4) Results of the delay measurements

Delays relative to Akureyri at Eskdalemuir, Kiruna and Kaptobin are presented in Tables 3, 4 and 5 as averages over 10 degree intervals in epicentral distance measured from Akureyri. (In Tables 3, 4, 5 and 6 the following notation is used: n = number of observations, \bar{X} = mean delay difference, $\hat{\sigma}$ = standard deviation, and α = standard error on the mean). Most of the data comes from the North Pacific between Alaska and Japan and are not sufficient to permit a separate consideration of azimuthal variations in delay. With the exception of measurements between Hveravellir and Eskdalemuir, all the data are culled according to the method described earlier. All estimates of errors are based on the culled data alone and are made according to Bessel-corrected standard deviations (Moroney 1951).

Figure 9 demonstrates clearly the similarity in delays at Akureyri relative to Eskdalemuir and Kaptobin in the 50 to 80 degree distance range, and the apparent absence of distance/azimuth variations over this range. Relative to Kiruna on the other hand, the delay is somewhat larger between 50 and 70 degrees but drops to be sensibly equal in the 70 to 90 degree range; this drop appears to be significant at the 95%

TABLE 3

Delay (AKU - EKA)

Δ°	n	\bar{X} sec	$\hat{\sigma}$	α
80's	4	1.83	0.93	0.47
70's	12	1.36	1.10	0.32
60's	24	1.45	0.69	0.14
50's	14	1.41	0.88	0.23
40's	12	1.76	0.71	0.21
all	66	1.50	0.83	0.10

TABLE 4

Delay (AKU - KIR)

Δ°	n	\bar{X} sec	$\hat{\sigma}$	α
80's	7	1.48	0.73	0.28
70's	24	1.50	0.48	0.10
60's	35	2.33	0.97	0.17
50's	27	2.23	0.56	0.11
40's	14	2.26	0.52	0.14
all	107	2.05	0.72	0.07

TABLE 5

Delay (AKU - KTG)

Δ°	n	\bar{X} sec	$\tilde{\sigma}$	α
80's	4	0.80	0.39	0.20
70's	15	1.38	0.61	0.16
60's	20	1.53	0.82	0.18
50's	14	1.36	0.96	0.26
40's	5	0.66	0.59	0.26
all	58	1.32	0.79	0.10

TABLE 6

Delay (AKU - REY) & Delay (AKU - SID)

DELAY	n	\bar{X} sec	$\tilde{\sigma}$	α
(A-R)	16	-.19	0.50	0.13
(A-S)	24	0.09	0.43	0.09

TABLE 7

Delay (HVR - EKA)

EVENT	Δ° HVR	D min sec	D max sec
A	63.3	1.4	1.6
B	69.8	1.4	1.4
C	78.2	1.9	2.1
D	71.5	1.0	1.2
all	—	1.4	1.6

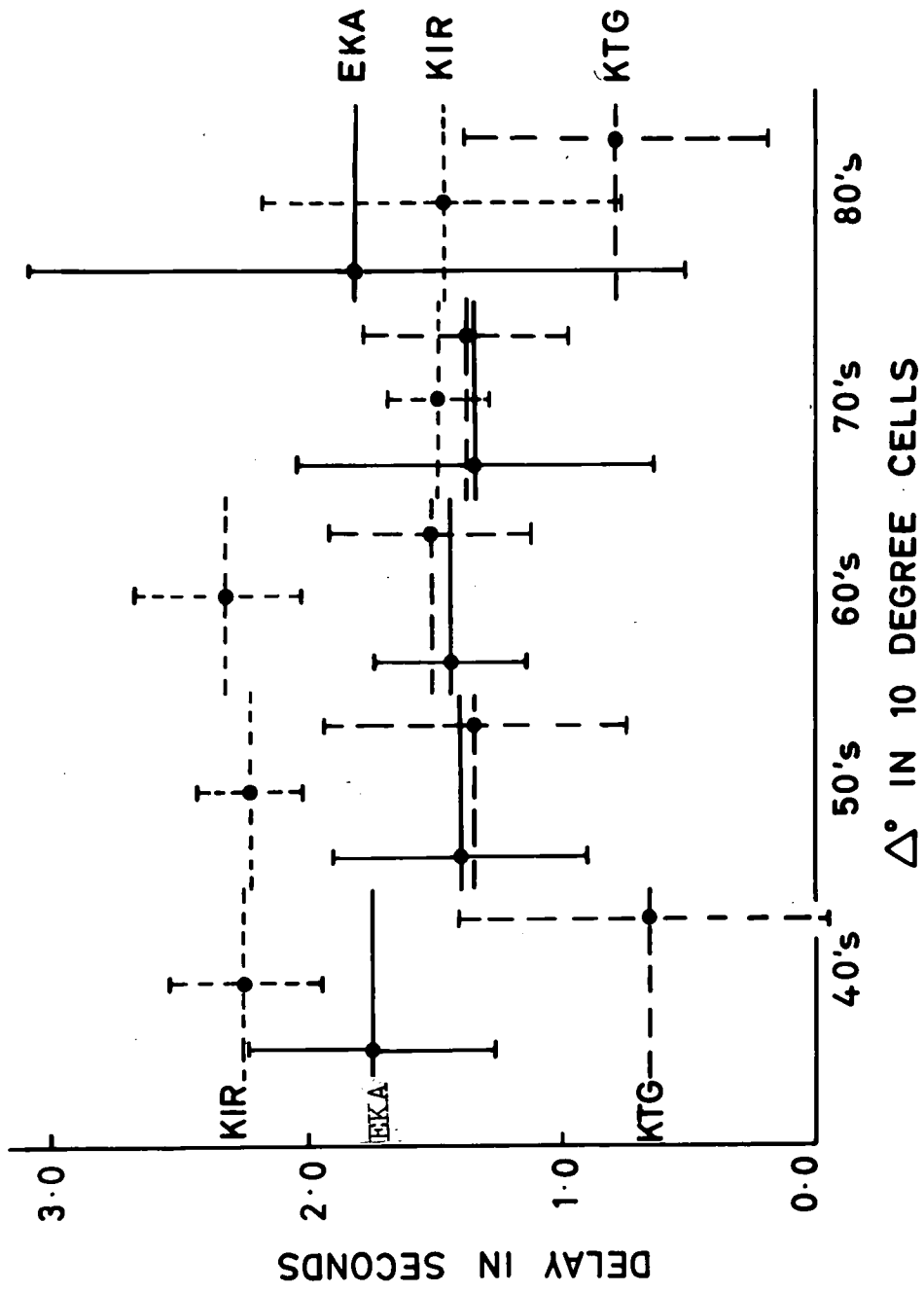


FIG. 9 DELAY RELATIVE TO AKUREYRI SHOWING
 Δ° IN 10 DEGREE CELLS
 95% CONFIDENCE LIMITS

confidence level. It is clear from the confidence levels shown on the figure that most of the observations below 50 degrees and above 80 degrees in distance are not very significant by themselves; this is due to the lack of data in these distance ranges.

The importance of the accuracy of the travel time tables can be seen by comparing the above delays with those deduced from the same data without applying Herrin's corrections (Fig. 10). Marked differences are seen between the relative delays at Eskdalemuir and at Kaptobin which vanish when the table corrections are applied. Furthermore, the scatter on the corrected data is reduced.

Delays at Reykjavic and Sida relative to those at Akureyri are shown in Table 6. These are averaged over all distance and azimuth ranges because of the small amount of data available. It may be seen that the delays are not significantly different from zero.

Measurements of the relative delays between Hveravellir and Eskdalemuir are shown in Table 7 for the four teleseismic events which are listed in Table 2. Errors here are due to possible timing errors at Hveravellir and the delays are given accordingly as maximum and minimum values. If the maximum allowance is made for possible timing errors at Hveravellir, then there is a range in the relative delay measurements of

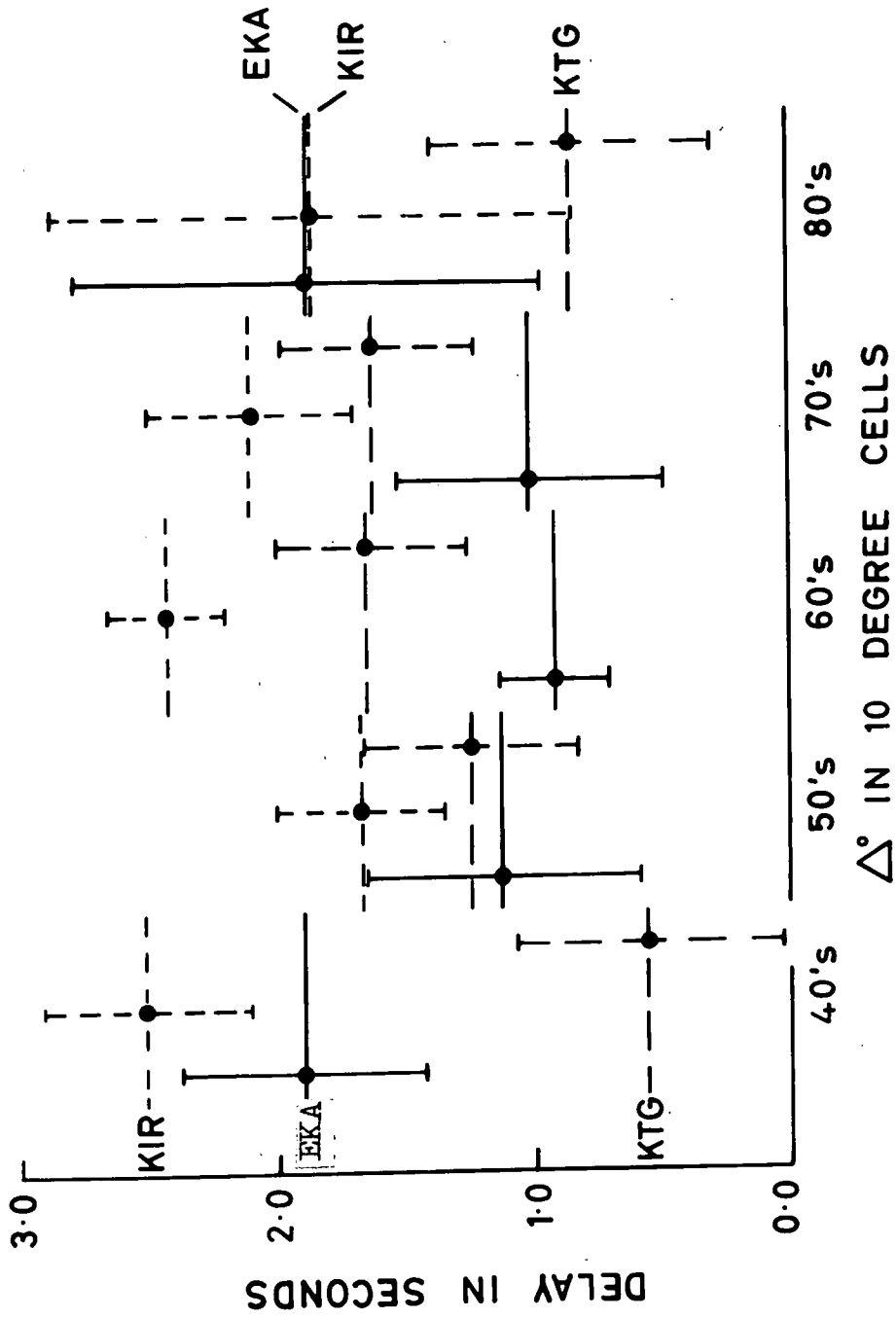


FIG.10 DELAY RELATIVE TO AKUREYRI WITHOUT HERRIN'S CORRECTIONS

at least 0.7 seconds for these four events. This is outside the range of reading errors and is unlikely to be accounted for by errors in the calculated (and corrected) travel times. Therefore this range of values reflects the inherent uncertainty in relative delay measurements which may be caused by (a) possible mislocation of the source, and (b) possible lateral variations in the structure beneath the source region. Thus it is likely that, however accurately the onsets may be determined, a single relative delay measurement from one earthquake is not reliable to within more than a few tenths of a second.

The average delay difference between Hveravellir and Eskdalemuir of 1.5 seconds is in good agreement with the value obtained for Akureyri and Eskdalemuir. It seems likely that a delay of 1.5 seconds relative to Eskdalemuir is, within the limits of error, constant over Iceland.

The distance variation in the relative delay at Kiruna is obviously caused either by the source region or by the structure beneath Kiruna. The latter explanation is considered unlikely as the delay measurements over Fennoscandia made by other authors (e.g. Cleary and Hales, 1966) are fairly constant implying lateral homogeneity over the region. Therefore it is considered unlikely that there are any lateral inhomogeneities beneath Kiruna which would cause the observed

change in delay time with distance and azimuth. A small change in the relative delay with distance is expected if Tryggvason's interpretation is correct (see later and Appendix 3), but this should result in a drop in the relative delay at Kiruna of only 0.1 seconds (approx.) between 65 and 75 degrees. Thus there is an unexplained drop in delay of 0.7 seconds.

It has been mentioned earlier that epicentral errors can cause errors in the observed delay difference. Thus if the direction or the magnitude of the epicentral errors changes for events more than 70 degrees from Akureyri then this could cause a change in the relative delay measured at Kiruna. However, there is little sign of such an effect on the relative delays at Eskdalemuir where the change should be smaller but of the same sign.

Most of the data used in this study come from earthquakes originating near the island arc structures between Alaska and Southern Honshu (Fig. 6). It is most probable that these arcs are the surface features marking the down-thrusting of an oceanic plate into the upper mantle (Sykes 1966, Oliver and Isacks 1967, Isacks et al 1968, Le Pichon 1968, Morgan 1968). This results in an anomalous zone in the mantle of the order of 100 km in width and extending to a depth of some 700 km in which the seismic velocities may be higher than in

the normal mantle by 1-2% (Oliver and Isacks 1967). As the earthquakes beneath the island arcs appear to lie above the anomalous zone, the structure may result in azimuthal variations in travel times (in an investigation of the Longshot explosion, Herrin and Taggart (1968b) found an azimuthally dependent source term with an amplitude of 1.3 seconds). The anomalous structure may cause a non-zero value for the difference term $T_e - T_e'$ thus producing an error in the relative delay between the two stations.

For example, if rays to Kiruna, from the more distant events, are travelling through normal mantle, while those to the other stations pass through the high-velocity plate for 500 km with a velocity increase of 1%, then the relative delay at Kiruna would change by approximately 0.5 seconds. Relative delay measurements at Kiruna, from events at similar distances but at different azimuths from Akureyri, are too few to enable this hypothesis to be checked.

The differences in the sub-Moho velocities beneath Kiruna and Eskdalemuir (Table 9) are consistent with a difference between the relative delays at the two stations and it is considered that 2.3 seconds is the more likely value for the delay at Akureyri relative to Kiruna. The general consistency of the delay times at the other stations suggests that this effect only occurs for the Kiruna data.

(3.5) Comparison with other delay time measurements

Delay times for some of the stations used here, and for the Greenland station at Scoresbysund - which is very close to Kaptobin - have been measured by several workers (Cleary and Hales 1966, Herrin and Taggart 1968a, Tryggvason 1964). Unlike those of the other authors, the delays measured by Herrin and Taggart are given in the form of $A + B \sin(\text{azimuth} + E)$ where A is the 'baseline' delay and the second term depends on the azimuth of the source from the station. For Reykjavik and Kaptobin, the second term is sensibly equal for each station ($B = 0.59$ and 0.46 respectively) and zero for events from due North. For Kiruna the azimuth variation is small ($B = 0.19$) and approximately 180 degrees out of phase with that for Reykjavik and Kaptobin. In order to make a comparison with the measurements presented here, only the 'baseline' delays given by Herrin and Taggart are considered.

The results of the various delay time measurements, expressed as delay differences, are given in Table 8. (N refers to the minimum number of observations used in each station pair). It can be seen that with the exception of Cleary and Hales measurements, which are based on only five observations at Reykjavik, the general agreement is good. The agreement with Herrin and Taggart's values is the best. Assuming that the delay difference between Reykjavik and

TABLE 8

SOURCE	STATIONS	DELAY sec	n
M.M. (40° - 70°)	AKU - KIR	2.3	76
M.M. (70° - 90°)	AKU - KIR	1.5	31
M.M. (40° - 90°)	AKU - KIR	2.1	107
Tryggvason	REY - KIR	2.9	94
Herrin and Taggart	REY - KIR	2.3	26
Cleary and Hales	REY - KIR	1.0	5
M.M.	AKU - KTG	1.3	58
Tryggvason	REY - SCO	1.7	26
Herrin and Taggart	REY - KTG	1.3	19
Herrin and Taggart	REY - SCO	1.0	26
Cleary and Hales	REY - SCO	.5	5

Akureyri is zero, then it appears that 2.3 seconds is the most likely value for the delay difference (AKU - KIR) rather than the value of 1.5 seconds which was measured here for distances between 70 and 90 degrees. The assumption that the delay difference (AKU - REY) is zero is supported by the agreement between the value reported here for the delay difference (AKU - KTG) and that reported by Herrin and Taggart for the delay difference (REY - KTG).

Both the results reported here, and those obtained by Herrin and Taggart, suggest that the relative delays obtained by Tryggvason may have been slightly overestimated.

(3.6) Interpretation of the delay times

The relative delay times between stations can be interpreted in terms of the differences in the crust and upper mantle structure beneath the stations. For certain regions delay times have been explained in terms of crustal structure alone (Barr and Robson 1963). In this case, an interpretation in terms of the crustal structure alone is impossible. The crustal structures beneath Iceland, Eskdalemuir and Kiruna (Table 9) are known in some detail and it is clear that the relatively thin, high-velocity crust beneath Iceland should lead to negative delay times. Thus the delay in Iceland must be due to a mantle anomaly. A unique interpretation cannot

be made on the basis of the data presented here as it is impossible to distinguish the effect of a change in layer thickness from that of a change in layer velocity. However, Tryggvason (1964) has suggested a method of interpretation which makes the assumption that the sub-Moho velocity beneath each station remains constant down to some common depth, H .

Using Tryggvason's method, the delays at Akureyri relative to Eskdalemuir and Kiruna have been used to determine the depth to the base of the 7.4 layer beneath Iceland. The derivations of the equations used in this method are given in Appendix 3. The calculations were made using the crustal structures given in Table 9 for Iceland (Bath, 1960), Eskdalemuir (Agger and Carpenter, 1964) and Kiruna (Tryggvason 1961b) where H_c = the crustal thickness, V_c = the crustal velocity and V_m = the sub-Moho velocity.

The depths, H , are shown in Table 10 for observations in each 10 degree interval where the error α corresponds to the standard error in the mean of the relative delay in each distance interval. It can be seen that, with the exception of delays relative to Kiruna between 70 and 90 degrees, which are regarded as incorrect, the values of H for both the Eskdalemuir and the Kiruna data are in good agreement. The mean value of H , taken from the weighted averages of the values from the individual cells is 200 km. (Excluding data

TABLE 9

Region :-	ICELAND	ESKDALEMUIR	KIRUNA
Hc km	18	25	35
Vc km/sec	6.7	6.12	6.2
Vm km/sec	7.4	8.0	8.36

TABLE 10

Δ°	STATIONS	X sec	n	H km	α km
80's	AKU - EKA	1.83	4	240	42
70's		1.36	12	191	29
60's		1.45	24	195	12
50's		1.41	14	186	19
40's		1.76	12	211	17
80's	AKU - KIR	1.48	7	167	19
70's		1.50	24	165	6
60's		2.33	35	207	10
50's		2.23	27	198	6
40's		2.26	14	194	7

For AKU - EKA mean H = 197 km (all Δ)

AKU - KIR mean H = 165 km ($\Delta = 70^\circ - 90^\circ$)

AKU - KIR mean H = 202 km ($\Delta = 40^\circ - 60^\circ$)

(Using mean H = $\sum nH / \sum n$)

from Kiruna between 70 and 90 degrees and taking mean $H = \sum nH / \sum n$). The effect of errors in epicentral position may alter H by ± 25 kms.

If the calculations are repeated using delays at Eskdalemuir or Kiruna relative to Reykjavik, Sida or Hveravellir, then H is changed by less than 20 km, though this variation in H is probably not significant. As one would expect from the difference in delay times, the value of H calculated here is less than the 240 km calculated by Tryggvason. The results obtained here are in good agreement with those obtained by Francis (1969) from $dt/d\Delta$ measurements for the axis of the Mid-Atlantic Ridge near Iceland. Francis interpreted his data in terms of a linear increase of velocity with depth which resulted in a geometric mean velocity of 7.38 km/sec for the uppermost 200 km.

The delays relative to Kaptobin cannot be interpreted directly as we have no knowledge of the crustal structure beneath the station. However, the similarity of the relative delays at Kaptobin and Eskdalemuir may indicate a structural symmetry in a northwest-southeast direction about Iceland. As it is most probable that Greenland and Europe were part of one land mass before continental drift took place (Einarsson 1967), such a symmetry might be expected. It is notable that, while delay times at Kaptobin are typical of a tectonic

region, those at Nord in the northeast and at Godhavn in the west of Greenland are typical of a shield region (Cleary and Hales 1966, Herrin and Taggart 1968).

The interpretation of the relative delay times in terms of a constant mantle velocity to a common depth is probably an oversimplification. The delay times basically reflect the differences between the upper mantle structures beneath ocean ridges (Iceland), tectonic regions (Eskdalemuir and probably Kaptobin) and shields (Kiruna). Consistent regional trends in delay times measured by other authors (Cleary and Hales 1966, Herrin and Taggart 1968a) show that P-wave arrivals are early in shield and late in tectonic regions. Apart from Icelandic delays, data on ocean ridges are sparse. While data on the P-wave velocity structure of the upper mantle is incomplete, a fairly detailed picture of the shear velocity structure is presented from Love wave dispersion data.

Figure 11 shows the oceanic, tectonic and shield models of the mantle derived from Love wave data by Toksoz et al (1967).

It is clear that the main differences between the regions are in the structure of the low-velocity zone (l.v. zone) in the upper-most 350 km. The l.v. zone is shallower and more pronounced under oceans than elsewhere. The "lid" on the l.v. zone becomes thicker and higher in velocity as we progress from ocean to tectonic to shield. The velocities in the l.v. zone

Shear velocity (km/s)

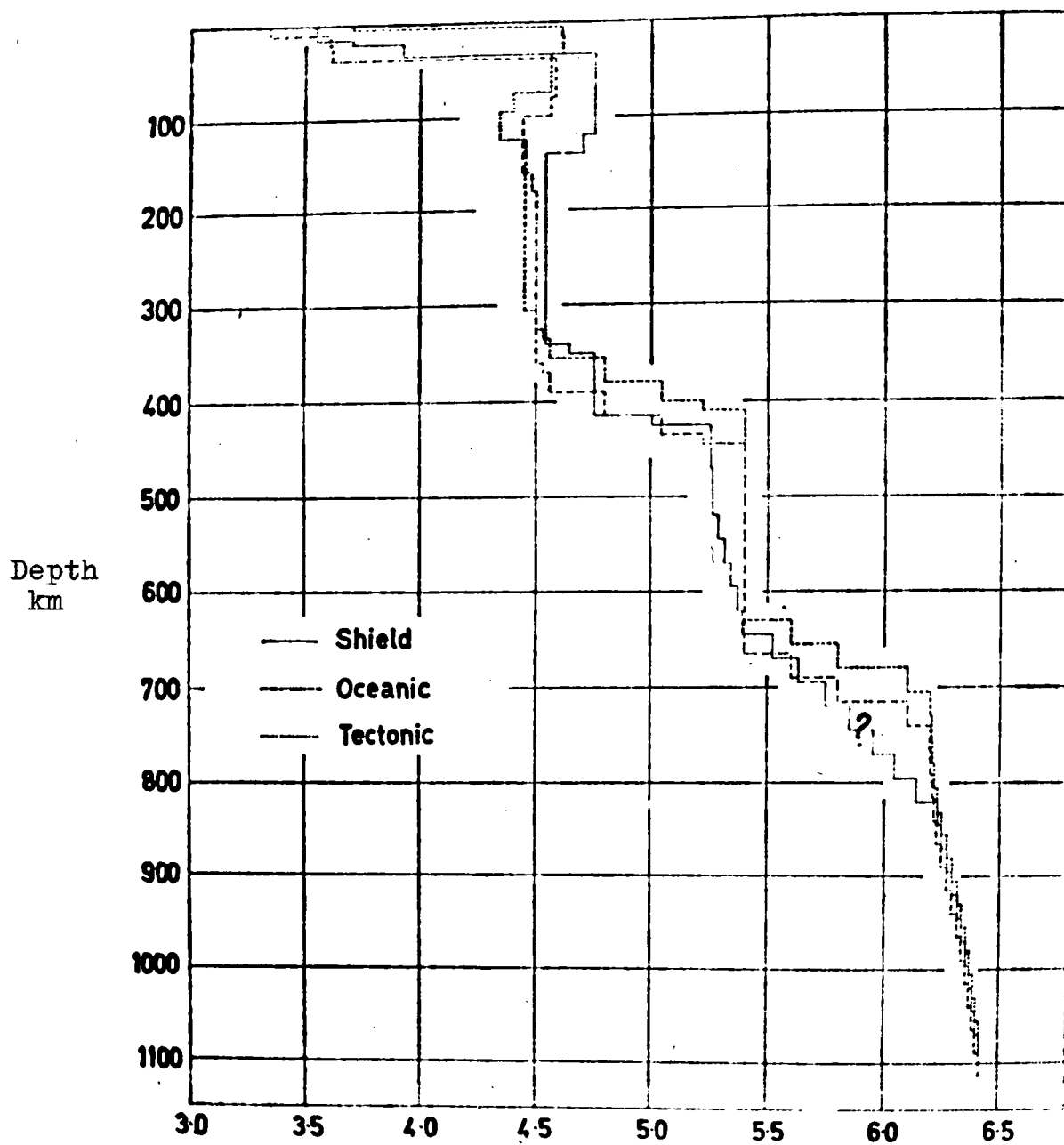


Fig. 11

also show a progression to higher values beneath shields and the depth to the top of the zone decreases from about 120 km beneath shields to about 80 km beneath oceans, while the tectonic mantle represents an intermediate situation.

We may use the shear-wave velocity models in Figure 11 to obtain the approximate P-wave delays for stations on oceanic, tectonic and shield regions caused by differences in the low velocity zone in the uppermost 350 km. Taking the models in Figure 11 and assuming that the ratio $\alpha/\beta = 1.76$ (Anderson and Toksoz 1963) and superimposing the crustal structure for Iceland, Eskdalemuir and Kiruna we can calculate the relative delay times for vertical P-wave arrivals. Modifying the oceanic model for Iceland so that the low-velocity spur extends to the base of the crust, we derive the sub-moho velocities 7.64, 8.36 and 8.08 km/sec for Iceland, Kiruna and Eskdalemuir respectively. Considering the structures down to 350 km, we derive the relative delay times: (AKU-EKA) = 0.5 sec and (EKA-KIR) = 0.6 sec. For the model calculated earlier, using Tryggvason's method, the relative delay times for vertical arrivals are: (AKU-EKA) = 1.2 sec and (EKA-KIR) = 0.6 sec.

It is clear that the Eskdalemuir and Kiruna delays are reasonably well satisfied by the model, yet the Icelandic delay is too small even after modifying the oceanic curve to

continue the low-velocity spur to the base of the crust. The assumption of a constant ratio of α/β for all regions is probably incorrect but, with the likelihood of partial fusion within the oceanic mantle, which would affect β more drastically than α , the Icelandic delay calculated above is probably overestimated. (If we consider the difference in structure below 350 km, where in Figure 11 the oceanic velocities are higher than those for tectonic and shield regions, then the fit to the data is made worse.) Therefore the mantle beneath Iceland must be considerably modified from the structure indicated for oceanic regions in order to explain the observed delay times.

(3.7) Gravity and seismological data on the mantle beneath Iceland

In order to evaluate possible mantle models to explain the anomalous structure beneath Iceland, it is necessary to consider the gravity and the seismic data together as this puts an additional constraint on the solution.

The arguments outlined in the first part of this section closely follow those given by Bott (1965a, 1965b). The average Boug^uer anomaly in Iceland is +15 mgal (Einarsson 1954). If the upper mantle beneath Iceland were normal, this would

suggest that the Icelandic crust is of continental thickness. However, seismic evidence suggests that the crust is only about 17 km thick and that it has a high average P-wave velocity (Stefansson 1967). Combining these observations, Bott suggests that the upper mantle beneath Iceland possesses an anomalously low density which contributes a gravity anomaly of about -250 mgal. This could be caused by a reduction in density of 0.03 g/cm^3 extending over a vertical thickness of at least 225 km, or 0.3 g/cm^3 over at least 23 km.

Thermal expansion and changes in the depth of such phase changes as basalt-eclogite appear to be inadequate as an explanation of the low-density mantle and the hydration of olivine to low-density serpentine is prohibited by the high geothermal gradient of Iceland. The empirical relationships between P-wave velocity and density suggest that a velocity of 7.4 km/sec implies a density which is at least 0.15 g/cm^3 lower than the average for the topmost mantle. If this were spread over a vertical extend of 200 km, in accordance with the delay time requirements, it would cause a mass deficiency of more than four times the necessary value. This suggests that the low density is not caused by common rock types with relatively low density. The remaining explanation is that the low-density and the low-velocity upper mantle is the result of partial fusion.

As Iceland overlies, or is part of, the Mid-Atlantic Ridge, then on the convection current hypothesis, it overlies an uprising convection cell (Bott 1967, Oxburgh and Turcotte 1968). Partial fusion in the upper mantle is most likely to occur in an uprising convection cell as the temperatures are highest there for any given depth. Taking the minimum estimate of the difference between the adiabatic and fusion gradients as 1.0°C/km , the specific heat as 1.2 J/g and the heat of fusion as 400 J/g , Bott (1965b) calculated that the amount of fusion possible in a 33 km rise is 10% . The magma produced in this way would tend to rise towards the surface owing to its low density thus forming a network of dykes and magma chambers in the layer overlying the convection cell, so the mass deficiency is probably partly within the topmost part of the upwelling convection current and partly within the overlying layer where it may build up to a substantial fraction locally.

Experiments by Daly (1944) show that basalt undergoes a reduction in density of approximately 10% or 0.3 g/cm^3 on fusion. As the fused fraction of an ultrabasic parent rock is likely to undergo a similar reduction in density, then a fused fraction on 10% will cause an overall reduction in density of 0.03 g/cm^3 . Extending over a depth of 200 km this is sufficient to account for the observed gravity. Thus the

picture which emerges is that the gravity anomaly in Iceland is caused primarily by the reduction in density of the upper mantle due to partial fusion. (Similarly, partial fusion provides an attractive mechanism to explain the uplift of ocean ridges elsewhere.)

The effect of partial fusion on velocity is difficult to evaluate. Generally, seismic velocities will be lowered though the effect on the shear velocity will be greatest so the ratio α/β will be increased (Oxburgh and Turcotte 1968). Expressions for the elastic moduli of two-phase (all solid) materials have been derived by Hashin (1966) and by Wu (1968). Walsh (1968) has examined the problem of the effect of partial melting on attenuation using Wu's equations and substituting a complex function of viscosity for the rigidity of the liquid phase. Using Walsh's equations it is possible to obtain an expression for P-wave velocity as a function of the melt concentration. Using values of bulk modulus, rigidity and density given by Bullen (1963) corresponding to a P-wave velocity of 7.95 km/sec, and taking the viscosity of the melted fraction as 10^{10} dynes sec/cm² and the bulk modulus as 10^{11} dynes/cm², then a fusion fraction of 10% results in a reduction of the P-wave velocity to approximately 6.5 km/sec for a 1cps arrival.

However, the resulting P-wave velocity depends very much on the value chosen for the viscosity of the liquid phase.

Measurements on silicate-water systems vary from 10^{14} dyne sec/cm² at 635°C and nearly zero H₂O, to 10^5 dyne sec/cm² at about 800°C and 6% H₂O (Shaw 1963). Further complications arise from the possibilities of different distributions of the melt within the solid phase as these can result in different effective elastic constants for the same melt concentration.

While it appears that partial fusion in the mantle beneath Iceland can result in a marked reduction of the P-wave velocity, without more detailed information on the elastic properties of fused mantle material and on its distribution within the solid, it has not been found possible to find a definite relationship between velocity and the concentration of the melt phase.

(3.8) Discussion

A model for the upper mantle beneath Iceland with partial fusion as the dominant cause of the low velocity and the low density, is in keeping with the results of other workers in similar areas. Hales and Doyle (1967) discussed the implications of the large ratio of S to P travel time residuals in the western United States. They concluded that the large ratio could not be explained in the terms of temperature unless one component of the system approaches its melting point or some new thermoelastic effect occurs. They also showed that the relationship between the P-wave travel time residuals

and the gravity anomalies is not consistent with the Birch (1961) relation between velocity and density. Further, Francis' (1969) work on $dt/d\Delta$ in the Mid-Atlantic Ridge near Iceland revealed a large ratio of α/β . While further measurements are needed to verify this last observation, it is compatible with the partial fusion hypothesis.

On the other hand, Talwani et al (1965) produced models to explain the gravity anomalies over the Mid-Atlantic Ridge, at approximately 35 degrees North, of which the most important feature, in this context, is that the low-density material extends to a maximum depth of about 40 km. This implies the presence of normal mantle material below 40 km which is compatible neither with the results presented here from P-wave delays nor with the velocity structure deduced by Francis. However, in their calculations, Talwani et al assumed that the densities and velocities are empirically related according to the curve given by Nafe and Drake (Talwani et al 1959). If there is partial fusion within the upper mantle beneath ocean ridges, then the empirical relationships between velocity and density break down, in which case the model deduced by Talwani et al may not be valid.

While certain features of Iceland, i.e. its isostatic equilibrium, high heat flow and the presence of the 7.4 layer, indicate that it is similar to the mid-ocean ridge system as

a whole, the fact that it has such a thick crust and that it is an island and not below sea level, suggest that it is not typical of the ridge system. It is therefore possible that the great vertical extent of the 7.4 layer, which is required to explain the P-wave delays in Iceland, is not necessarily present beneath the other parts of the Ridge which are remote from Iceland. This possibility could be investigated by measuring P-wave delays elsewhere on the Ridge using ocean-bottom seismometers. The presence of partially fused material should produce a large ratio of S to P delays and it should also result in high attenuation of shear waves. The measurement of these two factors in Iceland would produce a valuable, and highly desirable, check on the partial fusion hypothesis.

Conclusions

The delay measurements presented here clearly show that teleseismic arrivals recorded at Akureyri in Iceland are delayed by approximately 1.5 seconds relative to those recorded at the Eskdalemuir Array Station in Scotland; relative to Kiruna in Sweden, the delay at Akureyri is approximately 2.3 seconds. Delay measurements at Hveravellir relative to Eskdalemuir, and at Reykjavik and Sida relative to Akureyri, suggest that a delay of 1.5 seconds relative to Eskdalemuir is constant over Iceland. The delays at Eskdalemuir and Kaptobin in Greenland are approximately equal, which may indicate a structural symmetry about the Mid-Atlantic Ridge in Iceland.

The interpretation of the delays in Iceland relative to those at Eskdalemuir and Kiruna, suggests that the 7.4 layer extends to a depth of 200 km beneath Iceland. It is recognised that the interpretation of delay times in terms of a constant velocity down to some fixed depth is probably an oversimplification, but a more sophisticated approach is not possible on the basis of delay times alone. A comparison with the shear wave velocity-depth profiles for Oceanic, Tectonic and Shield regions show that while the profiles are compatible with the relative delays between Kiruna and Eskdalemuir, the upper mantle beneath Iceland must be consider-

ably modified from the normal Oceanic velocity-depth structure in order to explain the Icelandic delays.

The great vertical extent of the 7.4 layer which is necessary to explain the Iceland delay times, is incompatible with the models produced by Talwani et al for the Mid-Atlantic Ridge further South. It is suggested that either the model deduced by Talwani et al is incorrect or Iceland is an anomalous part of the Mid-Atlantic Ridge. This conflict can best be resolved by delay time measurements elsewhere on the Ridge and by a comparison of P and S wave delays in Iceland.

REFERENCES

- Agger, H. E. and Carpenter, E. W. 1964 A crustal study in the vicinity of the Eskdalemuir seismological array station, Geophys. J. R. astr. Soc., 2, 69-83.
- Anderson, D. L. and Toksoz, M. N. 1963 Surface waves on a spherical earth, 1, Upper structure from Love waves, J. Geophys. Res., 68, 3483-3500.
- Avery, G. et. al. 1968 An aeromagnetic survey of the Norwegian Sea, J. Geophys. Res., 73, 4583-4600.
- Barr, K. G. and Robson, G. R. 1963 Seismic delays in Eastern Caribbean, Geophys. J. R. astr. Soc., 7, 342-350.
- Bath, M. 1960 Crustal structure of Iceland, J. Geophys. Res., 65, 1793-1807.
- Birch, F. 1961 Velocity of compressional waves in rocks up to 10 kilobars, J. Geophys. Res., 66, 2199.
- Birtill, J. W. and Whiteway, F. E. 1965 The application of phased arrays to the analysis of seismic body waves, Phil. Trans. R. Soc., A, 258, 421-493.
- Blundell, D. J. and Parks, R. 1967 A study of the crustal structure beneath the Irish Sea, Geophys. J. R. astr. Soc., 17, 45-62.
- Bodvarsson, G. and Walker, G. P. L. 1964 Crustal drift in Iceland, Geophys. J. R. astr. Soc., 8, 285-300.

- Bott, M. H. P. 1965a The upper mantle beneath Iceland, Geophys. J. R. astr. Soc., 9, 275-277.
- _____ 1965b Formation of ocean ridges, Nature, 207, 840-843.
- _____ 1967 Terrestrial heat flow and the mantle convection hypothesis, Geophys. J. R. astr. Soc., 14, 413-428.
- Bullen, K. E. 1963 Introduction to the theory of Seismology, Cambridge University Press.
- Carder, D. A. 1964 Travel times from central Pacific nuclear explosions and inferred mantle structure, Bull. Seism. Soc. Am., 56, 2271-2294.
- _____ 1966 Analysis of surface-foci travel times, Bull. seism. Soc. Am. 56, 818-840.
et. al.
- Carmichael, I. S. E. 1964 The petrology of Thingmuli, a tertiary volcano in eastern Iceland, J. Petrol., 5, 435-460.
- Cleary, J. and 1966 An analysis of the travel times of Hales, A. L. P waves to North American stations, in the distance range 30° to 100°, Bull. seism. Soc. Am., 56, 467-489.
- Daly, R. A. 1944 Volcanism and petrogenesis as illustrated in Hawaiian Islands, Bull. geol. Soc. Am., 55, 1363.
- Einarsson, T. 1954 A survey of gravity in Iceland, Soc. Sci. Islandica, publication 30.

-
- 1967 Early history of the Scandic area and some chapters of the geology of Iceland, in Iceland and Mid-Ocean Ridges, Soc. Sci. Islandica 'Rit' 38, edited by S. Bjornsson, 13-31.
- Ewing, J. and
Ewing, M. 1959 Seismic-refraction measurements in the Atlantic Ocean basins, in the Mediterranean Sea, on the Mid-Atlantic Ridge, and in the Norwegian Sea, Bull. geol. Soc. Am., 70, 291-318.
- Francis, T. J. G. 1969 Upper mantle structure along the axis of the Mid-Atlantic Ridge near Iceland, Geophys. J. R. astr. Soc., 17, 507-520.
- Girdler, R. W. 1963 Geophysical studies of rift valleys, Physics and Chemistry of the Earth, 5, 122-154.
- Greensfelder, R. W. 1965 The Pg-Pn method of determining depth of focus with applications to the Nevada Earthquakes, Bull. seism. Soc. Am., 55, 391-403.
- Hales, A. L. and
Doyle, H. A. 1967 P and S travel time anomalies and their interpretation, Geophys. J. R. astr. Soc., 13, 403-415.
- Hashin, Z 1966 The elastic moduli of heterogeneous materials, J. appl. Mech., 29, 143-150.
- Heirtzler, J. R.
et. al. 1966 Magnetic anomalies over the Reykjanes Ridge, Deep Sea Research, 13, 427-445.

- Hermance, J. F. and Garland, G. D. 1968 Magnetotelluric deep-sounding experiments in Iceland, Earth & Planet. Sci. Lett., (Neth) 4, 469-474.
- Herrin, E. et. al. 1968 Estimation of surface focus P travel times, Bull. seism. Soc. Am., 58, 1273-1291.
- Herrin, E. and Taggart, J. 1968a Regional variations in P travel times, Bull. seism. Soc. Am., 58, 1325-1337.
- Herrin, E. and Taggart, J. 1968b Source bias in epicentre determination, Bull. seism. Soc. Am., 58, 1791-1796.
- Isacks, B. et. al. 1968 Seismology and the new global tectonics, J. geophys. Res., 73, 5855-5899.
- Jeffreys, H. and Bullen, K. E. 1940 Seismological tables, Brit. Assn. Grey-Milne Trust.
- Le Pichon, X. 1968 Sea-floor spreading and continental drift, J. geophys. Res., 73, 3661-3697.
- Lilwall, R. C. and Douglas, A. 1969 A quest for a P travel time standard, Nature, 222, 975-977.
- Long, R. E. 1968 Temporary seismic array stations, Geophys. J. R. astr. Soc., 16, 37-45.
- Marshall, P. D. et. al. 1966 Some seismic results of the Longshot explosion, A.W.R.E. report No. 067/66, H.M.S.O.

- McBirney, 1967 Relations of oceanic volcanic rocks to mid-ocean rises and heat flow, *Earth & Planet. Sci. Lett. (Neth)*, 2, 265-276.
- Moorbath, S. et. al. 1968 K-Ar ages of the oldest exposed rocks in Iceland, *Earth & Planet. Sci. Lett. (Neth)*, 4, 197-205.
- Morgan, W. J. 1968 Rises, trenches, great faults, and crustal blocks, *J. geophys. Res.*, 73, 1959-1982.
- Moroney, M. J. 1951 Facts from figures, A, 236, Penguin Books Ltd., Middlesex.
- Oliver, J. and Isacks, B. 1967 Deep earthquake zones, anomalous structures in the upper mantle, and the lithosphere, *J. geophys. Res.*, 72, 4259-4275.
- Oxburgh, E. R. and Turcotte, D. L. 1968 Mid-ocean ridges and geotherm distribution during mantle convection, *J. geophys. Res.*, 73, 2643-3661.
- Palmason, G. 1963 Seismic refraction investigation of the basalt lavas in northern and eastern Iceland, *Jökull* 13, 40-60.
- _____ 1967a Upper crustal structure in Iceland, Iceland and Mid-Ocean Ridges, *Soc. Sci. Islandica 'Rit'* 38, edited by S. Björnsson, 67-79.
- _____ 1967b On heat flow in Iceland in relation to the Mid-Atlantic Ridge, Iceland and Mid-Ocean Ridges, *Soc. Sci. Islandica 'Rit'* 38, edited by S. Björnsson 111-127.

- Pitman, W. C. and Heirtzler, J. R. 1966 Magnetic anomalies over the Pacific-Antarctic Ridge, *Science*, 154, 1164-1171.
- Raitt, R. W. 1956 Seismic refraction studies of the Pacific ocean basin, 1, Crustal thickness of the central equatorial Pacific, *Bull. geol. Soc. Am.*, 67, 1623-1640.
- Richter, C. F. 1958 *Elementary Seismology*, Freeman, San Francisco.
- Shaw, H. R. 1963 Obsidian, H₂O viscosities at 100 and 2000 bars in the temperature range 700° to 900°C, *J. geophys. Res.*, 68, 6337.
- Sigurdsson, H. 1967 The Icelandic basalt plateau and the question of sial, a review, *Iceland and Mid-Ocean Ridges*, *Soc. Sci. Islandica 'Rit'* 38, edited by S. Björnsson, 32-46.
- Sigurgeirsson, T. 1967 *Aeromagnetic Surveys of Iceland and its neighbourhood*, *Iceland and Mid-Ocean Ridges*, *Soc. Sci. Islandica 'Rit'* 38, edited by S. Björnsson, 91-108.
- Stefansson, R. 1966 Methods of focal mechanism studies with application to two Atlantic earthquakes, *Tectonophysics*, 3, 210-242.
- Stefansson, R. 1967 Some problems of seismological studies on the Mid-Atlantic Ridge, *Iceland and Mid-Ocean Ridges*, *Soc. Sci. Islandica 'Rit'* 38, edited by S. Björnsson, 80-90.

- Sykes, L. R. 1965 The seismicity of the Arctic, Bull. seis. Soc. Am., 55, 501-518.
-
- 1966 The seismicity and deep structure island arcs, J. geophys. Res., 71, 2981-3006.
-
- 1967 Mechanisms of earthquakes and nature of faulting on the mid-ocean ridges, J. geophys. Res., 72, 2131-2153.
- Talwani, M. 1959 A crustal section across the Puerto et.al. Rico trench, J. geophys. Res., 64, 1545-1555.
-
- 1965 Crustal structure of the mid-ocean ridges 2. Computed model from gravity and seismic refraction data, J. geophys. Res., 70, 341-352.
- Tarling, D. H. and 1965 Isotopic dating and paleomagnetic Gale, N. H. polarity in the Faroe Islands, Nature, in Press.
- Thirlaway, H. I. S. 1965 Depth of focus discrimination within the crust at first-zone distances, vesiac special advisory report, No. 1, 2-17.
- Toksoz, M. N. 1967 Inhomogeneities in the earth's et. al. mantle, Geophys. J. R. astr. Soc., 13, 31-59.
- Tryggvason, E. 1959 Longitudinal wave velocity in the earth's crust in Iceland, Natturufraedingurinn, 29, 80-84.

- _____ 1961a Wave velocity in the upper mantle below the Arctic-Atlantic Ocean and Northwest Europe, *Annali Geofis.*, XIV, 379-392.
- _____ 1961b Crustal thickness in Fennoscandia from phase velocities of Rayleigh waves, *Annali Geofis.*, XIV, 267-293.
- _____ and 1961 Upper crustal structure of Iceland, *J. geophys. Res.*, 66, 1913-1925.
Bath, M.
- Tryggvason, E. 1962 Crustal structure of the Iceland region from dispersion of surface waves, *Bull. seism. Soc. Am.*, 52, 359-388.
- _____ 1964 Arrival times of P waves and upper mantle structure, *Bull. seism. Soc. Am.*, 54, 727-736.
- Vine, F. J. 1966 Spreading of the ocean floor: New evidence, *Science*, 154, 1405-1415.
- Walker, G. P. L. 1959 Geology of the Reydarfjordur area, eastern Iceland, *Quart. J. Geol. Soc. Lond.*, 114, 367-391.
- _____ 1965 Evidence of crustal drift from Icelandic geology, *Phil. Trans. R. Soc., A*, 258, 199-204.
- Walsh, J. B. 1968 Attenuation in partially melted material, *J. geophys. Res.*, 73, 2209-2216.
- Ward, P. L. 1969 Microearthquake survey and the Mid-Atlantic Ridge in Iceland, *J. geophys. Res.*, 74, 665-684.
et. al.

- Wilson, J. T. 1965 Submarine fracture zones, aseismic ridges and the international council of scientific unions line: Proposed western margin of the East Pacific Rise, Nature 207, 907-911.
- Wu, F. T. 1968 The effect of inclusion shape on the elastic moduli of a two-phase material, Intern. J. Solids. Structures, 2, 1.
- Young, J. B. and 1968 Gedess: a series of computer programs for deriving information at selected seismic recording sites for signals from known hypocentres, A.W.R.E. report no. 054/68 H.M.S.O.
- Gibbs, P.G.

APPENDIX 1Array layouts at Hveravellir and Myvatn

The array layouts at Hveravellir and Myvatn are described in terms of the Cartesian co-ordinates (X and Y) with the units metres. For Hveravellir, the Y-axis lies 47 deg East of North. For Myvatn, the Y-axis lies 8 deg East of North. The X and Y co-orindates of the Hveravellir array are given in Table 1 and those of the Myvatn array are given in Table 2. The pit heights above mean sea level are quoted in metres. For both arrays, all chann&els except numbers 3 and 4 refer to vertical seismometers.

TABLE 1

Array layout at Hveravellir

Channel no.	Co-ordinates		Pit height h
	X	Y	
1	240	-20	624
2,3,4	755	-10	632
5	1320	15	640
6	1805	45	640
7	2905	-50	652
8	-15	-295	630
10	-50	-790	640
12	-70	-1325	646
13	-90	-1840	654
14	-165	-2885	690

The crossover point of the array (0,0) is at $64^{\circ} 51' 27''$ North, $19^{\circ} 32' 15''$ West. Channel 3 is aligned with the X-axis and channel 4 is aligned with the Y-axis.

TABLE 2

Array layout at Myvatn

Channel no.	Co-ordinates		Pit height h
	X	Y	
1	-20	-256	280
2,3,4	20	-747	285
5	20	-1258	290
6	20	-1760	285
7	30	-2850	290
8	256	10	280
10	746	20	285
12	1250	-20	290
13	1750	-20	290
14	2750	-10	300

The crossover point of the array (0,0) is at $65^{\circ} 33' 36''$ North, $16^{\circ} 56' 42''$ West. Channel 2 is aligned with the X-axis and channel 3 is aligned with the Y-axis.

APPENDIX 2The data used in the delay time measurements at Akureyri, Eskdalemuir, Kiruna and Kaptobin

The data used in the delay time measurements are listed on the pages following. The epicentral data correspond to the U.S.C.G.S. final data reports. Epicentral distances to Akureyri, Eskdalemuir, Kiruna and Kaptobin are given in the columns headed DELA, DELE, DELKR, DELKG respectively. The event azimuth, AZI, is measured from Akureyri clockwise from North.

The delay times for each station are given relative to the delay at Akureyri, firstly using the J-B tables and secondly, using Herrin's corrections to the J-B tables. These are listed in the columns headed DLAY EK1, DLAY EK2, DLAY KR1, DLAY KR2, DLAY KG1, DLAY KG2 referring to the relative delays, firstly using J-B tables and secondly using Herrin's corrections to the J-B tables, at Eskdalemuir, Kiruna and Kaptobin respectively. For example, $DLAY EK1 = (\text{delay at Akureyri} - \text{delay at Eskdalemuir})$ using the J-B tables.

Where a station did not report an event, or where it was reported as eP - and therefore not used in the analysis - the relevant columns are asterisked.

YEAR	M	D	ORIGIN TIME			EPICENTRE		DEPTH	MAG	DELA	AZI	DELE	DELKR	DELKG	DLAY	DLAY	DLAY	DLAY	DLAY	DLAY
			HR	MN	SEC	NORTH	EAST			KM	MB	DEG	DEG	DEG	DEG	DEG	EK1	EK2	KR1	KR2
1964	8	4	17	24	29.2	46.5	-151.1	101	5.9	67.8	8	76.2	60.1	****	0.6	1.1	3.0	2.7	****	****
1964	8	4	18	24	50.5	56.9	-152.1	39	5.6	52.9	330	65.3	55.4	****	1.7	1.7	2.8	2.6	****	****
1964	8	8	14	59	41.2	31.7	140.2	110	5.7	81.5	19	****	71.1	****	****	****	1.9	1.3	****	****
1964	8	12	6	51	49.9	48.9	153.7	127	5.6	65.6	6	74.3	58.4	****	1.1	1.7	2.5	2.3	****	****
1964	8	12	19	26	26.1	31.0	49.8	33	5.1	53.1	96	44.3	40.7	****	1.7	2.2	0.9	1.6	****	****
1964	8	17	11	51	19.3	46.3	151.9	33	4.9	68.1	8	****	61.7	****	****	****	0.0	0.0	****	****
1964	8	17	14	54	1.4	42.6	142.8	33	5.1	71.0	15	****	7.7	****	****	****	1.8	1.1	****	****
1964	8	19	9	33	10.0	28.2	52.6	50	5.6	56.7	95	****	44.1	****	****	****	1.1	1.9	****	****
1964	8	19	15	20	13.9	28.2	52.7	52	5.6	56.8	95	****	44.1	****	****	****	1.4	2.2	****	****
1964	8	20	5	8	50.3	28.1	52.6	47	5.1	56.8	95	****	44.2	****	****	****	1.3	2.1	****	****
1964	8	20	5	39	47.7	28.2	52.6	52	5.5	56.8	95	****	44.2	****	****	****	1.1	1.9	****	****
1964	9	26	0	46	2.8	30.1	80.7	50	6.2	66.5	69	****	51.3	****	****	****	2.3	2.4	****	****
1964	9	27	15	50	54.7	56.6	-152.0	27	5.4	53.2	330	****	55.7	****	****	****	2.6	2.4	****	****
1964	9	28	5	4	55.5	-1.2	-24.1	35	5.5	66.9	187	****	75.5	****	****	****	2.1	2.7	****	****
1964	10	15	20	26	53.5	44.7	149.8	49	5.2	69.2	9	****	61.5	65.0	****	****	2.9	2.4	2.3	1.9
1964	10	15	23	9	25.1	56.9	-151.7	33	5.3	52.8	330	****	55.4	****	****	****	2.9	2.7	****	****
1964	10	16	7	21	42.7	44.2	149.4	33	5.2	70.0	10	****	61.9	****	****	****	1.3	0.7	****	****
1964	10	16	8	18	28.3	44.6	149.4	33	5.2	70.0	10	****	61.9	****	****	****	2.3	1.7	****	****
1964	10	16	9	18	16.6	44.5	149.1	33	5.6	70.0	10	****	61.9	65.2	****	****	1.1	0.5	1.2	0.8
1964	10	16	9	54	30.9	44.1	149.3	33	4.4	70.0	10	****	61.9	65.2	****	****	2.5	1.9	0.0	0.0
1966	4	21	3	57	58.0	49.8	78.0	0	5.5	48.3	60	47.0	32.2	****	1.4	1.5	2.4	2.2	****	****
1966	4	22	23	27	20.5	57.5	-152.1	22	5.9	52.3	331	64.8	54.8	47.5	-0.8	-0.9	1.3	1.1	-0.3	0.0
1966	5	1	16	22	56.3	-8.5	-74.3	165	5.7	84.6	236	86.4	99.6	****	-1.9	-1.9	0.9	1.1	****	****
1966	5	5	14	21	22.7	24.4	122.6	60	5.7	85.3	35	****	72.1	****	****	****	5.4	4.8	****	****
1966	5	9	0	42	55.6	34.5	26.5	33	5.5	40.8	118	****	33.6	44.3	****	****	3.6	3.1	-0.2	-0.3
1966	5	11	14	26	41.6	49.0	156.2	33	5.5	56.6	4	74.6	58.9	****	0.5	1.2	3.2	3.0	****	****
1966	5	11	15	6	2.1	34.4	26.5	34	4.9	40.9	118	****	33.7	****	****	****	4.0	3.5	****	****
1966	5	12	12	16	59.2	48.7	156.3	26	4.9	65.9	4	****	59.2	****	****	****	4.0	3.7	****	****
1966	5	15	14	46	6.5	51.5	-178.4	31	5.8	62.2	346	****	60.1	****	****	****	2.9	2.9	****	****
1966	5	17	7	3	30.1	0.8	29.9	15	5.5	73.2	129	****	67.2	****	****	****	5.1	4.7	****	****
1966	5	19	7	6	26.8	54.1	-164.1	28	5.8	57.8	337	69.8	58.3	52.8	0.8	1.4	3.5	3.5	2.3	2.6
1966	5	22	22	19	35.2	51.9	174.9	33	4.9	62.3	351	****	59.1	****	****	****	2.4	2.4	****	****
1966	5	23	8	39	44.4	30.0	139.8	28	5.5	83.1	19	****	72.6	****	****	****	1.8	1.2	****	****
1966	5	28	0	3	56.8	24.4	122.5	33	5.7	85.3	36	88.1	72.1	****	3.0	2.9	3.3	2.7	****	****
1966	6	1	2	33	56.3	51.5	176.2	15	5.1	62.6	350	73.5	59.6	57.7	0.4	1.2	1.8	1.7	0.8	0.8
1966	6	2	3	27	53.3	51.1	176.0	41	6.0	63.0	350	73.9	60.0	58.1	0.9	1.7	2.3	2.3	1.4	1.3
1966	6	4	5	11	54.2	36.3	70.8	207	5.7	57.1	74	52.3	42.2	57.2	1.7	2.0	0.7	1.6	0.2	0.2
1966	6	4	23	48	17.8	46.5	152.5	27	5.9	67.9	7	76.5	60.4	63.3	-0.6	0.0	1.0	0.5	1.7	1.4
1966	6	6	7	46	16.2	36.3	71.2	225	6.3	57.3	74	52.5	42.3	57.3	2.0	2.3	1.8	2.7	0.5	0.5
1966	6	8	19	56	21.3	53.1	171.1	20	5.4	61.3	354	****	57.4	****	****	****	1.6	1.6	****	****
1966	6	14	2	45	57.0	38.1	42.8	38	4.7	44.1	98	35.1	32.2	****	3.2	2.9	3.2	2.7	****	****

YEAR	M	D	ORIGIN TIME			EPICENTRE		DEPTH	MAG	DELA	AZI	DELE	DELKR	DELKG	DLAY	DLAY	DLAY	DLAY	DLAY	DLAY
			HR	MN	SEC	NORTH	EAST			KM	MB	DEG	DEG	DEG	DEG	DEG	EK1	EK2	KR1	KR2
1966	621	23	6	25.9	50.1	157.8	14	5.8	64.5	3	73.7	58.1	59.8	1.0	1.7	3.5	3.3	1.1	0.9	
1966	622	11	38	53.7	61.4	-147.6	53	5.2	47.8	330	60.3	50.8	****	3.1	2.5	1.9	1.7	****	****	
1966	623	5	1	42.2	43.8	139.9	218	5.5	69.5	17	76.4	59.8	65.3	0.9	1.3	2.1	1.5	1.2	0.8	
1966	629	6	57	58.1	49.9	78.0	0	5.7	48.3	60	****	33.1	****	****	****	2.3	2.1	****	****	
1966	630	8	59	48.3	43.6	132.2	454	5.4	68.6	23	****	57.8	****	****	****	2.6	2.1	****	****	
1966	7 1	5	50	39.2	24.8	122.5	117	6.4	84.9	35	87.7	71.2	81.8	1.6	1.6	2.6	1.9	0.5	0.4	
1966	7 4	2	55	35.9	51.8	176.4	28	5.7	62.3	350	73.2	59.3	57.4	0.4	1.1	2.0	2.0	1.0	1.0	
1966	7 5	2	21	43.8	52.2	-178.4	66	4.9	61.5	35	****	59.5	56.5	****	****	10.9	10.9	0.4	0.4	
1966	8 8	8	2	45.8	19.3	-108.1	33	5.4	72.6	278	****	85.4	****	****	****	1.4	2.0	****	****	
1966	810	22	5	35.0	38.4	69.6	4	5.5	54.8	74	****	39.9	****	****	****	0.9	1.7	****	****	
1966	812	20	16	59.8	52.9	-161.6	31	5.6	58.5	335	70.7	59.6	****	0.8	1.5	2.0	2.0	****	****	
1966	815	2	15	33.8	28.7	78.9	50	5.8	67.0	71	****	52.0	****	****	****	1.3	1.3	****	****	
1966	815	13	36	23.7	60.4	-146.0	9	5.3	48.4	328	60.9	51.7	****	1.6	1.0	2.2	2.0	****	****	
1966	816	2	16	19.7	36.4	70.8	199	5.7	57.0	74	52.2	42.1	****	1.4	1.7	0.7	1.5	****	****	
1966	817	20	58	35.9	52.3	174.9	32	5.6	61.9	351	72.7	57.8	****	1.4	2.1	2.7	2.7	****	****	
1966	818	10	33	16.5	14.6	-91.7	76	5.9	70.0	261	****	84.6	****	****	****	-0.6	0.2	****	****	
1966	820	7	43	27.6	-3.2	-77.2	116	5.6	80.7	240	83.6	****	****	1.0	1.1	****	****	****	****	
1966	820	9	32	31.7	43.1	140.6	161	5.8	70.3	16	77.2	60.6	****	-0.3	0.1	1.0	0.4	****	****	
1966	820	11	59	12.1	39.3	40.9	37	5.4	42.3	99	****	30.7	****	****	****	2.1	1.6	****	****	
1966	10 7	20	55	56.0	61.6	-150.1	56	5.7	48.2	332	60.5	50.7	****	2.3	1.7	3.1	2.9	****	****	
1966	1017	21	41	56.3	-10.7	-78.7	38	0.0	88.2	239	****	****	89.5	****	****	****	****	0.9	0.9	
1966	11 1	7	1	0.4	43.2	143.4	127	4.8	70.5	14	77.8	61.3	66.2	0.8	1.3	3.0	2.4	2.2	1.8	
1966	1112	12	49	43.6	41.8	144.1	33	5.8	72.0	14	****	62.8	67.6	****	****	2.1	1.4	1.6	1.3	
1966	1122	6	29	53.5	48.2	146.7	453	5.6	65.8	11	73.8	57.5	61.4	1.3	1.9	2.0	1.8	1.9	1.7	
1966	1210	13	6	32.6	14.3	-92.0	70	0.0	70.4	261	77.7	****	****	0.3	0.8	****	****	****	****	
1966	1218	4	57	57.8	49.9	77.7	0	5.9	48.1	60	46.8	33.0	****	0.9	1.0	1.7	1.5	****	****	
1967	1 4	20	15	55.8	10.7	-62.5	74	5.5	62.7	231	64.0	77.5	64.8	1.4	1.5	0.6	1.6	1.6	1.7	
1967	1 5	0	14	40.4	48.1	102.8	33	6.4	57.8	43	59.8	43.9	55.3	1.2	1.2	1.0	1.8	1.7	1.8	
1967	1 5	0	42	13.3	48.4	103.1	33	5.6	57.6	43	59.7	43.8	55.1	0.1	0.1	1.1	1.9	1.2	1.3	
1967	1 6	0	4	2.7	41.8	143.3	35	5.5	71.9	15	****	62.6	67.6	****	****	2.1	1.4	1.2	0.9	
1967	111	11	20	45.7	34.1	45.7	34	5.6	48.7	98	39.7	36.8	50.8	1.4	1.7	2.6	2.8	0.7	0.8	
1967	114	12	4	50.7	52.1	175.4	41	5.1	62.1	351	72.9	58.9	57.1	1.8	2.6	3.2	3.2	2.2	2.2	
1967	117	11	59	31.5	38.3	142.1	44	5.9	75.2	16	82.1	65.5	71.0	1.3	1.7	3.2	2.5	2.3	2.1	
1967	118	5	34	32.6	56.6	120.8	11	6.1	54.1	27	59.5	42.9	50.5	0.9	0.7	2.8	3.5	2.9	3.2	
1967	118	8	18	22.0	52.5	-168.3	37	5.7	60.0	339	71.8	59.8	55.1	0.3	1.0	3.3	3.3	2.6	2.7	
1967	118	15	28	2.7	47.3	152.1	140	4.8	67.0	7	****	****	62.5	****	****	****	****	1.1	0.8	
1967	120	1	57	23.1	48.0	102.9	33	6.1	57.9	43	59.9	44.0	55.4	2.1	2.1	2.3	3.1	0.5	0.6	
1967	123	20	25	38.3	19.9	-109.3	56	5.3	72.5	280	****	****	70.5	****	****	****	****	-1.6	-1.7	
1967	124	3	5	39.0	41.4	141.9	69	5.7	72.1	16	79.1	62.6	69.9	-0.5	-0.1	3.2	2.5	2.1	2.0	
1967	125	1	50	19.4	36.6	71.6	281	5.7	57.2	73	52.6	42.2	57.2	2.3	2.6	1.7	2.5	1.2	1.2	
1967	128	13	52	58.3	52.4	-169.5	47	0.0	60.2	340	****	59.9	55.3	****	****	3.5	3.5	2.7	2.8	

YEAR	M	D	ORIGIN TIME			EPICENTRE		DEPTH	MAG	DELA	AZI	DELE	DELKR	DELKG	DLAY	DLAY	DLAY	DLAY	DLAY	DLAY
			HR	MN	SEC	NORTH	EAST													
1967	131		17	43	56.2	42.8	145.4	44	5.1	71.1	13	****	62.2	66.7	****	****	2.9	2.3	2.7	2.3
1967	2	7	14	53	13.9	56.7	-157.2	67	5.6	54.1	334	****	55.8	49.2	****	****	3.5	3.4	2.1	2.5
1967	2	9	15	24	47.2	2.9	-74.9	58	6.3	74.2	240	****	89.3	75.5	****	****	1.2	1.7	1.6	1.7
1967	214		1	36	4.7	13.7	96.5	27	0.0	87.3	62	****	****	86.3	****	****	****	****	-3.2	-3.2
1967	215		16	11	11.8	-9.0	-71.3	597	6.2	84.1	233	****	98.9	85.9	****	****	0.3	0.5	0.5	0.5
1967	3	2	2	47	31.7	-0.3	-78.7	121	5.8	78.5	243	82.0	93.7	79.6	0.0	0.2	0.7	1.0	0.8	0.8
1967	319		4	1	36.7	45.4	151.3	33	0.0	68.9	8	****	61.2	64.4	****	****	3.4	2.9	3.2	2.8
1967	327		8	58	25.5	38.4	116.5	61	5.4	70.4	36	****	57.3	****	****	****	6.0	5.4	****	****
1967	4	1	5	54	19.1	45.8	151.8	40	5.7	68.6	8	77.0	****	****	-0.1	0.4	****	****	****	****
1967	4	1	5	57	9.1	46.3	152.0	40	5.5	68.1	7	76.6	60.5	****	0.0	0.5	2.0	1.6	****	****
1967	4	1	12	23	35.5	45.7	151.8	40	5.9	68.7	8	****	61.0	****	****	****	2.9	2.5	****	****
1967	4	1	14	0	33.8	45.8	151.7	23	5.4	68.6	8	****	60.9	****	****	****	3.1	2.7	****	****
1967	413		19	53	42.4	27.3	128.7	38	6.0	83.9	29	88.0	71.6	80.3	2.1	2.1	2.8	2.1	1.5	1.4
1967	913		18	41	15.4	52.7	172.5	34	5.7	61.7	353	72.3	58.0	56.7	0.3	1.0	1.0	1.0	0.1	0.1
1967	922		8	8	4.3	-0.7	-20.1	33	5.3	66.3	182	****	73.9	****	****	****	1.2	1.8	****	****
1967	922		10	17	59.9	44.5	149.4	60	5.6	69.7	10	77.9	61.6	65.2	0.3	0.8	4.6	4.2	3.1	2.7
1967	928		15	44	55.7	59.5	-147.1	28	5.6	49.5	329	61.9	52.6	44.7	1.1	0.6	2.1	1.9	1.0	1.3
1967	1012		12	53	46.9	52.2	152.5	476	5.5	62.2	7	70.9	55.1	57.6	1.6	2.2	3.1	3.1	1.6	1.6
1967	1015		8	0	50.3	11.9	-86.0	162	6.2	70.2	255	76.2	85.1	70.3	2.4	2.8	-0.3	0.5	0.6	0.6
1967	1017		5	3	58.0	49.8	78.1	0	5.7	48.4	60	47.1	33.3	47.3	1.8	1.9	2.7	2.5	0.7	0.8
1967	1030		6	3	57.9	49.8	78.1	0	5.5	48.4	60	47.1	33.3	47.3	1.9	2.0	2.4	2.2	0.6	0.7
1967	1123		8	35	49.5	14.5	52.1	3	0.0	68.8	102	****	57.1	71.1	****	****	6.5	6.3	5.4	5.6
1967	1210		22	51	24.3	17.7	73.9	33	6.0	74.9	81	68.3	60.3	75.4	3.3	2.9	2.0	1.1	0.2	0.2
1967	1213		10	38	23.4	47.6	152.6	124	5.5	66.8	7	75.4	59.4	****	0.9	1.3	3.0	2.7	****	****
1967	1216		20	53	58.3	51.2	157.7	24	5.5	63.4	3	72.6	57.1	58.7	1.1	1.8	2.0	2.0	1.2	1.2
1967	1224		20	3	10.9	17.4	-61.1	24	6.4	56.0	232	57.8	70.8	58.0	-0.2	-0.2	1.3	1.8	1.7	1.7
1968	1	8	20	22	15.6	8.2	-38.2	33	5.4	59.1	203	****	70.9	63.0	****	****	3.2	3.9	1.4	1.5
1968	129		5	0	10.0	36.3	70.4	225	5.5	57.0	74	52.1	42.1	57.1	2.2	2.5	1.0	1.8	0.8	0.8
1968	129		10	19	5.6	43.6	146.7	40	0.0	70.4	12	78.2	61.8	****	0.4	0.9	3.2	2.6	****	****
1968	129		16	42	50.4	43.5	147.2	36	5.7	70.6	11	78.4	62.0	66.1	1.9	2.4	3.6	3.0	2.0	1.6
1968	130		1	30	12.7	43.3	146.8	12	5.3	70.7	12	****	62.1	66.3	****	****	2.8	2.2	1.9	1.5
1968	2	3	11	30	44.4	43.2	146.8	33	5.5	70.8	12	****	62.2	66.4	****	****	2.6	2.0	1.8	1.4
1968	220		2	19	49.6	12.4	-46.9	13	5.6	56.7	214	****	70.1	60.0	****	****	1.6	2.2	1.2	1.2
1968	221		6	21	3.6	52.3	-175.3	107	5.3	61.1	344	72.5	59.6	56.1	1.2	2.0	2.6	2.6	1.7	1.7
1968	226		10	50	16.7	22.7	121.5	24	0.0	86.7	37	****	73.3	83.6	****	****	5.4	4.8	5.1	5.1
1968	322		20	34	46.3	37.4	142.4	18	5.3	76.1	16	****	66.4	****	****	****	-1.4	-2.1	****	****
1968	4	1	7	13	17.6	32.3	132.1	32	5.7	79.6	25	84.7	****	****	0.7	0.9	****	****	****	****
1968	4	3	16	24	45.7	51.7	174.2	38	5.3	62.6	351	73.3	****	****	2.2	3.0	****	****	****	****
1968	423		20	29	14.5	58.7	-150.0	23	6.3	50.8	330	63.2	****	****	0.5	0.2	****	****	****	****
1968	426		2	58	22.1	35.1	50.2	21	5.3	49.7	93	41.5	****	****	2.0	2.4	****	****	****	****
1968	429		17	1	57.6	39.2	44.3	34	5.3	43.8	96	35.2	****	****	2.7	2.5	****	****	****	****

APPENDIX 3

Tryggvason's method.

(A3.1) Crustal effect on the travel time

Because of the large variations in its thickness and velocity, seismic travel times must be corrected for the effect of the crust. This correction is computed here so that the corrected travel time is equal to the travel time after the crust at the recording station has been replaced by materials with wave velocity equal to that in the upper mantle. As the wave velocity is lower in the crust than in the mantle, the time correction will be negative.

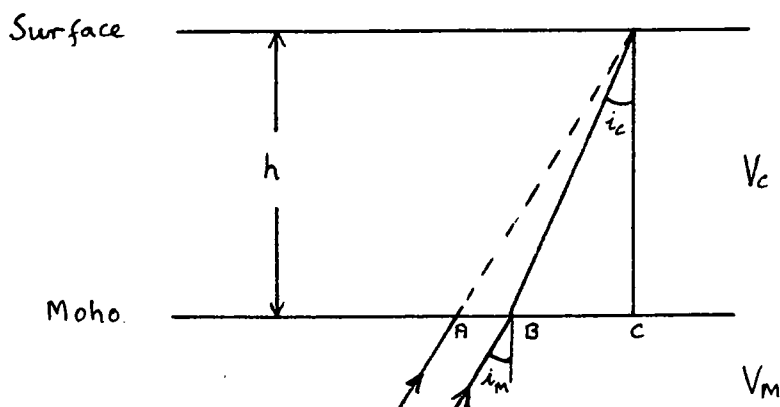


Figure 1

Introducing the following notation:

V_c = P-wave velocity in the crust, assumed constant.

V_m = P-wave velocity in the upper mantle.

V_a = Apparent P-wave velocity along the surface.

h = the crustal thickness.

dt = the time correction due to the crust.

i_c = Angle of incidence at the top of the crust.

i_m = angle of incidence at the base of the crust.

Other notations are indicated on Figure 1.

Neglecting the earth's curvature, we obtain the following equation for the time correction:

$$dt = AD/V_m - AB/V_a - BD/V_c \quad (1)$$

Also, $\sin i_c = V_c/V_a \quad (2a)$

$$\sin i_m = V_m/V_a \quad (2b)$$

$$AD = h/\cos i_m \quad (3a)$$

$$BD = h/\cos i_c \quad (3b)$$

$$\text{and } AB = AC - BC = h(\tan i_m - \tan i_c) \quad (4)$$

On substituting the values given in equations (3) and (4) into equation (1) we obtain:

$$dt = h/V_m \cos i_m - h/V_c \cos i_c - h/V_a(\tan i_m - \tan i_c) \quad (5)$$

and substituting (2) into (5) we get:

$$dt = h(V_a/V_m K_m - V_a/V_c K_c - V_m/V_a K_m + V_c/V_a K_c) \quad (6)$$

$$\text{where, } K_m = \sqrt{V_a^2 - V_m^2}, \text{ and } K_c = \sqrt{V_a^2 - V_c^2}$$

(A3.2) Computation of the mantle anomaly

Provided that the crustal structures and the difference in travel time to two stations ($t_1 - t_2$) are known, then the difference of wave velocity at different depths, h , below the stations, $(V_h)_1 - (V_h)_2$, can be estimated to fit the known data. If the epicentral distance to each station is known, then an approximate equation giving the relation between $(t_1 - t_2)$, $(V_h)_1$, $(V_h)_2$ and H can be written in the form:

$$\begin{aligned} t_1 - t_2 = & \int_{h=0}^H \frac{dh}{(V_h \cos ih)_1} - \int_{h=0}^H \frac{dh}{(V_h \cos ih)_2} \\ & + 1/V_a \int_{h=0}^H \frac{R \tan (ih)_2 dh}{(R - h)} \\ & - 1/V_a \int_{h=0}^H \frac{R \tan (ih)_1 dh}{(R - h)} \end{aligned} \quad (7)$$

where, the subscript 1 refers to location 1 and 2 refers to location 2, R is the radius of the earth and H is the depth below which no horizontal variation in velocity exists.

The angle between the vertical and the seismic ray (ih) may vary with h and so may the velocity V_h . Equation (7) cannot be solved in its general form, but by introducing some simplifying assumptions, it can be solved. If we assume that $(V_h)_1 = V_1$ and $(V_h)_2 = V_2$ are constant from $h = 0$ to $h = H$, then equation (7) can be solved to find H (Figure 2). The simplified equation then becomes:

$$t_1 - t_2 = AB R/V_a(R - H) + AS/V_1 - BS/V_2 \quad (8)$$

$$\text{Where, } AS = H/\cos i_1 \quad (9a)$$

$$BS = H/\cos i_2 \quad (9b)$$

$$AB = OB - OA = H(\tan i_2 - \tan i_1) \quad (10)$$

$$\sin i_1 = V_1/V_a \quad (\text{Approx.}) \quad (11a)$$

$$\sin i_2 = V_2/V_a \quad (\text{Approx.}) \quad (11b)$$

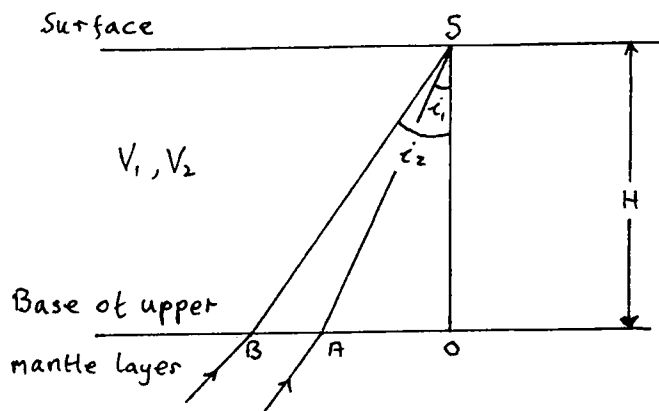


Figure 2

On substituting (9), (10) and (11) into equation (8), and noting the relations between the trigonometric functions, we have:

$$t_1 - t_2 = H \left[\frac{RV_2}{(R-H)V_a C_2} - \frac{RV_1}{(R-H)V_a C_1} - \frac{V_a}{V_2 C_2} + \frac{V_a}{V_1 C_1} \right] \quad (12)$$

where $C_1 = \sqrt{V_a^2 - V_1^2}$ and $C_2 = \sqrt{V_a^2 - V_2^2}$

Equation (12) is not exact as the curvature of the earth along the distance OB (Fig. 2) is neglected, but if H is much less than R, and if V_a is considerably greater than both V_1 and V_2 , then the error caused by the inaccuracy is negligible.

(A3.3) Application to the delay time data

Using the equations for the crustal correction (6) and for the effect of the upper mantle (12), we can relate the differences in travel time ($t_1 - t_2$) to two stations equidistant from the event, to the depth H, providing the other factors in the equations are known. Where the distances to the two stations are not equal, we may use the equations to relate H to the difference in delay times ($Dt_1 - Dt_2$) at the two stations. Thus we may write:

$$Dt_1 - Dt_2 = (t_1 - t_2) - (dt_1 - dt_2) \quad (13)$$

A computer program was written to relate $Dt_1 - Dt_2$ to the depth H , for relative delays between Akureyri and Eskdalemuir and between Akureyri and Kiruna. The crustal structures in Table 9 (page 62) were assumed and the sub-Moho velocity was taken as constant down to the depth H beneath each station. The apparent surface velocities, V_a , were taken from Richter (1958). The calculations were made for observations at 10 degree distance intervals from Akureyri, using apparent velocities appropriate for the mid-point of each distance range.



FIG. 5A.2. Event recorded at Hveraveiditr. This is a high-speed, high-gain playback of the event shown in Figure 5A.1.

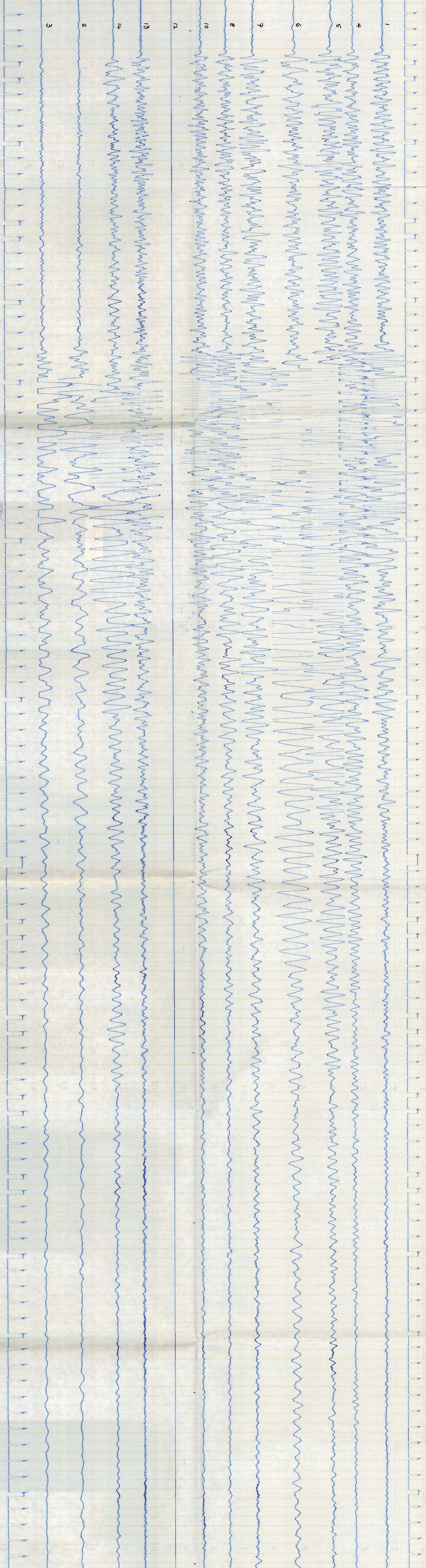
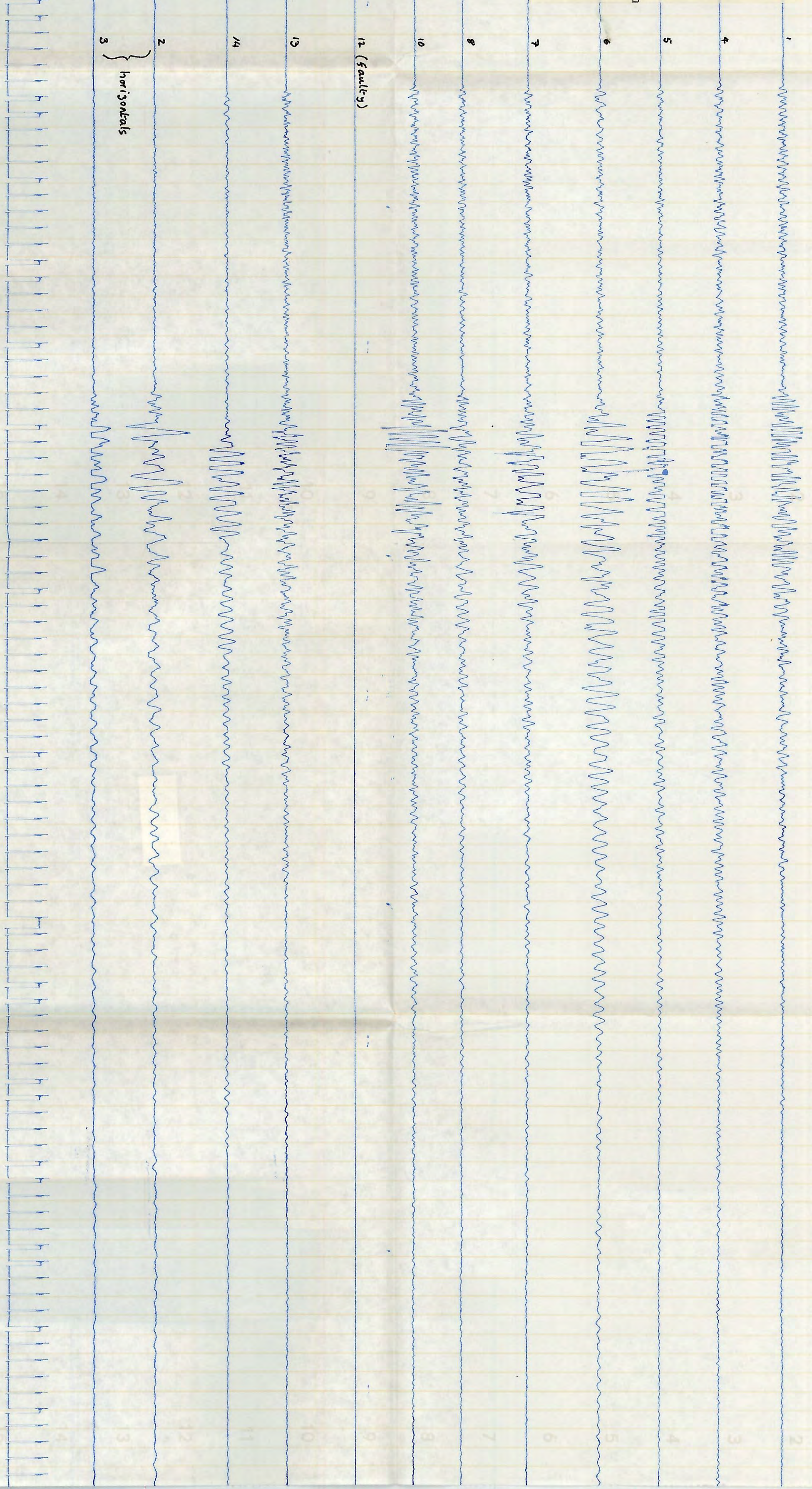


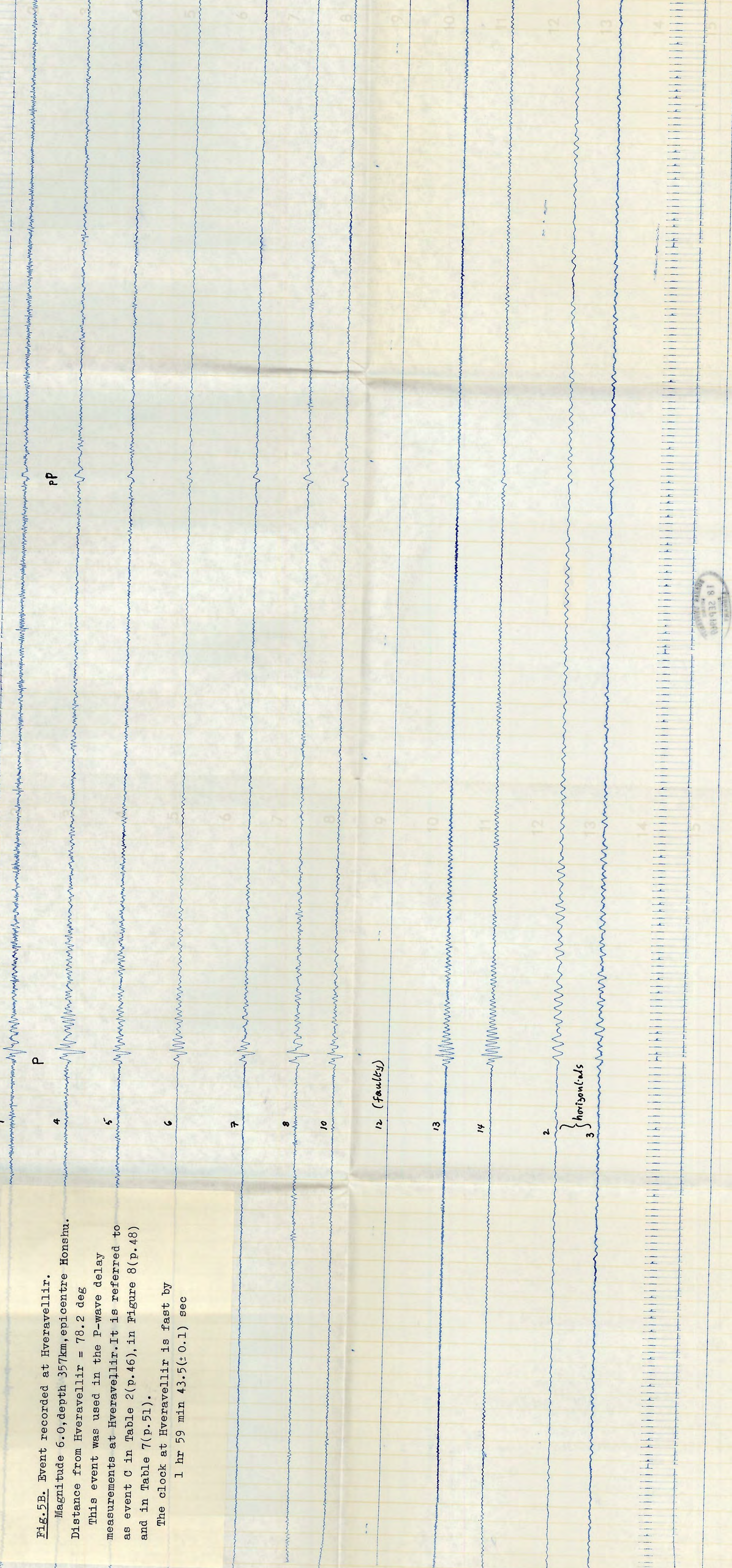
Fig. 5A.1. Event recorded at Hveraveillir.
 Approx. origin time : 0131 hr Aug. 17th 1967.
 Epicentre : off the North coast of Iceland
 near no. 4 on Figure 3 (p. 25).
 The clock correction at Hveraveillir is not
 known exactly. Onset-time analysis gives an
 apparent velocity of 6.3 km/sec and an azimuth
 of 16 deg East of North.
 The P-wave arrivals from this event are
 shown more clearly in Fig. 5A.2.



22 hrs 18 min Aug 1956

Fig. 5B. Event recorded at Hveravellir.
 Magnitude 6.0, depth 357km, epicentre Honshu.
 Distance from Hveravellir = 78.2 deg
 This event was used in the P-wave delay
 measurements at Hveravellir. It is referred to
 as event C in Table 2 (p. 46), in Figure 8 (p. 48)
 and in Table 7 (p. 51).

The clock at Hveravellir is fast by
 1 hr 59 min 43.5 (± 0.1) sec



094932 81
 18
 1956